U.PORTO

MESTRADO EM ONCOLOGIA

ONCOLOGIA LABORATORIAL

Studying the chemosensitizing effect of Pirfenidone in non-small cell lung cancer cell lines

Helena Isabel de Freitas Branco

M

2021

U.PORTO

Helena Isabel de Freitas Branco. Studying the chemosensitizing effect of Pirfenidone in non-small cell lung cancer cell lines

Studying the chemosensitizing effect of Pirfenidone in non-small cell lung cancer cell lines

Helena Isabel de Freitas Branco

M.ICBAS **2021**

INSTITUTO DE CIÊNCIAS BIOMÉDICAS ABEL SALAZAR

Helena Isabel de Freitas Branco

Studying the chemosensitizing effect of Pirfenidone in non-small cell lung cancer cell lines

Dissertação de Candidatura ao grau de Mestre em Oncologia submetida ao Instituto de Ciências Biomédicas de Abel Salazar da Universidade do Porto.

Orientador – Doutora Cristina Pinto Ribeiro Xavier

Categoria – Investigador de Pós-Doutoramento

Afiliação – Grupo Cancer Drug Resistance do Instituto de Patologia e Imunologia Molecular da Universidade do Porto/Instituto de Investigação e Inovação em Saúde da Universidade do Porto

Co-orientador – Prof. Doutora Maria Helena da Silva de Vasconcelos Meehan

Categoria – Professor Associado

Afiliação – Departamento de Ciências Biológicas da Faculdade de Farmácia da Universidade do Porto e Coordenadora do Grupo Cancer Drug Resistance do Instituto de Patologia e Imunologia Molecular da Universidade do Porto/Instituto de Investigação e Inovação em Saúde da Universidade do Porto

Co-orientador – Prof. Doutor Lúcio José de Lara Santos

Categoria – Professor Associado

Afiliação – Instituto de Ciências Biomédicas de Abel Salazar da Universidade do Porto e Coordenador do Grupo de Patologia e Terapêutica Experimental do Instituto Português de Oncologia do Porto

“Every scientist dreams of doing something that can help the world.”

TU YOUYOU

Nobel Prize in Physiology or Medicine 2015

Scientific Communications

ORAL

- **Helena Branco**, Catarina Antunes, Cristina P.R. Xavier, Júlio Oliveira, Lúcio L. Santos, M. Helena Vasconcelos. Pirfenidone sensitizes non-small cell lung cancer cell lines to the effect of chemotherapeutic agents. Young Researchers Meeting 14th Edition, May 05-07, 2021. Online meeting.

POSTER

- **Helena Branco**, Catarina Antunes, Júlio Oliveira, Lúcio L. Santos, M. Helena Vasconcelos, Cristina P.R. Xavier. Pirfenidone sensitizes non-small cell lung cancer cell lines to Vinorelbine treatment. II ASPIC-ASEICA International Meeting, October 14-15, 2021. Online meeting.
- **Helena Branco**, Catarina Antunes, Júlio Oliveira, Lúcio L. Santos, M. Helena Vasconcelos, Cristina P.R. Xavier. Estudo pré-clínico do efeito combinado da Pirfenidona com fármacos antitumorais em linhas celulares de cancro do pulmão de não-pequenas células. 3º Encontro Nacional de Jovens Investigadores em Oncologia, September 24th, 2021. Porto, Portugal.

This work was funded in part by Programa Operacional Regional do Norte and co-funded by European Regional Development Fund under the project "The Porto Comprehensive Cancer Center" with the reference NORTE-01-0145-FEDER-072678 - Consórcio PORTO.CCC – Porto.Comprehensive Cancer Center.

Acknowledgements | Agradecimentos

Antes de terminar esta importante etapa da minha vida, gostaria de agradecer a todos aqueles que me acompanharam ao longo deste percurso, contribuindo, de uma forma ou de outra, para a minha formação enquanto pessoa e profissional.

Agradeço à comissão científica do Mestrado em Oncologia, em particular à Professora Doutora Carmen Jerónimo, pela oportunidade de ingressar neste ciclo de estudos, permitindo-me aprofundar conhecimentos nesta área que tanto me fascina com o auxílio de alguns dos melhores profissionais em oncologia.

Agradeço à Prof. Doutora Maria Helena Vasconcelos, líder do grupo Cancer Drug Resistance e co-orientadora do trabalho que aqui apresento, por me ter concedido a oportunidade de integrar o seu grupo de investigação e pela imensa dedicação e empenho com que me acompanhou ao longo deste percurso. Agradeço-lhe por toda a confiança depositada no meu trabalho e por tudo aquilo que me tem vindo a ensinar. A Professora inspira-me, dia após dia, a superar-me e trabalhar para me tornar numa melhor cientista e, acima de tudo, num melhor ser humano. Obrigada!

Agradeço à Doutora Cristina Xavier, orientadora da minha dissertação de mestrado, pelo papel absolutamente fundamental que desempenhou ao longo deste último ano. Agradeço pela forma calorosa como me recebeu desde o primeiro dia e pelo rigor e entrega com que sempre se apresentou. Agradeço-lhe pela confiança depositada em mim e no meu trabalho e pela liberdade que me concedeu para pensar e discutir ciência. Agradeço-lhe pela disponibilidade constante e por todas as palavras de incentivo. Agradeço-lhe pela amizade. Por tudo isto e por muito mais: Obrigada!

Agradeço ao Prof. Doutor Lúcio Lara Santos, co-orientador deste projeto, pela contribuição valiosa que a sua expertise clínica e translacional trouxe ao trabalho que aqui apresento, realçando o impacto que este trabalho possa vir a ter na prática clínica.

Ao Dr. Júlio Oliveira, médico oncologista no IPO-Porto, agradeço pela partilha de conhecimentos e incentivo constante deste projeto.

A todos os membros do grupo Cancer Drug Resistance, agradeço pela amizade, companheirismo e profissionalismo demonstrados ao longo deste último ano. Cada uma de vocês contribuiu diariamente para que esta etapa se tornasse inesquecível. Em particular, agradeço às minhas queridas Rita, Sara e Bárbara pelos seres humanos absolutamente incríveis que são. Poder partilhar o entusiasmo e paixão pela ciência com cada uma de vocês todos os dias é uma sorte.

Agradeço e felicito os meus colegas do Mestrado em Oncologia com os quais pude trocar conhecimentos e crescer nos últimos dois anos. Levo-vos comigo para a vida!

Aos amigos de sempre e àqueles que a Universidade do Porto colocou no meu caminho, o meu sincero obrigada. Agradeço por todos os sorrisos e gargalhadas trocados em momentos de vitória e pelo apoio nos momentos mais difíceis. Nada na vida se alcança sozinho e poder partilhar a vida convosco é uma dádiva.

Por fim, mas não menos importante, agradeço à minha família pela presença constante e apoio incondicional não só ao longo dos últimos 5 anos, mas em toda a minha vida. Aos meus pais, agradeço por todos os esforços feitos para que eu pudesse estar aqui hoje. Agradeço por acreditarem em mim e me incentivarem a perseguir os meus sonhos. Tudo o que sou hoje a vocês o devo. Um obrigada não é suficiente.

A todos vocês,

Obrigada!

Abstract

Lung cancer is the leading cause of cancer-related deaths worldwide and non-small cell lung cancer (NSCLC) accounts for roughly 85% of the cases. Despite the advances that have been made in the development of new early-detection techniques, lung cancer continues to be diagnosed at a late stage, with a 5-year survival rate of only 5%. Chemotherapy is the primary treatment option for patients with advanced NSCLC without targetable alterations and low PD-L1 expression, and is commonly used as a neo-adjuvant measure. Nonetheless, NSCLC is a highly desmoplastic type of tumor and drug resistance frequently occurs as a result of its highly fibrotic profile. Thus, the development of new and more effective therapeutic strategies becomes crucial.

Drug repurposing has emerged in oncology as a strategy to identify antitumor properties in drugs already approved or under investigation for the treatment of other diseases. This approach enables the development of new therapeutic options in a more timely and cost-effective manner. Recently, Pirfenidone (PF) – an antifibrotic drug approved for the treatment of idiopathic pulmonary fibrosis – demonstrated antitumor potential against different types of cancers by interfering with proliferation and migration. Furthermore, the sensitizing effect of PF to the treatment with some antitumor agents has also been described. Preliminary results obtained by another Master student from our research group demonstrated that PF sensitizes the NSCLC NCI-H460 cell line to Vinorelbine (VR) treatment.

The main aim of this dissertation was to study the sensitizing effect of PF to several chemotherapeutic drugs currently used in the clinical practice, in various NSCLC cell lines. Our long-term goal is to verify the possibility of repurposing PF for the treatment of NSCLC.

To achieve this goal, three NSCLC cell lines (A549, NCI-H322 and NCI-H460) were used to assess the effect of PF in combination with Etoposide, Gemcitabine, VR or Paclitaxel (PAC) on cell growth, using the sulforhodamine B (SRB) assay. The combined drug treatments that presented statistically significant advantage in terms of cell growth inhibition over the treatment with each drug individually, were further tested to assess their effect on: 1) cell viability (with the trypan blue exclusion assay); 2) cell cycle profile (by flow cytometry analysis following propidium iodide staining); 3) cell proliferation (with the bromodeoxyuridine incorporation assay); and 4) cell death (by flow cytometry analysis following Annexin V-FITC/PI staining). Moreover, the effect of the combined treatment of VR and Carboplatin (CBP), which is currently used in the clinical practice, with PF on cell

growth of the three NSCLC cell lines under study was also analyzed. Finally, the effect of the combined drug treatments on cell growth of non-tumorigenic cell lines (MCF-10A and MCF-12A) were also assessed recurring to the SRB assay.

Our results demonstrated that PF sensitizes the A549 and NCI-H322 lung adenocarcinoma cell lines to VR treatment, causing a significant reduction in the % of viable and proliferating cells and an increase in the % of cell death. Therefore, our results validated in two additional NSCLC cell lines, what had been previously found in the preliminary results from our research group. Furthermore, PF also sensitized the three NSCLC cell lines under study to the combined effect of VR with CBP, leading to a statistically significant increase in the % of cell growth inhibition. Moreover, our data also revealed that PF sensitizes the NCI-H460 cell line to PAC treatment, causing a statistically significant reduction in cell growth and viability, alterations in the cell cycle profile and an increase in the % of cell death. Importantly, none of these drug combinations increased the cytotoxicity of non-tumorigenic cells, when compared with the corresponding individual treatments with chemotherapeutic drugs.

Future work will validate the drug combination consisting of PF with VR and CBP, using xenograft mice models of NSCLC cell lines.

Keywords: Non-Small Cell Lung Cancer; Drug Repurposing; Pirfenidone; Vinorelbine; Paclitaxel; Carboplatin.

Resumo

O cancro do pulmão é a principal causa de morte relacionada com cancro a nível mundial, e o cancro do pulmão de não-pequenas células (NSCLC) é responsável por cerca de 85% dos casos. Apesar dos avanços que se têm vindo a registar no desenvolvimento de novas técnicas de deteção precoce, o cancro do pulmão continua a ser diagnosticado numa fase tardia, com uma taxa de sobrevida a 5 anos de apenas 5%. A quimioterapia é a opção terapêutica de eleição para pacientes com NSCLC avançado não elegíveis para terapia dirigida e com baixa expressão de PD-L1, sendo habitualmente utilizada como uma medida neo-adjuvante. No entanto, NSCLC é um tumor desmoplásico e a resistência a fármacos ocorre frequentemente devido ao perfil altamente fibrótico que caracteriza esta doença. Assim, o desenvolvimento de novas estratégias terapêuticas mais eficazes torna-se essencial.

O reposicionamento de fármacos surgiu em oncologia como uma estratégia para identificar propriedades anti-tumorais em medicamentos já aprovados ou em investigação para o tratamento de outras doenças. Este método permite o desenvolvimento de novas opções terapêuticas de uma forma mais rápida e economicamente rentável. Recentemente, a Pirfenidona (PF) – fármaco anti-fibrótico aprovado para o tratamento da fibrose idiopática pulmonar – demonstrou potencial anti-tumoral em diferentes tipos de cancro ao interferir com a proliferação e disseminação celular. Além disso, o efeito sensibilizante da PF ao tratamento com alguns agentes anti-tumorais foi também descrito. Resultados preliminares obtidos por outra estudante de Mestrado do nosso grupo de investigação demonstraram que a PF sensibiliza a linha celular de NSCLC NCI-H460 para o tratamento com Vinorelbina (VR).

O objetivo principal desta dissertação foi estudar o efeito sensibilizador da PF para o tratamento com fármacos quimioterápicos atualmente utilizados na prática clínica, em várias linhas celulares de NSCLC. O nosso objetivo a longo prazo consiste em verificar a possibilidade de reposicionar a PF para o tratamento de NSCLC.

Para atingir este objetivo, três linhas celulares de NSCLC (A549, NCI-H322 e NCI-H460) foram utilizadas para avaliar o efeito de PF em combinação com Etoposídeo, Gemcitabina, VR ou Paclitaxel (PAC) no crescimento celular, utilizando o ensaio de sulforrodamina B (SRB). Os tratamentos combinados que mostraram vantagem estatisticamente significativa em termos de inibição do crescimento celular sobre o tratamento com cada um dos fármacos individualmente foram avaliados para o seu efeito

sobre: 1) a viabilidade celular (com o ensaio de exclusão de azul de tripano), 2) o perfil do ciclo celular (por análise de citometria de fluxo após marcação com iodeto de propídeo), 3) a proliferação celular (com o ensaio de incorporação de bromodeoxiuridina), e 4) a morte celular (por análise de citometria de fluxo após marcação com Anexina V-FITC/PI). Para além disso, o efeito do tratamento combinado de VR e Carboplatina (CBP), atualmente usado na prática clínica, com a PF no crescimento celular das três linhas celulares de NSCLC foi também analisado. Finalmente, o efeito dos tratamentos combinados no crescimento de linhas celulares não-tumorigénicas (MCF-10A e MCF-12A) foi também avaliado, recorrendo ao ensaio de SRB.

Os nossos resultados demonstraram que a PF sensibiliza as linhas celulares de adenocarcinoma pulmonar A549 e NCI-H322 para o tratamento com VR, causando uma redução significativa na % de células viáveis e de proliferação celular e um aumento na % de morte celular. Assim, os nossos resultados validaram em duas linhas celulares adicionais de NSCLC os resultados preliminares anteriormente descritos pelo nosso grupo de investigação. Para além disso, a PF também sensibilizou as três linhas celulares de NSCLC em estudo para o efeito combinado de VR com CBP, levando a um aumento estatisticamente significativo na % de inibição do crescimento celular. Adicionalmente, os nossos dados também revelaram que a PF sensibiliza a linha celular NCI-H460 para o tratamento com PAC, causando uma redução estatisticamente significativa no crescimento e viabilidade celular, alterações no perfil de ciclo celular e um aumento na % de morte celular. É importante realçar que nenhuma destas combinações de fármacos aumentou a citotoxicidade de células não-tumorigénicas quando comparadas com os tratamentos individuais com fármacos quimioterápicos correspondentes.

Trabalho futuro irá validar o tratamento combinado de PF com VR e CBP, utilizando modelos xenografos de linhas celulares de NSCLC.

Palavras-Chave: Cancro do Pulmão de Não-Pequenas Células; Reposicionamento de Fármacos; Pirfenidona; Vinorelbina; Paclitaxel; Carboplatina.

List of Abbreviations

A

Akt	Protein Kinase B
ALK	Anaplastic Lymphoma Kinase
ATCC	American Type Culture Collection

B

BRAF	Raf Murine Sarcoma Viral Oncogene Homolog B1
BrdU	5-Bromo-2'-Deoxyuridine
BSA	Bovine Serum Albumin

C

C	Cysteine
CAF	Cancer-Associated Fibroblast
CBP	Carboplatin
CCGen	Cell Culture and Genotyping
ChT	Chemotherapy
CTLA-4	Cytotoxic T-Lymphocyte Antigen-4

D

DAPI	4′,6-Diamidino-2-Phenylindole
DMEM	Dulbecco's Modified Eagle Medium

E

E	Glutamate
ECACC	European Collection of Authenticated Cell Cultures
EGFR	Epidermal Growth Factor Receptor
EMA	European Medicines Agency
ERK	Extracellular Signal-Regulated Kinase
ETP	Etoposide

F

FBS	Fetal Bovine Serum

FDA	Food and Drug Administration

G

G	Glycine
GI_{50}	50% Cell Growth Inhibition Concentration

H

HER2	Human Epidermal Growth Factor Receptor 2
HS	Horse Serum

I

IARC	International Agency for Research on Cancer
ILK	Integrin-Linked Kinase

K

KRAS	Kirsten Rat Sarcoma Viral Oncogene Homologue

L

LCa	Lung Cancer

M

M	Methionine
MET	Mesenchymal Epithelial Transition Factor

N

NGS	Next Generation Sequencing
NSAID	Non-Steroidal Anti-Inflammatory Drug
NSCLC	Non-Small Cell Lung Cancer

P

PAC	Paclitaxel
PBS	Phosphate-Buffered Saline
PD-1	Programmed Death-1
PF	Pirfenidone

PFA	Paraformaldehyde
PI	Propidium Iodide
PI3KCA	Phosphatidylinositol-4,5-Bisphosphate 3-Kinase Catalytic Subunit α
PS	Performance Status

R

RB1	Retinoblastoma 1
ROS1	ROS Proto-Oncogene 1
RPMI	Roswell Park Memorial Institute

S

SCLC	Small Cell Lung Cancer
SMAD	Mothers Against Decapentaplegic Homolog
SRB	Sulforhodamine B
STK11	Serine/Threonine Kinase 11

T

T	Threonine
TCA	Trichloroacetic Acid
TGF	Transforming Growth Factor
TP53	Cellular Tumor Antigen p53
TTF-1	Transcription Factor 1
TKI	Tyrosine Kinase Inhibitor

V

V	Valine
VEGF	Vascular Endothelial Growth Factor
VR	Vinorelbine

W

WHO	World Health Organization
Wnt	Wingless/Integrated

Table of Contents

Index of Figures

Index of Tables

Chapter

1 Introduction

1.1. Lung Cancer

1.1.1. Epidemiology and Etiology

Lung cancer (LCa) is the second most commonly diagnosed cancer and the leading cause of cancer-related deaths worldwide. In 2020, LCa was estimated to be responsible for 11.4% of all diagnosed malignancies and 18% of cancer-associated deaths, meaning that the mortality rate of this type of cancer exceeds the one registered for colorectal and liver cancers together (**Figure 1**) [1]. Importantly, according to the International Agency for Research on Cancer (IARC), LCa mortality rate is expected to increase up to ~ 60% by 2040, which is partially associated with a rise in worldwide tobacco use [2, 3].

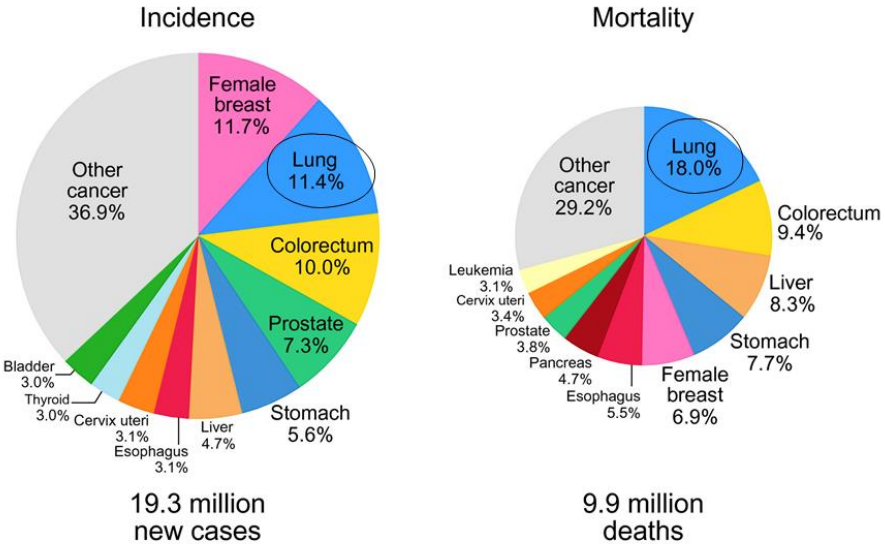

Figure 1 – Estimated 2020 worldwide cancer incidence and mortality rates for both genders. Source: GLOBOCAN. Adapted from [1] and [4].

Interestingly, LCa incidence and mortality rates present a heterogeneous distribution across the globe. LCa rates tend to be higher in developed regions, particularly in Europe and Northern America, when compared to the ones observed for underdeveloped countries, for instance in Africa or South America [1, 4]. However, due to an increase in tobacco use

together with a limited smoking regulation in less developed areas, this tendency is shifting [5].

Concerning gender, LCa mortality and incidence rates are about twice as high in men as in women [1, 4]. Nonetheless, a study by G. Cariolli *et al.* demonstrated that LCa rates in the European Union declined 9.2% in men and increased 6.0% in women within 2015 and 2020, moving in the opposite direction of what is the current reality [6].

As many other oncological diseases, LCa rates show an increase in older age groups for both genders [1]. Furthermore, despite the efforts that have been made in the development of new early-detection techniques, one of the key factors behind LCa high mortality rates is the fact that roughly 57% of patients are diagnosed at a locally-advanced or metastatic stage of the disease, with a 5-year survival rate of only 5% [7, 8].

The major environmental factor associated with the development of LCa is tobacco smoke. In fact, only 10-25% of all diagnosed LCa cases correspond to people who never smoked. However, other environmental factors such as passive smoking and exposure to asbestos, radon or air pollution have also been described as important drivers of LCa carcinogenesis [5, 9].

Similarly to other oncological disorders, genetic susceptibility is also a key factor to consider, particularly in younger age groups [10].

1.1.2. Classification

LCa comprises a heterogeneous group of diseases that can be classified into two major histologic types: small cell lung cancer (SCLC) and non-small cell lung cancer (NSCLC) [11].

1.1.2.1. Small Cell Lung Cancer (SCLC)

Accounting for approximately 15% of LCa cases, SCLC is a neuroendocrine carcinoma pointed out as an aggressive, high-proliferative, and highly metastatic disease [12]. In fact, nearly 60% of patients have advanced metastatic disease, which dictates the extremely poor prognosis that characterizes this disease [13]. Chemotherapy plays a major role in the treatment of this histologic type, which frequently presents as a centrally positioned tumor with lymph node involvement [12, 14].

A strong association with cigarette smoking has been found for this type of malignancy, with only 2% of the cases being diagnosed in people who never smoked. The inactivating mutations in the retinoblastoma 1 (*RB1*) and cellular tumor antigen p53 (*TP53*)

tumor suppressor genes are also linked with SCLC carcinogenesis [12]. Importantly, the subtype SCLC exhibits an increase in telomerase activity [14].

1.1.2.2. Non-Small Cell Lung Cancer (NSCLC)

NSCLC is responsible for 85% of LCa cases with a 5-year survival rate of 15.9%. Histologically, NSCLC can be divided into three major subtypes – adenocarcinoma (40%), squamous cell carcinoma (25-30%) and large cell carcinoma (5-10%) – highlighting the marked heterogeneity that characterizes this disease (**Figure 2**) [3, 11, 15].

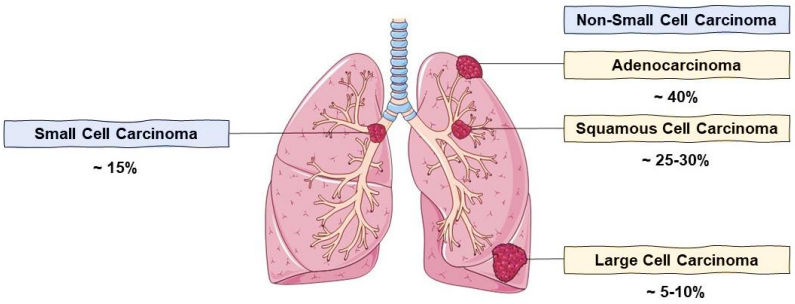

Figure 2 – The most common anatomical location of the four major histological types of LCa and their respective prevalence. Created with Servier Medical Art (smart.servier.com).

For the last decades, an epidemiological switch from a squamous to an adenocarcinoma histology has been observed, making adenocarcinoma the most frequently diagnosed subtype, particularly in people who never smoked [5]. Adenocarcinoma is a malignant epithelial tumor with glandular histological features that tends to develop in the peripheral airways. Positive stains for the transcription factor 1 (TTF-1) and keratin 7 are critical for adenocarcinoma histopathological identification [15]. Depending on the amount of invasiveness, the World Health Organization (WHO) classifies adenocarcinoma into three main categories: adenocarcinoma *in situ*, minimally invasive adenocarcinoma, and invasive adenocarcinoma. These histological patterns can be found in the same patient [16].

Squamous cell carcinoma is the second most commonly diagnosed subtype, accounting for approximately 40% of NSCLC cases. This type of malignancy tends to develop in central airways, presenting a pseudostratified columnar epithelium, and is strongly associated with tobacco use [5, 15]. Keratinization is one of the most noticeable characteristics of squamous cell carcinoma, but it is not always present. Therefore, in the absence of clear keratinization, immunohistochemical detection of squamous biomarkers, such as p40 or p63, becomes essential [16].

The NSCLC subtype with lower representation is the large cell carcinoma, which is characterized to be poorly differentiated and to lack any small, glandular, or squamous cell

histological features [15]. The diagnosis of this type of malignancy is based on the morphological and immunohistochemical exclusion of the previously referred subtypes. In fact, as a result of an improved ability to detect poorly differentiated adenocarcinomas and squamous cell carcinomas, large cell carcinoma incidence rates have been suffering a reduction [3, 16]. Nonetheless, even in its early stages, an accurate diagnosis is critical as it is an aggressive disease with rapid growth and dissemination [17].

1.1.3. Diagnosis and Staging

LCa diagnosis and staging are often performed simultaneously and are of great importance since the applied therapeutic strategy will often rely on them. The most commonly reported symptoms associated with this oncological disease include cough, chest pain, hemoptysis, weight loss and dyspnea [5]. However, these symptoms can be confounded with those of other respiratory diseases, leading to a delay in diagnosis.

Depending on the tumor stage, diagnosis methodologies may include less invasive imaging approaches, such as computerized tomography, positron emission tomography, magnetic resonance imaging, transesophageal ultrasonography, or endobronchial ultrasound. Nevertheless, for a complete diagnosis, cytological, histological, and molecular analysis recurring to invasive methods, such as surgical open biopsy or needle biopsy, are required [5, 18].

LCa staging is based on the TNM staging system, in which the T stands for tumor size and burden, the N for lymph node involvement, and the M for the existence of distant metastases. Each of these criteria uses a numeric scale to represent the severity of the disease, which increases with the number. The combination of them allows the categorization of LCa into four stages (I-IV) with a successively increase in malignancy degree [19].

1.1.4. Treatment Options

LCa comprises a heterogeneous group of diseases, thus presenting distinct treatment options based on stage, histology, molecular profile, and patient performance status [5]. Regardless of the histological type, therapeutic options in LCa include surgery, radiotherapy, chemotherapy, immunotherapy, and molecularly targeted therapy [14].

Platinum-based chemotherapy, particularly the combined treatment of cisplatin/carboplatin with etoposide, is considered the gold standard treatment for SCLC, as most of the patients present an unresectable tumor at the time of diagnosis [12]. For this particular histologic type, radiotherapy can also be implemented either alone or in combination with chemotherapy in both neo-adjuvant and palliative settings [20].

Surgery is considered the standard approach for patients with early-stage (I, II or IIIA) NSCLC who are fit enough [5]. Lobectomy is the most commonly applied surgery in clinical practice, even though segmentectomy is raising interest due to its association with a better preservation of the pulmonary function [21]. Nevertheless, a recent meta-analysis did not find statistically significant differences in the overall survival of patients undergoing lobectomy or segmentectomy [22]. Despite that, as previously stated, the vast majority of patients is diagnosed with advanced-stage disease and, therefore, unable to undergo tumor resection.

For patients with early-stage NSCLC who are medically unfit or refuse surgery, radiofrequency ablation therapy can be used to reduce tumor burden [23]. Radiotherapy is also recommended together with chemotherapy for the treatment of unresectable stage III NSCLC, and is widely used as a palliative measure, allowing patients' quality of life to be improved through the control of specific symptoms [14].

Over the past decades, chemotherapy has been applied for the treatment of NSCLC, either alone or in combination with other therapeutic modalities. Adjuvant platinum-based chemotherapy, including therapeutic duplets consisting of Cisplatin or Carboplatin with Paclitaxel, Gemcitabine or Vinorelbine, is recommended for patients with resectable stage II/III NSCLC, improving the overall survival rate [5, 28]. Depending on patients' performance status, single or combined chemotherapy regimens are also being used for the treatment of locally-advanced or advanced NSCLC [14]. Particularly, tubulin inhibitors (*e.g.* Paclitaxel or Vinorelbine) have been used and efforts are being made to improve their antitumoral potential [27].

Table 1 – Mechanism of action of some cytotoxic agents used for the treatment of NSCLC.

Drug	Family	Mechanism of Action
Carboplatin	Alkylate	Inhibition of DNA replication [24]
Etoposide	Topoisomerase II Inhibitor	Inhibition of DNA synthesis [25]
Gemcitabine	Nucleoside Analog	Inhibition of DNA synthesis [26]
Paclitaxel	Taxane	Inhibition of microtubule depolymerization [27]
Vinorelbine	Vinka-alkaloid	Inhibition of microtubule polymerization [27]

The treatment of patients with advanced NSCLC is becoming increasingly customized, taking into account the molecular profile of the disease. For the last couple of years, several targetable alterations have been associated with LCa carcinogenesis, particularly with lung adenocarcinoma, such as gene rearrangements, proto-oncogene amplification or activating mutations, as well as tumor suppressor gene inactivation [29]. Thus, efforts are being undertaken to develop novel targeted therapies for those described alterations [30].

Epidermal growth factor receptor (*EGFR*) mutations occur in 10-50% of NSCLC cases, being the molecular alterations for which most targeted therapies are approved [30]. Indeed, three generations of EGFR-tyrosine kinase inhibitors (TKIs) are currently applied in the clinical practice. First-generation TKIs (including Gefitinib and Erlotinib) act by reversely preventing EGFR autophosphorylation, while second-generation TKIs (such as Afatinib) covalently bind to EGFR [31, 32]. On the other hand, the approved third-generation TKI (Osimertinib) targets both EGFR-sensitizing mutations and the T790M mutation, which is known to be a driver of EGFR-TKIs resistance [33].

Kirsten rat sarcoma viral oncogene homologue (*KRAS*) mutations are present in approximately 25% of NSCLC adenocarcinoma cases and are generally mutually exclusive of *EGFR* and human epidermal growth factor receptor 2 (*HER2*) alterations [33]. Therapeutic options for patients carrying alterations in this proto-oncogene are limited since they are often associated with poor responses to EGFR-TKIs and chemotherapy [11]. Nevertheless, this may be changing as the United States Food and Drug Administration (FDA) has recently approved Sotorasib as the first therapy targeting *KRAS* G12C mutation [34]. Furthermore, patients harboring *KRAS* alterations have been associated with higher levels of programmed-death-1 (PD-1) expression and therefore, better responses to immunotherapy [35].

A smaller proportion of NSCLC patients carries alterations in anaplastic lymphoma kinase (*ALK*), ROS proto-oncogene 1 (*ROS1*) or mesenchymal epithelial transition factor (*MET)* genes [36]. These alterations can be targeted using Crizotinib [33]. Raf murine sarcoma viral oncogene homolog B1 (*BRAF*) mutations also play a role in LCa carcinogenesis, accounting for 0-3% of all LCa cases. The most common *BRAF* mutation in LCa is *BRAF* V600E, which is associated with a poor prognosis. The treatment with anti-BRAF inhibitors, such as Vemurafenib, Dabrafenib, Trametinib and Encorafenib is currently applied in clinical settings [37].

Immunotherapy has emerged as one of the most promising therapeutic strategies in oncology. The immune checkpoint inhibitors targeting PD-1 (*e.g.* Nivolumab,

Pembrolizumab or Atezolizumab) or the cytotoxic T-lymphocyte antigen-4 (CTLA-4) (*e.g.* Ipilimumab) pathways have been widely studied in NSCLC [38, 39]. Nowadays, immunotherapy alone or in combination with other therapeutic approaches is considered the standard of care for patients with advanced NSCLC without targetable alterations [36, 40].

Targeting the anti-angiogenic pathways is also considered in NSCLC treatment, as a reduction in tumor surroundings' irrigation may slow down tumor growth and dissemination [41]. The monoclonal antibody targeting the vascular endothelial growth factor (VEGF), Bevacizumab, is approved for the treatment of advanced NSCLC when in association with platinum-based chemotherapy [42].

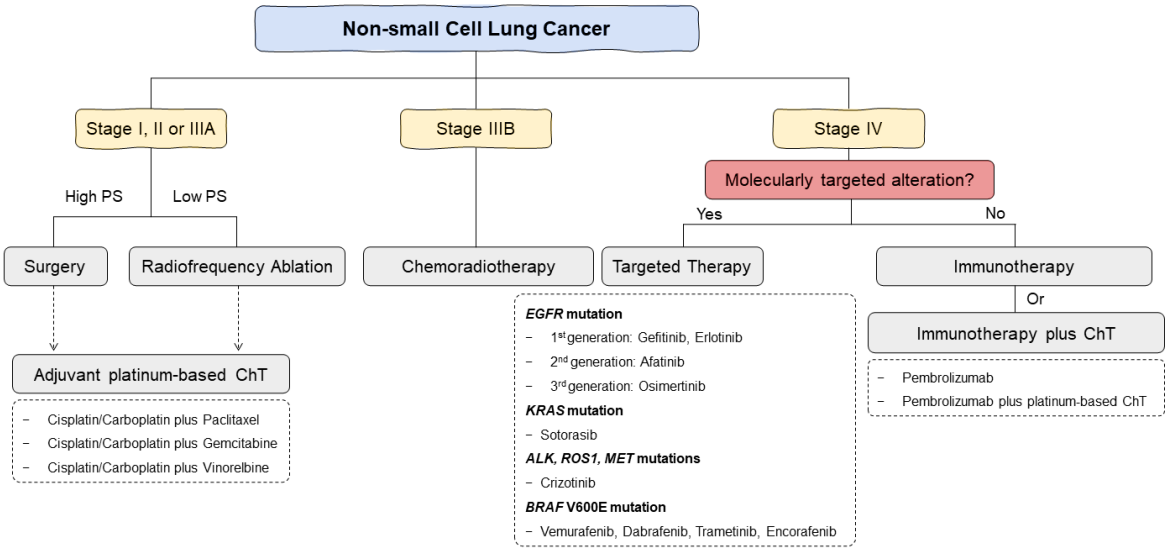

Figure 3 – Summary of the current therapeutic approaches available for the treatment of non-small cell lung cancer (NSCLC). ChT, Chemotherapy; PS, Performance Status.

1.1.5. Therapeutic Challenges

Despite recent breakthroughs in LCa management, particularly with the introduction of immune- and targeted therapies, this disease remains associated with a poor prognosis owing to its metastatic potential and ultimate development of drug resistance [43, 44].

Surgery is the only therapeutic approach with curative potential, providing a 5-year survival rate of 77% for patients with stage I NSCLC [45]. However, due to the presence of undetectable micro-metastases or to the spread of cancer cells during surgery, 30-50% of these patients end up suffering tumor recurrence and disease-related death [46]. Cancer cells can spread through different mechanisms, including their entrance into the blood and lymphatic routes [43]. Targeting these mechanisms is a challenge that must be addressed.

Regardless of the encouraging results obtained from targeted therapy, a significant number of patients will inevitably relapse. In fact, during targeted therapy, secondary mutations, activation of alternative signaling pathways and downstream modifications can eventually occur, leading to drug resistance [44]. Several secondary mutations have been identified after treatment with first- and second-generation of EGFR-TKIs. The *EGFR* T790M mutation is the most frequently recognized secondary mutation, for which the third-generation Osimertinib was established. Nonetheless, tertiary mutations are already being identified in response to third-generation TKIs and there is an urgent need for the development of novel drugs [47].

Immunotherapy allows patients who failed to be treated with targeted therapies to extend their lives. However, due to secondary genetic alterations and/or tumor microenvironment modifications, around 40-50% of patients can suffer rapid progression following the first cycles of immunotherapy [48]. The processes underlying immunotherapy resistance are still not fully understood, making its study imperative.

Regardless the efforts to make cancer treatment more personalized, chemotherapy still plays a significant role in NSCLC treatment. Nevertheless, as happen with other therapeutic modalities, several intrinsic and acquired chemoresistance mechanisms have been described in NSCLC, including epigenetic alterations, induction of drug efflux pumps, overexpression of integrin-linked kinase (ILK) and deregulation of DNA repair mechanisms and microRNAs [49].

Importantly, LCa is surrounded by a highly fibrotic stroma being considered a desmoplastic tumor [50]. In this situation, drug delivery to the tumor is hampered by this physical obstacle, resulting in diminished therapeutic efficacy and in the development of chemoresistance [51]. Therefore, alternative therapies that take into account the tumor microenvironment, more precisely the fibrotic profile, are required.

Taken together, despite recent advances, LCa remains a disease with significant epidemiological implications and the development of new diagnostic tools and therapeutic approaches is of great interest.

1.2. Drug Repurposing: A Milestone in Drug Discovery

De novo drug discovery and development is an extremely time-consuming, expensive, and uncertain process, associated with a high degree of failure. In fact, a new drug takes 10 to 17 years to enter into the market, and only one out of five drugs that follow clinical trial ends up being approved [52-54].

Due to the intention to overcome the drawbacks associated with traditional drug discovery process, Ashburn and Thor in 2004 introduced the concept of drug repurposing as a strategy to identify therapeutic applications for drugs already approved or under investigation that are not related to their original medical indication [54, 55]. This approach is established over two fundamental ideas: a) distinct diseases can interfere with similar biological pathways and b) the pleiotropic effects of a drug can be effective against other diseases [56]. The application of these premises through drug repurposing involves distinct stages, including 1) the selection of the candidate drug, 2) the mechanistic evaluation of the drug in pre-clinical models (*in vitro* and *in vivo* studies) and 3) the efficacy validation in clinical trials [57]. The identification of the specific candidate drug is the most critical step in this process and can be accomplished through computational and experimental approaches (**Figure 4**) [57, 58].

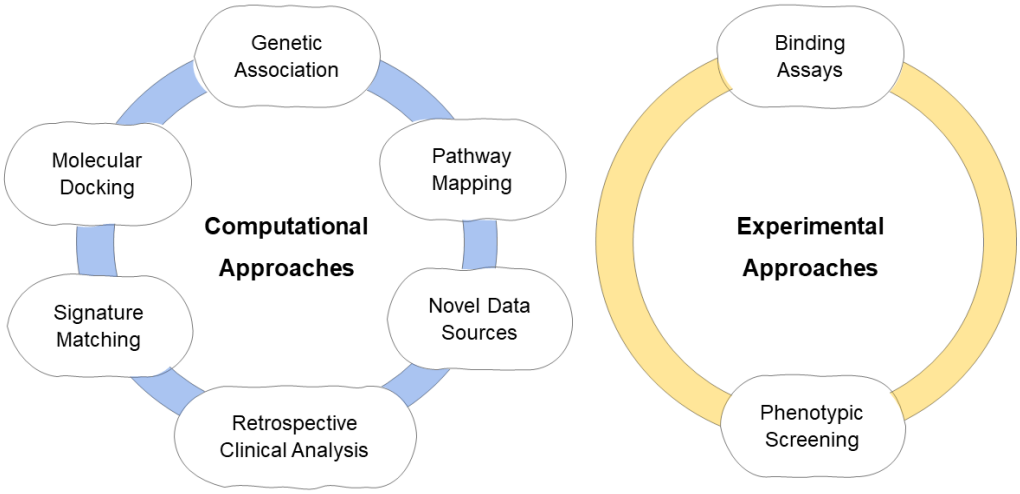

Figure 4 – Methodologies used to identify candidate drugs for drug repurposing. Computational and experimental approaches can be implemented individually or in association to detect novel drug-disease relationships. Adapted from [57].

There are several aspects to take into consideration when comparing drug repurposing with conventional drug discovery and development that are associated with time, costs and safety profiles. Indeed, drug repurposing enables a reduction of 5 to 7 years in the average time required for drug approval and a decrease of roughly 85-90% in the associated costs [52, 59]. These differences arise from the fact that drug repurposing avoids most of the steps associated with initial pharmacological development, which are related with safety, toxicity, pharmacokinetics and pharmacodynamics studies (**Figure 5**) [57, 60].

In oncology, drug repurposing emerged as a tool for the identification of both anti-tumor and palliative properties in drugs approved or under study for the treatment of other diseases, providing patients with new therapeutic alternatives [61]. Furthermore, for the last

couple of years has been an increase in oncology treatment associated prices, and the idea of repurposing generic drugs for cancer treatment could represent a way to make it more affordable to patients from all socioeconomic backgrounds [62]. Nonetheless, despite all the advantages associated with this approach, there are still some difficulties concerning repurposed drug's intellectual property and clinical application. In fact, as most of these drugs are already approved for the treatment of other diseases, acquiring a patent registration becomes a challenge. Moreover, due to the lower incomes associated with repurposed drugs, pharmaceutical companies have no interest in supporting or advertising them, resulting in limited funding opportunities for this area of study [63].

Interestingly, several studies have demonstrated the possibility of repurposing statins, non-steroidal anti-inflammatory drugs (NSAIDs), β-blockers and anti-fungal agents for the treatment of NSCLC [64]. These agents have been tested either alone or in combination with other therapeutic approaches that are already used in the clinical practice. In fact, most of the repurposed drugs are investigated in combinational regimens allowing the decrease of the conventional chemotherapeutic drug concentration, thus reducing drug-related toxicity and the risk of drug resistance [65].

Taken together, drug repurposing emerged as a promising strategy to be applied in drug discovery, and may be a process to consider in the search of new drugs for the treatment of oncological disorders, which are in need for rapid and cost-effective drug development. However, overcoming patent and regulatory constraints, as well as increasing funding for this field of research are crucial [57].

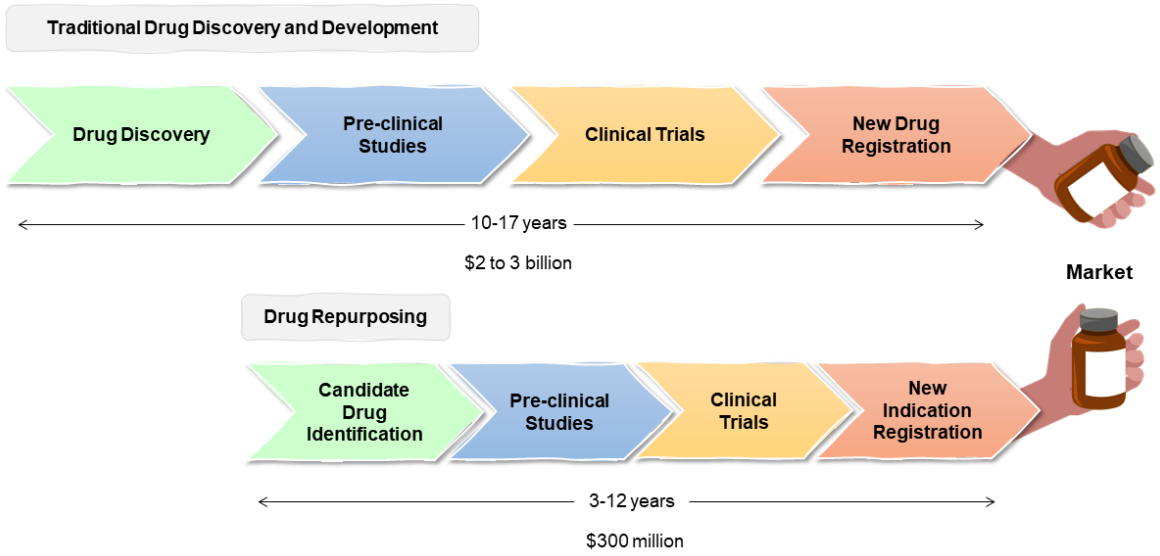

Figure 5 – Comparison between drug repurposing and traditional drug discovery and development processes.

1.3. Pirfenidone: A Potential Candidate Drug for Drug Repurposing

Pirfenidone (PF) is an anti-fibrotic, anti-inflammatory and anti-oxidant drug approved by the FDA and the European Medicines Agency (EMA) for the treatment of Idiopathic Pulmonary Fibrosis [66, 67].

In the last couple of years, PF has been demonstrating anti-tumor potential against different types of cancer. Indeed, research conducted by Zou W. J. *et al.* (2017) demonstrated that PF caused a reduction in proliferation and an increase in programmed cell death of hepatocellular carcinoma cells through the Wnt/β-catenin pathway. They observed that PF induced a reduction in β-catenin and phosphorylated-β-catenin that was reverted following treatment with a β-catenin activator [68]. Likewise, Li C. *et al.* (2018) showed that PF reduced proliferation of mesothelioma cells through the ERK/Akt signaling pathway and caused a reduction in the expression of extracellular matrix associated genes *in vivo* [69]. Furthermore, another study revealed PF ability to downregulate the transforming growth factor (TGF)-β expression in malignant glioma cells [70].

More recently, in 2019, Ishii K. *et al.* demonstrated that PF suppresses prostate cancer cell lines' proliferation through G0/G1 cell cycle arrest, whereas Usugi E. *et al.* (2019) showed the same effect on pancreatic cancer cell lines. In both studies, after treatment with PF, the percentage of cells in G0/G1 stages of the cell cycle increased whereas the number of cells in S/G2 phases decreased. Furthermore, both studies revealed that PF increased p21 expression, which corroborated with the cell cycle arrest on the G0/G1 phases [71, 72].

Interestingly, the effect of PF in the tumor microenvironment has also been described. Kozono *et al.* (2013), using *in vitro* and *in vivo* models, demonstrated that PF reduces pancreatic cancer associated desmoplasia through a reduction on the proliferation and dissemination of pancreatic stellate cells [73]. Moreover, another study used a microfluidic cell culture device to demonstrate that PF reduces migration of both cancer-associated fibroblasts (CAFs) and breast cancer cells. They also observed a reduction in CAFs' immunosuppressive properties over breast cancer cells [74].

Concerning studies involving PF on NSCLC, Marwitz *et al.* (2019) showed that PF reduces cancer cell proliferation, decreases the expression of proliferation specific markers and induces G0/G1 cell cycle arrest. Furthermore, PF downregulated SMAD, TGF-β and Survivin expression levels, as well as reduced cell migration in NSCLC cells. Interestingly, PF also showed to increase immune cells tumor infiltration *in vivo* [75]. Moreover, some studies revealed that PF interferes with the epithelial-to-mesenchymal transition (EMT) in NSCLC, using *in vitro* and *in vivo* models [76, 77]. Additionally, more recently (in 2020) PF showed to inhibit NSCLC cell motility through the urokinase system [78].

The role of PF in combination with other therapeutic modalities has also been explored in oncology settings. In fact, PF increased Gemcitabine ability to suppress tumor growth and dissemination in an *in vivo* pancreatic cancer model [73]. Choi S. *et al.* (2015) also demonstrated that PF sensitizes radio-resistant Lewis lung carcinoma tumors to the combination of radiotherapy with Sunitinib, through a reduction of the TGF-β-induced collagen deposition [79]. Interestingly, a study by Polydorou *et al.* (2017) pointed out the potential effect of PF in enhancing drug delivery to desmoplastic tumors. These authors demonstrated that PF increases the sensitivity to Doxorubicin treatment by reducing the expression of several extracellular matrix components, using two orthotopic breast cancer models [80].

Regarding NSCLC, Mediavilla-Varela *et al.* (2016) revealed that the combined treatment of PF with Cisplatin was effective against NSCLC and its associated fibroblasts, in both *in vitro* and *in vivo* models. In particular, these authors verified that this combined treatment induced programmed cell death in CAFs and NSCLC cells *in vitro*, which was then validated *in vivo* by showing a decrease in tumor growth after treatment with the mentioned combined treatment in the presence of CAFs [81]. Recently, Qin W. *et al.* (2020) demonstrated that PF enhanced the anti-tumor immunogenicity when combined with an anti-PD-L1 antibody, in an *in vivo* NSCLC model [82].

Additionally, preliminary results obtained by another Master (MSc) student from our research group demonstrated that PF increased the sensitivity of the NSCLC NCI-H460 cell line to Vinorelbine treatment (currently used in the clinical practice for patients with advanced NSCLC) [83]. In particular, these results revealed that this drug combination reduced NCI-H460 cell growth, viability and proliferation. Furthermore, this drug combination caused a slight alteration in the cell cycle profile with an increase in the % of cells in the sub-G1 phase of the cell cycle, suggestive of apoptosis.

In summary, as demonstrated in all these reported studies, PF has been shown to be active against several of the cancer hallmarks described by Hanahan and Weinberg in 2011 (**Figure 6**) [84]. For instance, PF has the ability to 1) induce cancer cell death, 2) suppress tumor cell proliferation by interfering with the cell cycle profile or specific signal transduction pathways, 3) increase immune cell infiltration into the tumor by enhancing tumor response to PD-L1 blockades, and 4) inhibit tumor cell motility and migration through the EMT process.

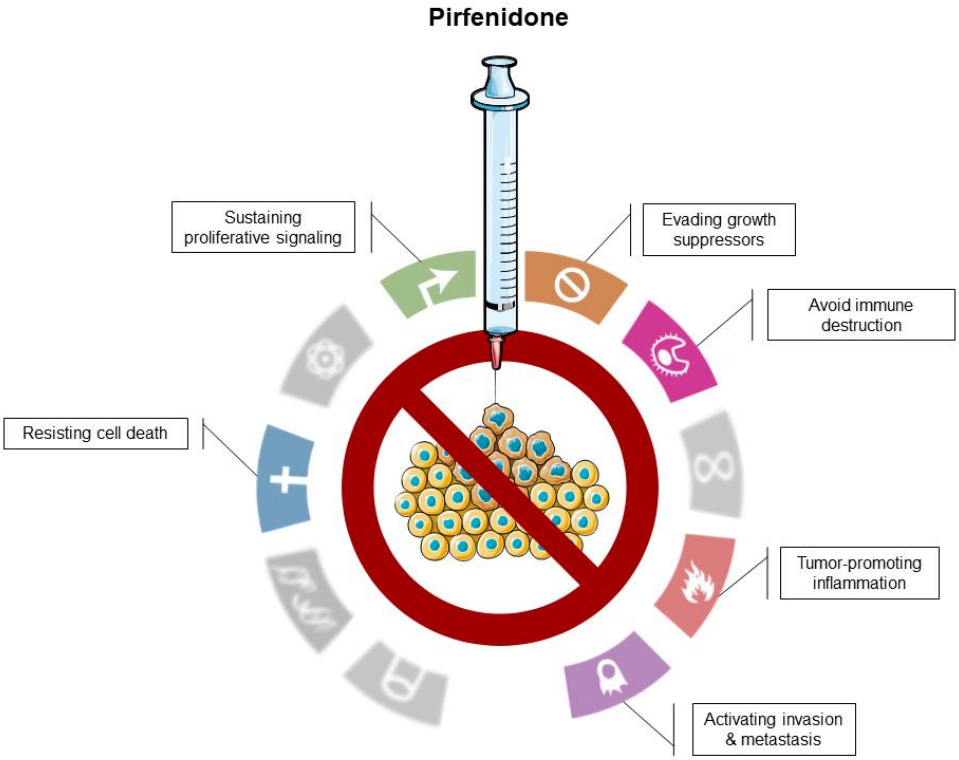

Figure 6 – Possible effects of Pirfenidone on the cancer hallmarks. Adapted from [84]. Created with Servier Medical Art (smart.servier.com).

One of the ideas of drug repurposing is that different diseases might act through similar biological processes. Interestingly, a correlation between biological pathways underlying LCa and Idiopathic Pulmonary Fibrosis has been suggested. In fact, these two diseases share a number of genetic and molecular processes, including genetic and epigenetic alterations, activation of particular signaling pathways, myofibroblasts persistent activation and aberrant expression of specific microRNAS [85, 86]. Remarkably, a retrospective study found that patients with Idiopathic Pulmonary Fibrosis treated with PF had a statistically significant lower incidence of LCa cases [87]. Moreover, Yamamoto Y. *et al.* (2020) suggested that the combined treatment of PF with carboplatin-based chemotherapy or immunotherapy is potentially safe as none of the patients with both Idiopathic Pulmonary Fibrosis and LCa treated with PF developed acute Idiopathic Pulmonary Fibrosis exacerbations [88].

Taking all these studies into consideration, PF might be considered a drug with potential to be repositioned for the treatment of NSCLC, either alone or in combination with other therapeutic modalities.

Chapter

2 Aims

Taking into consideration the previously described preliminary data (MSc dissertation of Catarina Antunes – [83]), the main aim of this master dissertation was to evaluate the sensitizing effect of Pirfenidone to several chemotherapeutic drugs currently used in clinical practice, in various NSCLC cell lines.

Thus, specific aims of this project were to:

1) Confirm the preliminary results previously obtained by some of us, regarding the effect of the combined treatment of Pirfenidone with Vinorelbine in NCI-H460 cells, in two additional NSCLC cell lines (A549 and NCI-H322);

2) Evaluate the sensitizing effect of Pirfenidone to other chemotherapeutic drugs also used in clinical practice, namely Etoposide, Gemcitabine and Paclitaxel, in three NSCLC cell lines (A549, NCI-H322 and NCI-H460);

The effect of the combined drug treatments were evaluated on: a) cell growth (measured by the Sulforhodamine B assay), b) cell viability (assessed by the Trypan Blue exclusion assay), c) cell proliferation (measured by the Bromodeoxyuridine incorporation assay), d) cell cycle profile (assessed by Flow cytometry following propidium iodide staining) and e) cell death (assessed by flow cytometry following Annexin V-FITC/PI staining).

3) Study the sensitizing effect of Pirfenidone to the treatment with the duplet consisting of Carboplatin with Vinorelbine (currently used in the clinical practice for patients with advanced NSCLC or as a neo-adjuvant measure) in the three NSCLC cell lines, using the SRB assay;

4) Evaluate the cytotoxic effect of the most promising drug combinations in two non-tumorigenic cell lines (MCF-10A and MCF-12A), using the SRB assay.

Chapter

Material and Methods 3

3.1. Cell Culture

In order to achieve the previously outlined aims, three epithelial NSCLC cell lines, A549, NCI-H322 and NCI-H460, and two epithelial non-tumorigenic cell lines, MCF-10A and MCF-12A, were included in this study (**Table 2**). The human NSCLC cell lines, A549 and NCI-H460, and the non-tumorigenic cell lines were purchased from the American Type Culture Collection (ATCC), whereas the NSCLC cell line NCI-H322 was acquired from the European Collection of Authenticated Cell Cultures (ECACC).

Table 2 – Relevant characteristics of the cell lines included in this study.

Cell Line	Tissue	Disease	Subtype	Known Mutational Status
A549	Lung	NSCLC	Adenocarcinoma	*KRAS, STK11* and *TP53*
NCI-H322	Lung	NSCLC	Adenocarcinoma	*TP53*
NCI-H460	Lung	NSCLC	Large Cell Carcinoma	*KRAS, PIK3CA, STK11* and *TP53*
MCF-10A	Breast	Fibrocystic Disease (Non-tumorigenic)	-	-
MCF-12A	Breast	Fibrocystic Disease (Non-tumorigenic)	-	-

-, non-applicable.

The A549 cell line was maintained in Dulbecco's Modified Eagle Medium (DMEM) supplemented with 4.5 g/L Glucose with UltraGlutamine™ w/ sodium pyruvate (Lonza, BE12-604F), enriched with 10% fetal bovine serum (FBS; Biowest, S181H-500). The NCI-

H322 and NCI-H460 cell lines were maintained in Roswell Park Memorial Institute (RPMI) 1640 medium supplemented with Ultraglutamine™ and 25 mM HEPES (Lonza, BE12-115F/U1), complemented with 10% FBS. The non-tumorigenic MCF-10A and MCF-12A cell lines were cultured in DMEM/F12 (Thermo Fischer Scientific, 11320033), supplemented with 5% inactivated Horse Serum (HS; Biowest, S0910), 0.5 mg/mL of hydrocortisone (Merck Life Science, H0888), 20 ng/mL of human epidermal growth factor (R&D systems, 236EG), 10 mg/mL of insulin (Merck Life Science, I9278), 100 ng/mL of cholera toxin (Merck Life Science, C8052), 100 units/mL penicillin and 100 mg/mL of streptomycin solution (100X, Corning, 30-002-CI). For the cell growth inhibition assay only (using the sulforhodamine B assay), cells were grown in medium supplemented with 5% FBS.

Cells were cultured in tissue culture flasks and maintained in a humidified chamber at 37 ºC and 5% CO_2. The cell number and viability were assessed with the trypan blue exclusion assay and all the experiments were carried out with cells at the exponential phase of growth and with more than 90% of viability.

To provide an appropriate maintenance of cells, the medium was changed on a regular basis. When 80% of confluence was reached, cells were washed with phosphate-buffered saline (PBS; P5493) and incubated for a short period with Gibco™ tripLE express (1x, Thermo Fischer Scientific, 12604021) to detach the cells from the flask surface (since all cell lines used in this study are adherent). Then, cells were resuspended with new culture medium and transferred to a new flask with new medium at the desired dilution.

Cells were routinely tested for mycoplasma at the Cell Culture and Genotyping (CCGen) Service of i3S, Porto, using the VenorGeM® Advance Mycoplasma Detection Kit (Minerva Biolabs) and genotyped at the Genomics Core Facility of i3S, Porto, using the PowerPlex® 16 HS System.

3.2. Cell Plating

For the subsequent assays, cells were plated in 6 or 96-well plates. For that, after trypsinization, the concentration of cells (cells/mL) in the initial cell suspension was calculated using the trypan blue exclusion assay. The cells were then plated at a previously determined optimal cell concentration (5.0×10^4 cells/mL) in a total volume of 2 mL/well or 100 µL/well for a 6 or 96-well plate, respectively.

3.3. Drug Treatments

Carboplatin (CBP, BP711), Etoposide (ETP, E1383), Gemcitabine (GEM, G6423), Paclitaxel (PAC, T7402), Vinorelbine (VR, Y0000463) and Pirfenidone (PF, Y0001769) were purchased from Merck Life Science. ETP, GEM and PAC were dissolved in dimethyl-

sulfoxide (DMSO; Merck Life Science, D2650) and CBP, VR and PF were dissolved in sterile Water for Molecular Biology (Merck Life Science, 95284). All drugs were stored at -20 ºC with the exception of CBP, which was stored at 4 ºC.

To determine the concentration of each drug that inhibits 50% of cell growth (GI_{50}), the NSCLC cell lines were treated with different conditions for 48 h: a) five serial dilutions of the tested drug; b) vehicle (at the higher concentration used to dilute the tested drugs); and c) medium alone (blank). The ranges of concentrations tested for each drug in each cancer cell line are presented in **Table 3**.

Table 3 – Range of concentrations (μM) tested for each drug in each cancer cell line.

		NSCLC Cell Line		
		A549	**NCI-H322**	**NCI-H460**
Drug Concentration Range (μM)	**CBP**	6.3 – 600.0	37.5 – 600.0	6.3 – 100.0
	ETP	0.6 – 10.0	-	0.2 – 2.5
	GEM	6.3×10^{-3} – 0.1	-	1.9×10^{-3} – 3.0×10^{-2}
	PAC	4×10^{-4} – 7×10^{-3}	6×10^{-4} – 10×10^{-3}	1.9×10^{-3} – 3.0×10^{-2}
	VR	6×10^{-4} – 20×10^{-3}	6×10^{-4} – 20×10^{-3}	-
	PF	313 – 5×10^{3}	313 – 5×10^{3}	-

-, non-applicable.

Concerning the effect of the combined drug treatments on the % of cell growth, the NSCLC cell line NCI-H460 was treated for 48 h with two different experimental designs: a) combined treatment of five serial dilutions of the determined GI_{50} concentration of ETP, GEM or PAC with the GI_{50} concentration of PF; or b) combined treatment of five serial dilutions of the GI_{50} concentration of PF with the GI_{50} concentration of ETP, GEM or PAC. The A549 cell line was treated with the combination of the GI_{50} concentration of ETP, GEM, PAC, or VR with the GI_{50} concentration of PF. The effects of the combined treatments proved to be advantageous, when compared to the treatment with each drug individually, for the A549 and NCI-H460 cell lines, were then validated in the NCI-H322 cell line. Moreover, in the last portion of the work, the three NSCLC cell lines under study were also treated with the combination consisting of the three drugs, VR, CBP and PF. The non-

tumorigenic MCF-10A and MCF-12A cell lines were treated with the most promising drug combinations. In all experimental designs, cells were also treated with vehicle at the highest concentration tested, as well as with medium alone (blank).

For the subsequent assays, cells were treated for 48 h with a) the individual concentration of each drug alone; b) the combined drug treatment; c) vehicle (at the higher concentration tested); and d) medium alone (blank).

3.4. Trypan Blue Exclusion Assay

The Trypan Blue Exclusion assay was carried out to: a) maintain cells at an appropriate density in the cell culture flasks; b) confirm the cell viability; and c) plate the same number of cells in each well for the drug treatments. This assay relies on the dye Trypan Blue, which penetrates into dead cells through their disrupted membrane, allowing to distinguish between alive (bright) and dead (blue) cells [89]. After drug treatments, cell suspensions were mixed with 0.2% (v/v) Trypan Blue dye (Sigma-Aldrich Aldrich, T8154), at a ratio of 1:1, and the cell number was counted using a Neubauer Chamber.

3.5. Sulforhodamine B (SRB) Assay

In order to determine the GI_{50} concentration of each drug individually (which causes 50% of cell growth inhibition) and to assess the effect of the combined drug treatments in the NSCLC cell lines, the sulforhodamine B (SRB) assay was performed. This assay measures the % of cell growth based on cellular protein content and relies on the ability of SRB – a bright-pink aminoxanthene dye – to bind stoichiometrically to the basic amino-acid residues of cells. As a result, the amount of dye taken from labeled cells is directly proportional to the cell mass, allowing an indirect determination of cell density based on the measurement of cellular protein content [90].

For this assay, cells were first plated in 96-well plates, as previously described, and further incubated for 24 h at 37 ºC. Then, cells were subjected to the desired drug treatment. After a 48 h incubation period, cells were fixed with 10% (w/v) ice-cold trichloroacetic acid (TCA; Merck Life Science, T0699) and left at 4 ºC for at least 1 h. Subsequently, cells were washed three times with distilled water and left to air-dry at room temperature. After staining the proteins with 0.4% (w/v) SRB (Merck Life Science, S9012) in 1 % (v/v) acetic acid (Merck Life Science, T0699) for 30 minutes, cells were washed three times with 1% (v/v) acetic acid to remove the unbound dye and left to air-dry at room temperature. The bound SRB was then solubilized with 10 mM Tris base solution in water (Merck Life Science, T6066) and absorbance was measured at 510 nm in a multi plate reader (Synergy™ Mx, Biotek Instruments Inc.), recurring to the Gen5™ software.

3.6. 5-Bromo-2'-deoxyuridine (BrdU) Incorporation Assay

The BrdU Incorporation Assay was used to verify the effect of the combined drug treatments on cell proliferation. This assay relies on the ability of BrdU, a thymidine analog, to incorporate into the DNA of cells during the synthetic phase of the cell cycle, meaning that it is incorporated into cells under proliferation [91].

For this assay, cells were first plated in 6-well plates and incubated for 24 h at 37 ºC. Approximately 4 h before cell collection, cells of each condition were incubated with BrdU (Merck Life Science, B5002) at a final concentration of 10 µM. After a 48 h incubation period with the desired drug treatments, the medium of which condition was collected. Then, cells were washed with PBS (also collected) and incubated with Gibco™ tripLE express for a short period. Afterwards, the trypsinized cells were resuspended with the previously referred medium plus PBS, allowing attached and floating cells to be collected.

After collection, cells were centrifuged for 5 minutes at 1200 rpm at room temperature. Then, the supernatant was discharged, and the cell pellet was resuspended in 1 mL of PBS. After a second centrifugation under the same conditions, cells were fixed with paraformaldehyde 4% (PFA; Merck Life Science, 1.04005) in PBS for 40 minutes. Then, cells were subjected to two sequential centrifugations under the same previously described conditions, resuspended in PBS and stored at 4 ºC.

After the cytospin preparation, cellular DNA denaturation was induced by treatment with 2 M HCl (Merck Life Science, 258148) for 20 minutes. Then, blocking was performed with a PBS with 0.5%Tween (Promega, H5152) and 0.05% Bovine Serum Albumin (BSA; Merck Life Science, A7906) solution. The cells were then incubated with the Monoclonal Mouse Anti-BrdU Clone Bu20a primary antibody (1:10; Dako, M0744) for 1 h, followed by incubation with the Polyclonal Rabbit Anti-Mouse Immunoglobulins/FITC secondary antibody (1:100; Dako, F0261) for 30 minutes. After that, slides were prepared with Vectashield mounting medium containing 4′,6-diamidino-2-phenylindole (DAPI; Vector Laboratories Inc., H-1200). The detection of BrdU incorporation was possible using the Zeiss Axio Imager Z1 (Carl Zeiss) microscope and the Axiovision 4.9 (Carl Zeiss) software. The evaluation of the % of proliferating cells was performed by counting a minimum of 200 cells per slide using the ImageJ 2.1.0 software.

3.7. Cell Cycle Profile Analysis

To verify the effect of the combined drug treatments on the cell cycle profile of NSCLC cell lines, flow cytometry cell cycle analysis using propidium iodide (PI) DNA staining was performed. This assay is based on the ability of PI to bind stoichiometrically to

the DNA content of cells. Therefore, as cells undergoing the S phase of the cell cycle have a bigger amount of DNA than the ones in the G0/G1 phases, cells in the S phase will release proportionally more fluorescence than those in the G0/G1 phases. Similarly, cells in the G2/M phases of the cell cycle will be approximately twice as bright as cells undertaking the G1 phase. PI reacts to both RNA and DNA, thus treatment with a RNase A is also necessary [92].

Cells were plated in 6-well plates and incubated for 24 h at 37 ºC. After a 48 h incubation period with the drug treatments, cells were collected as described in **section 3.6.** and centrifuged for 5 minutes at 1200 rpm, at 4 ºC. The supernatant was discharged, and cells were fixed and permeabilized with ice-cold 70% ethanol (Fischer Scientific, E/0650DF/C17) dropwise, while vortexing to minimize clumping. Cells were then left at 4 ºC for a period of at least 12 h to provide proper fixation. Subsequently, samples were subjected to a centrifugation under the same previously described conditions, and the supernatant discharged. The remaining ethanol was allowed to evaporate for a period of 10-15 minutes. Each cell pellet was resuspended in 300-400 µL of a PBS solution containing 0.137M NaCl, 0.0027M KCl, 0.01M NaH_2PO_4 (Merck Life Science, A420746) and 0.0018M KH_2PO_4 (Merck Life Science, A591973), which was then added 0.1 mg/mL RNase A (Invitrogen, 12091021) and 5 mg/mL PI (Merck Life Science, 537060), and kept in the dark for at least 30 minutes. Sample analysis was performed using the BD Accuri™ C6 Flow Cytometer (BD Biosciences) and the BDSamples software (BD Biosciences), after proper exclusion of cell debris and aggregates, and plotting at least 10 000 to 20 000 events per sample. The flow cytometry results were further analyzed using the FlowJo 7.6.5 Software (Tree Star, Inc.).

3.8. Cell Death Detection

The effect of the combined drug treatments on the % of cell death of the NSCLC cell lines under study was assessed using the Annexin V-FITC Apoptosis Detection Kit (eBioscience™, BMS500FI), according to manufacturer's instructions. This protocol allows the recognition of cell death based on the ability of fluorescent conjugated Annexin V to bind to the phosphatidyl serine exposed on the surface of apoptotic cells, as well as on the capability of PI to identify necrotic or late apoptotic cells, characterized by the loss of cellular and nuclear membrane permeability [93].

For this assay, cells were plated in 6-well plates, and incubated for 24 h at 37 ºC. Then, 1 h before cell collection, 200 µL of pure ethanol were added to the well correspondent to the positive control for necrosis. After a 48 h incubation period with the drug treatments, cells were collected as described in **section 3.6.** and centrifuged for 5

minutes at 1200 rpm at 4 ºC. The supernatant was discharged, and cells were resuspended in 400 µL of the binding buffer solution in water (1x). As indicated by the manufacturer's instructions, 195 µL of the cell suspension were then incubated with 5 µL of Annexin V-FITC for 10 minutes at room temperature, protected from light. Subsequently, 10 µL of PI were added to which condition and samples were analyzed using the BD Accuri™ C6 Flow Cytometer and the BDSamples software, after proper exclusion of cell debris and aggregates, and plotting at least 10 000 to 20 000 events per sample. The flow cytometry results were further analyzed using the BD Accuri™ C6 Software (BD Biosciences).

3.9. Next Generation Sequencing (NGS) Analysis using the Oncomine Focus Assay

In order to confirm the molecular profile of the NSCLC cell lines (A549, NCI-H322 and NCI-H460) used in this study a NGS analysis for a panel of specific genes was performed. NGS has emerged in oncology as a tool that allows the rapid, simultaneous, and increasingly affordable sequencing of a large number of genes of particular importance [94]. In our work, we used the Ion Torrent™ Oncomine™ Focus Assay (A42008; Thermo Fisher Scientific) that allows the detection of variants in 52 cancer-relevant genes in a single procedure (**Table 4**).

For that, 5 x 10^6 cells/pellet of the three NSCLC cell lines under study were collected for DNA and RNA extraction. Then, NGS analysis was performed at the Genomics Core Facility of i3S, Porto. The results were further analyzed using the Ion Reporter™ Software (Thermo Fisher Scientific).

Table 4 – Genes covered in the Oncomine Focus Assay (from Thermo Fisher Scientific).

Somatic Alteration		
Hotspot genes	**Copy Number Variants**	**Fusion Drivers**
AKT1, ALK, AR, BRAF, CDK4, CTNNB1, DDR2, EGFR, ERBB2, ERBB3, ERBB4, ESR1, FGFR2, FGFR3, GNA11, GNAQ, HRAS, IDH1, IDH2, JAK1, JAK2, JAK3, KIT, KRAS, MAP2K1, MAP2K2, MET, MTOR, NRAS, PDGFRA, PIK3CA, RAF1, RET, ROS1, SMO	*ALK, AR, BRAF, CCND1, CDK4, CDK6, EGFR, ERBB2, FGFR1, FGFR2, FGFR3, FGFR4, KIT, RAS, MET, MYC, MYCN, PDGFRA, PIK3CA*	*ABL1, AKT3, ALK, AXL, BRAF, EGFR, ERBB2, ERG, ETV1, ETV4, ETV5, FGFR1, FGFR2, FGFR3, MET, NTRK1, NTRK2, NTRK3, PDGFRA, PPARG, RAF1, RET, ROS1*

3.10. Statistical Analysis

All experiments were performed at least three independent times, and the results are expressed as mean ± SEM. The statistical analysis was performed using the two-tailed unpaired *t*-test, with GraphPad Prism 8.0 software. Statistical significance was considered whenever $p < 0.05$.

Chapter

Results and Discussion 4

4.1. Determination of drug concentrations causing 50% cell growth inhibition (GI_{50}) in several NSCLC cell lines

In order to study the combined effect of Pirfenidone with each chemotherapeutic agent, the cytotoxic effect of the individual drugs, Carboplatin (CBP), Etoposide (ETP), Gemcitabine (GEM), Paclitaxel (PAC), Vinorelbine (VR) and Pirfenidone (PF), were assessed in three NSCLC cell lines, using the SRB assay. For that, the A549, NCI-H322 and NCI-H460 cancer cell lines were treated for 48 h with five serial dilutions of each individual drug and dose-response curves were determined (**Figures 7, 8 and 9**). The GI_{50} concentrations were then calculated through an interpolation of the determined dose-response curves and are presented in **Table 5**.

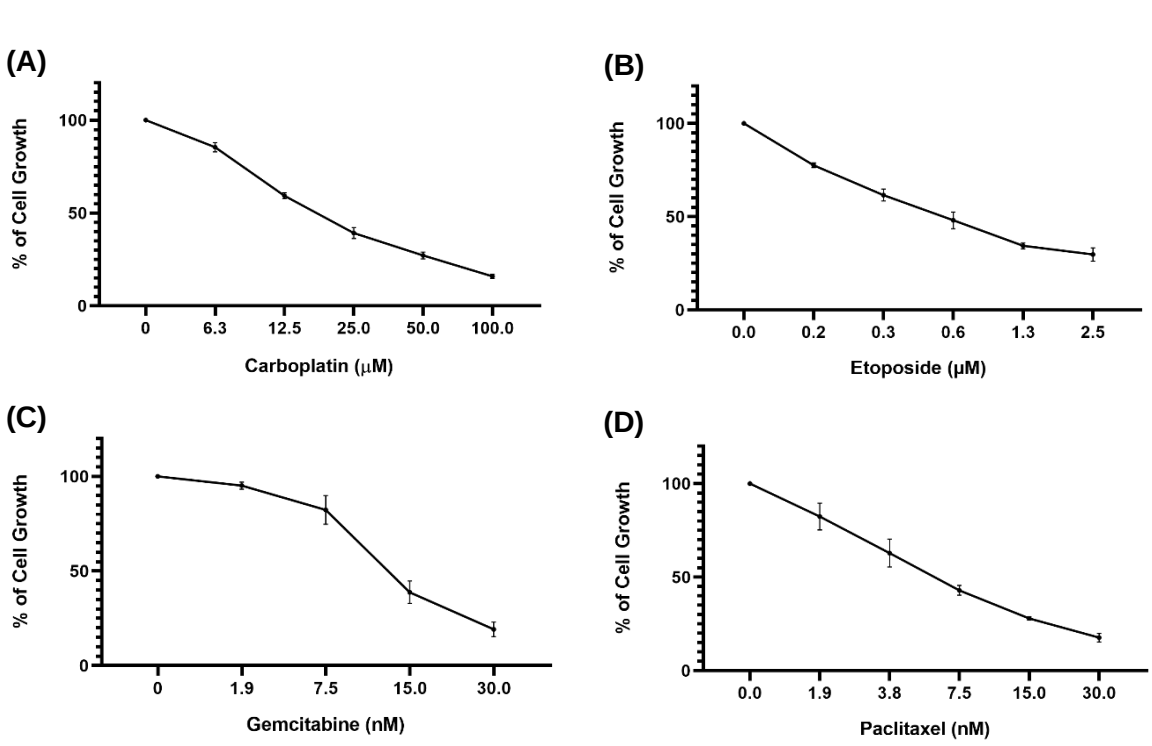

Figure 7 – Dose-response curves of the NCI-H460 cell line after treatment with (A) Carboplatin, (B) Etoposide, (C) Gemcitabine or (D) Paclitaxel. Cells were treated with five serial dilutions of each individual drug for 48 h and results were obtained by the SRB assay. Results are presented as a percentage (%) of cell growth and are the mean ± SEM of at least three independent experiments.

The dose-response curves of VR and PF for the human NSCLC NCI-H460 cell line were not determined since they had been previously determined by our research group (MSc dissertation of Catarina Antunes – [83]). The GI_{50} concentrations for VR and PF that had been previously obtained were $6.9 \times 10^{-3} \pm 5.0 \times 10^{-4}$ µM and $1.9 \times 10^{3} \pm 30.0$ µM, respectively.

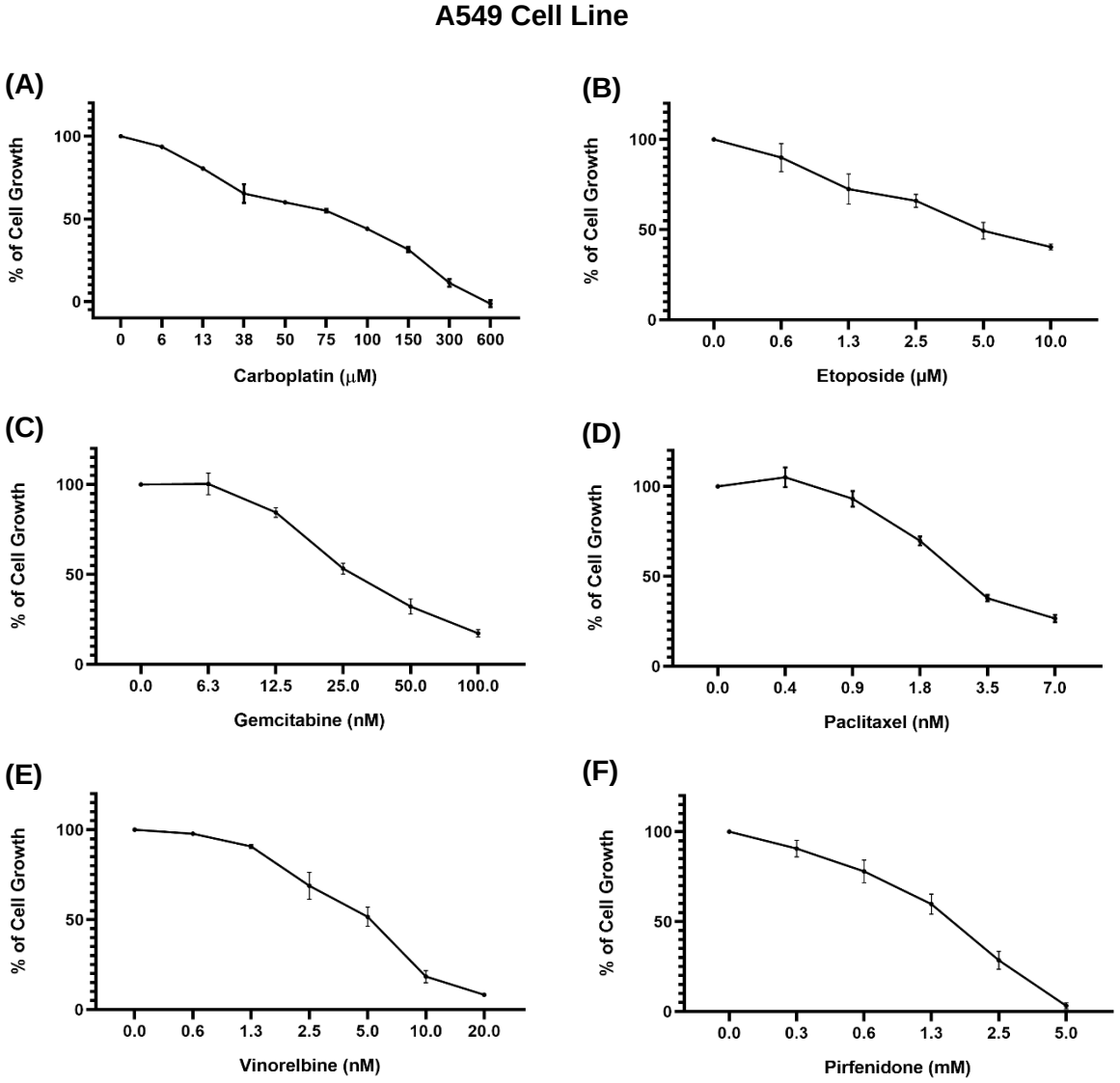

Figure 8 – Dose-response curves of the A549 cell line after treatment with (A) Carboplatin, (B) Etoposide, (C) Gemcitabine, (D) Paclitaxel, (E) Vinorelbine or (F) Pirfenidone. Cells were treated with five serial dilutions of each individual drug for 48 h and results were obtained by the SRB assay. Results are presented as a % of cell growth and are the mean ± SEM of at least three independent experiments.

In the NCI-H322 cell line, only the most promising drug treatments obtained in the NCI-H460 and A549 cancer cell lines (CBP, PAC, VR and PF) were further validated.

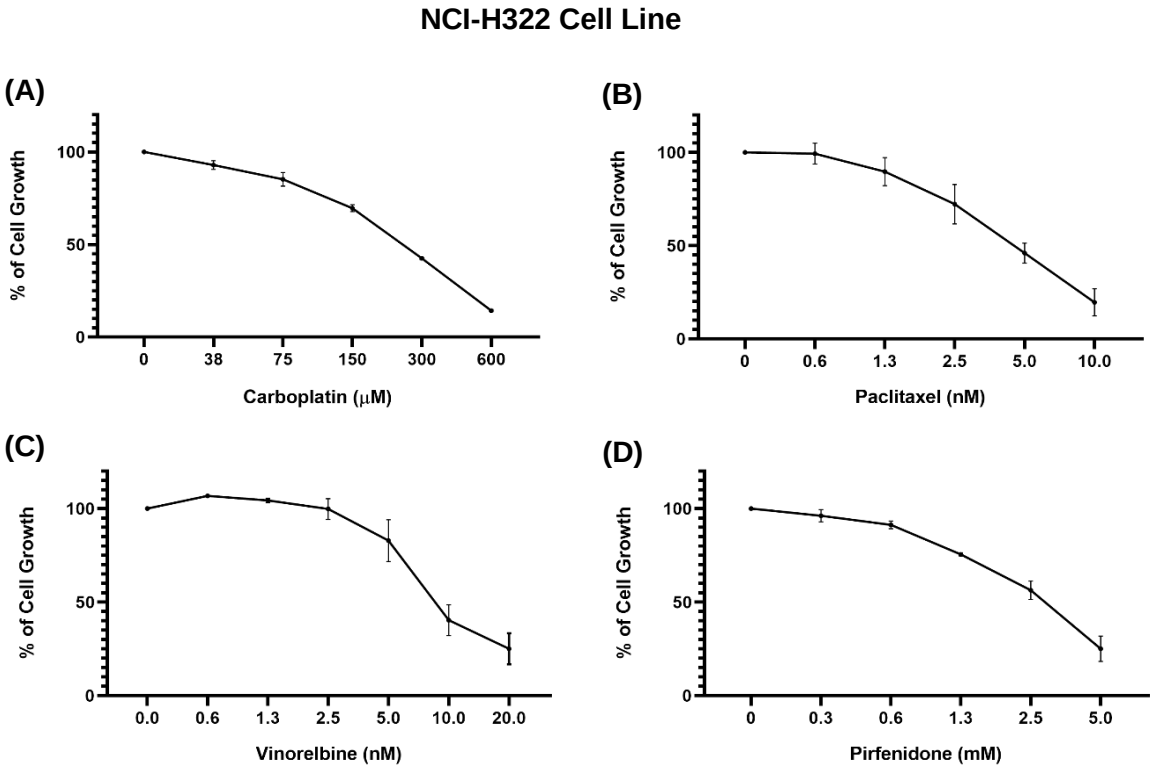

Figure 9 – Dose-response curves of the NCI-H322 cell line after treatment with (A) Carboplatin, (B) Paclitaxel, (C) Vinorelbine or (D) Pirfenidone. Cells were treated with five serial dilutions of each individual drug for 48 h and results were obtained by the SRB assay. Results are presented as a % of cell growth and are the mean ± SEM of at least three independent experiments.

Table 5 – GI_{50} concentrations of Carboplatin (CBP), Etoposide (ETP), Gemcitabine (GEM), Paclitaxel (PAC), Vinorelbine (VR) or Pirfenidone (PF) in A549, NCI-H322 and NCI-H460 cell lines. The concentration that causes 50% cell growth inhibition (GI_{50}) of CBP, ETP, GEM, PAC, VR or PF in A549, NCI-H322 and NCI-H460 human NSCLC cell lines, determined 48 h following drug treatment, using the SRB assay. Results are the mean ± SEM of at least three independent experiments.

		NSCLC Cell Line		
		A549	**NCI-H322**	**NCI-H460**
GI_{50} concentration (μM)	**CBP**	83.7 ± 3.4	247.0 ± 3.3	17.7 ± 1.2
	ETP	5.2 ± 0.8	-	0.6 ± 0.1
	GEM	$26.3 \times 10^{-3} \pm 1.8 \times 10^{-3}$	-	$12.6 \times 10^{-3} \pm 1.3 \times 10^{-3}$
	PAC	$2.7 \times 10^{-3} \pm 0.0$	$4.7 \times 10^{-3} \pm 4.7 \times 10^{-4}$	$5.7 \times 10^{-3} \pm 5.3 \times 10^{-4}$
	VR	$5.0 \times 10^{-3} \pm 4.9 \times 10^{-4}$	$8.9 \times 10^{-3} \pm 1.6 \times 10^{-3}$	-
	PF	$1.5 \times 10^{3} \pm 1.9 \times 10^{2}$	$2.8 \times 10^{3} \pm 1.5 \times 10^{2}$	-

-, not determined in the framework of this dissertation.

Our results together with the ones previously determined by our research group (MSc dissertation of Catarina Antunes – [83]) demonstrated that, among the chemotherapeutic drugs under study (which excludes PF from this analysis of results), VR and PAC were the ones for which all three NSCLC cell lines had higher sensitivity. On the other hand, CBP treatment demonstrated to be less effective in decreasing the growth of the three NSCLC cell lines. These findings are in agreement with other researchers, which showed higher cytotoxic effect (in the nM range) for VR and PAC and less cytotoxic effect (in the μM range) for CBP on NSCLC cell lines [95-99]. In fact, although CBP has been used in the clinical practice for NSCLC treatment, this chemotherapeutic drug is mainly used in combination regimens to allow a reduction in the final concentration of this alkylating agent [100].

The GI_{50} concentrations obtained for PF in the NSCLC cell lines were significantly higher (in the mM range) than those obtained for the chemotherapeutic drugs. This was expected since PF is a drug approved for the treatment of idiopathic pulmonary fibrosis, thus a strong tumor cell growth inhibitory capacity was not expected.

4.2. Study of the Drug Combination: Vinorelbine (VR) plus Pirfenidone (PF)

4.2.1. Effect on the % of Cell Growth of Human NSCLC cell lines

According to the preliminary results from our research group [83], PF sensitizes the lung large cell carcinoma cell line NCI-H460 to VR treatment. Those results showed that PF at 0.5, 1 or 2 mM combined with VR at 1.8, 3.5 or 7 nM had statistically significant advantage in terms of cell growth inhibition, when compared with each individual drug. Therefore, the validation of these findings in other lung adenocarcinoma cell lines (which is the histological subtype with highest representation) was carried out within the scope of this master dissertation. For that, two lung adenocarcinoma cell lines were included in this study: NCI-H322 (*KRAS* wild-type) and A549 (*KRAS* mutated).

First, the effectiveness of the drug combination consisting of PF plus VR was validated in the NCI-H322 cell line. For that, this lung adenocarcinoma cell line was treated through distinct experimental designs: 1) PF was fixed at a concentration of 2 mM and VR was applied at three increasing concentrations (from 1.8 to 7.0 nM) (**Figure 10A**) and 2) VR was fixed at a concentration of 7.0 nM and PF was applied at two increasing concentrations (1.0 and 2.0 mM) (**Figure 10B**). The obtained results demonstrated that the combination of VR at 7.0 nM with PF at 2.0 mM statistically significantly decreased NCI-H322 cell growth, when compared to the treatment with each drug individually.

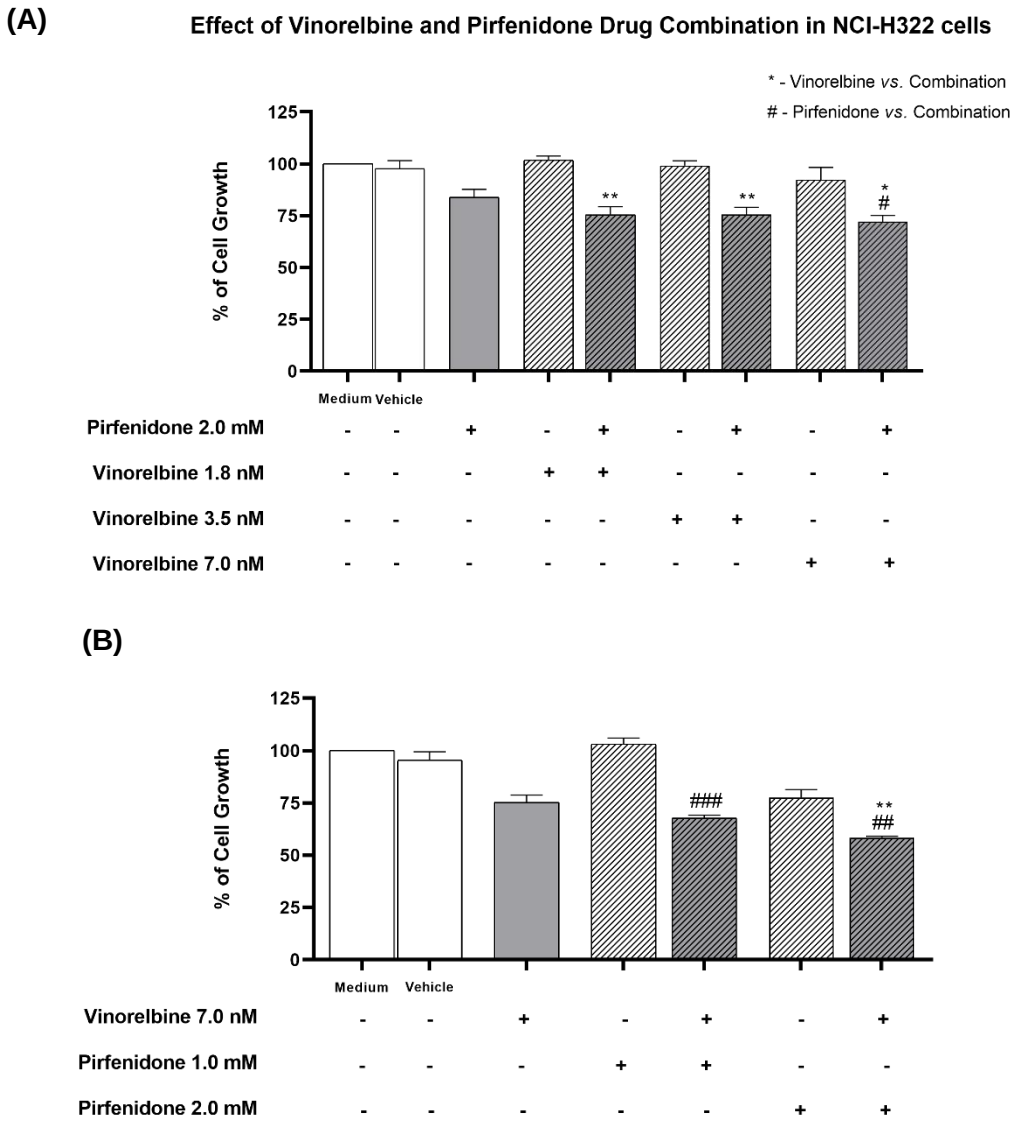

Figure 10 – Effect of the combined treatment with Vinorelbine and Pirfenidone at different concentrations on the % of cell growth of NCI-H322 cells, assessed by the SRB assay. Cells were treated with drug combinations consisting of **(A)** Pirfenidone at 2.0 mM with three serial dilutions of Vinorelbine; or **(B)** Vinorelbine at 7.0 nM with two serial dilutions of Pirfenidone, for 48 h. The effect of the vehicle at the highest concentration tested was also analyzed. Results are presented as a % of cell growth and are the mean ± SEM of at least three independent experiments. * or # $p < 0.05$, ** or ## $p < 0.01$ and *** or ### $p < 0.001$.

Further, the effect of the combined treatment of PF plus VR was validated in the A549 cell line. For that, these cells were treated with PF at a concentration of 1.5 mM and VR at a concentration of 5.0 nM, for 48 h. The results presented in **Figure 11** demonstrated that this drug combination statistically significantly decreased the % of cell growth, when compared to each drug individually.

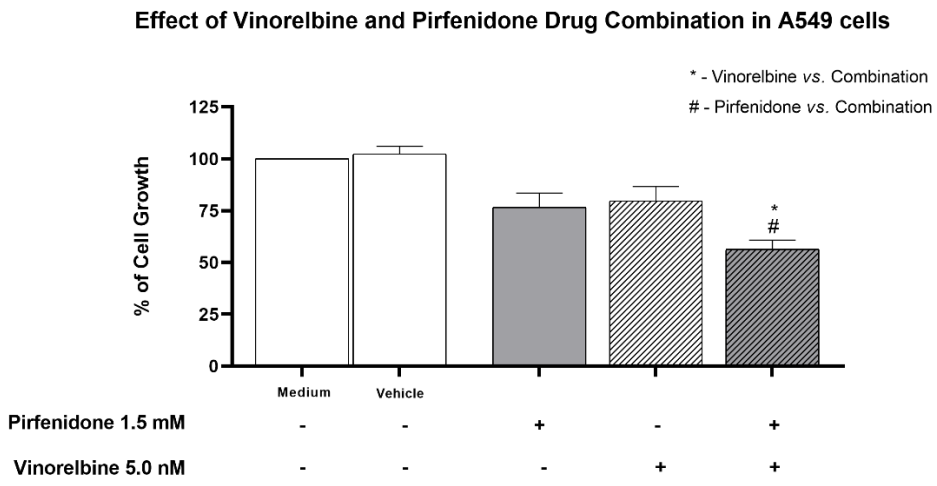

Figure 11 – Effect of the combined treatment with Vinorelbine and Pirfenidone on the % of cell growth of A549 cells, assessed by the SRB assay. Cells were treated with a drug combination consisting of Pirfenidone at 1.5 mM and Vinorelbine at 5.0 nM, for 48 h. The effect of the vehicle at the highest concentration tested was also analyzed. Results are presented as a % of cell growth and are the mean ± SEM of at least three independent experiments. * or # $p < 0.05$.

4.2.2. Effect on the Viability of Human NSCLC cell lines

The effect of the combined treatment of VR and PF on A549 and NCI-H322 cell viability was assessed using the trypan blue exclusion assay (**Figures 12 and 13**). The effect of this drug combination on the NCI-H460 cell viability had been previously assessed by our group, having been demonstrated that PF at 2 mM and VR at 7 nM significantly decreased cell viability (MSc dissertation of Catarina Antunes – [83]).

The present results demonstrated that both VR and PF individually induced a statistically significant reduction in the % of A549 and NCI-H322 viable cells. The results for PF are in agreement with those described by Marwitz S. *et al.* (2019), who demonstrated that PF reduced the viability of several lung adenocarcinoma cell lines, including the A549 cell line [75].

Importantly, the combined treatment of VR and PF statistically significantly reduced the viability of both A549 and NCI-H322 cells, when compared with each individual drug. These results are in line and support our results previously obtained using the SRB assay.

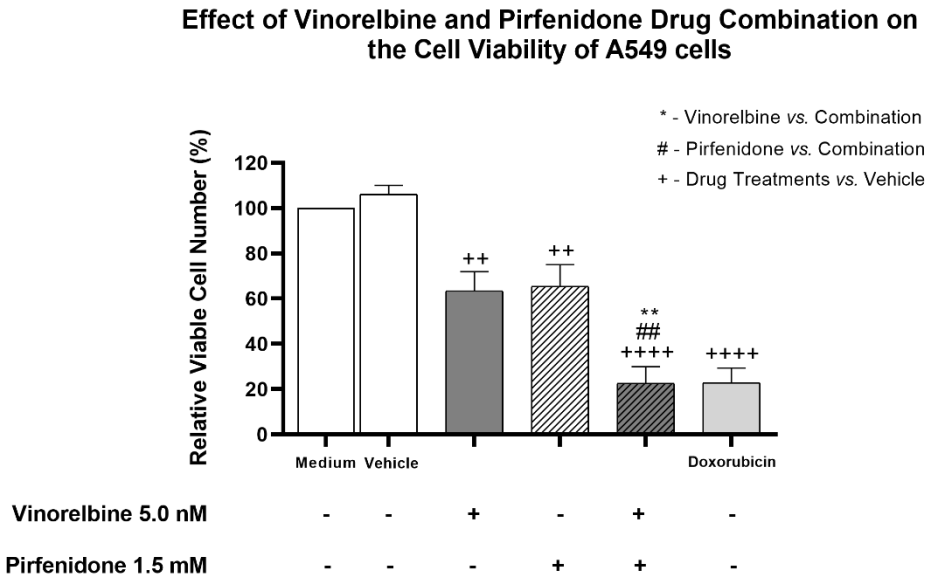

Figure 12 – Effect of the combined treatment with Vinorelbine and Pirfenidone on the viable cell number of A549 cells determined by the trypan blue exclusion assay. Cells were treated with Vinorelbine at 5.0 nM and Pirfenidone at 1.5 mM, either alone or in combination, for 48 h. The effect of the vehicle at the highest concentration tested was also analyzed. Doxorubicin (50 nM) was used as positive control. Results are the mean ± SEM of at least three independent experiments. **, ## or ++ $p < 0.01$ and ++++ $p < 0.0001$.

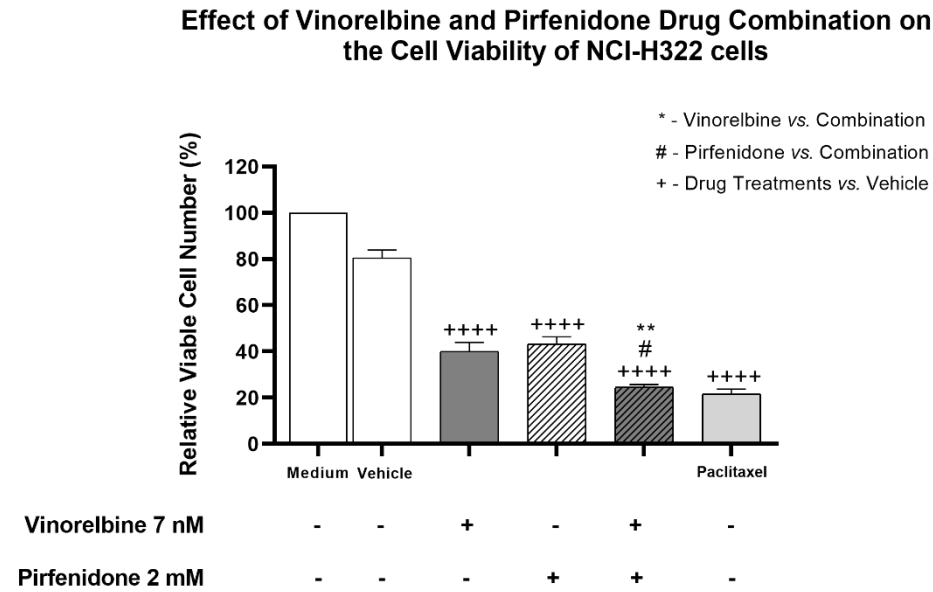

Figure 13 – Effect of the combined treatment with Vinorelbine and Pirfenidone on the viable cell number of NCI-H322 cells determined by the trypan blue exclusion assay. Cells were treated with Vinorelbine at 7 nM and Pirfenidone at 2 mM, either alone or in combination, for 48 h. The effect of the vehicle at the highest concentration tested was also analyzed. Paclitaxel (20 nM) was used as positive control. Results are the mean ± SEM of at least three independent experiments. # $p < 0.05$, ** $p < 0.01$ and ++++ $p < 0.0001$.

4.2.3. Effect on the Proliferation of Human NSCLC cell lines

As previously mentioned, the effect of the combined treatment of VR with PF on the proliferation of the NCI-H460 cells had been previously evaluated by our research group [83]. Those results demonstrated that this combined drug treatment significantly reduced NCI-H460 cell proliferation. Thus, the effect of this drug combination on the proliferation of the two adenocarcinoma cell lines, A549 and NCI-H322, was here further investigated using the BrdU incorporation assay.

As presented in **Figures 14 and 15,** the treatment of A549 and NCI-H322 cells with VR or PF alone statistically significantly reduced the % of proliferating cells. These results with VR are in line with those presented by Liu H. *et al.* (2020), which described a reduction in the % of proliferating cells after treatment with VR in another lung adenocarcinoma cell line, H1975 [101]. Furthermore, Marwitz *et al.* (2019) also demonstrated the anti-proliferative effect of PF in several NSCLC cell lines (A549, H838, H1650, H1975 and H520) [75].

Regarding the drug combination, our results showed that VR in combination with PF statistically significantly reduced the % of proliferating cells, when compared with either of the drugs individually, in both A549 and NCI-H322 cells.

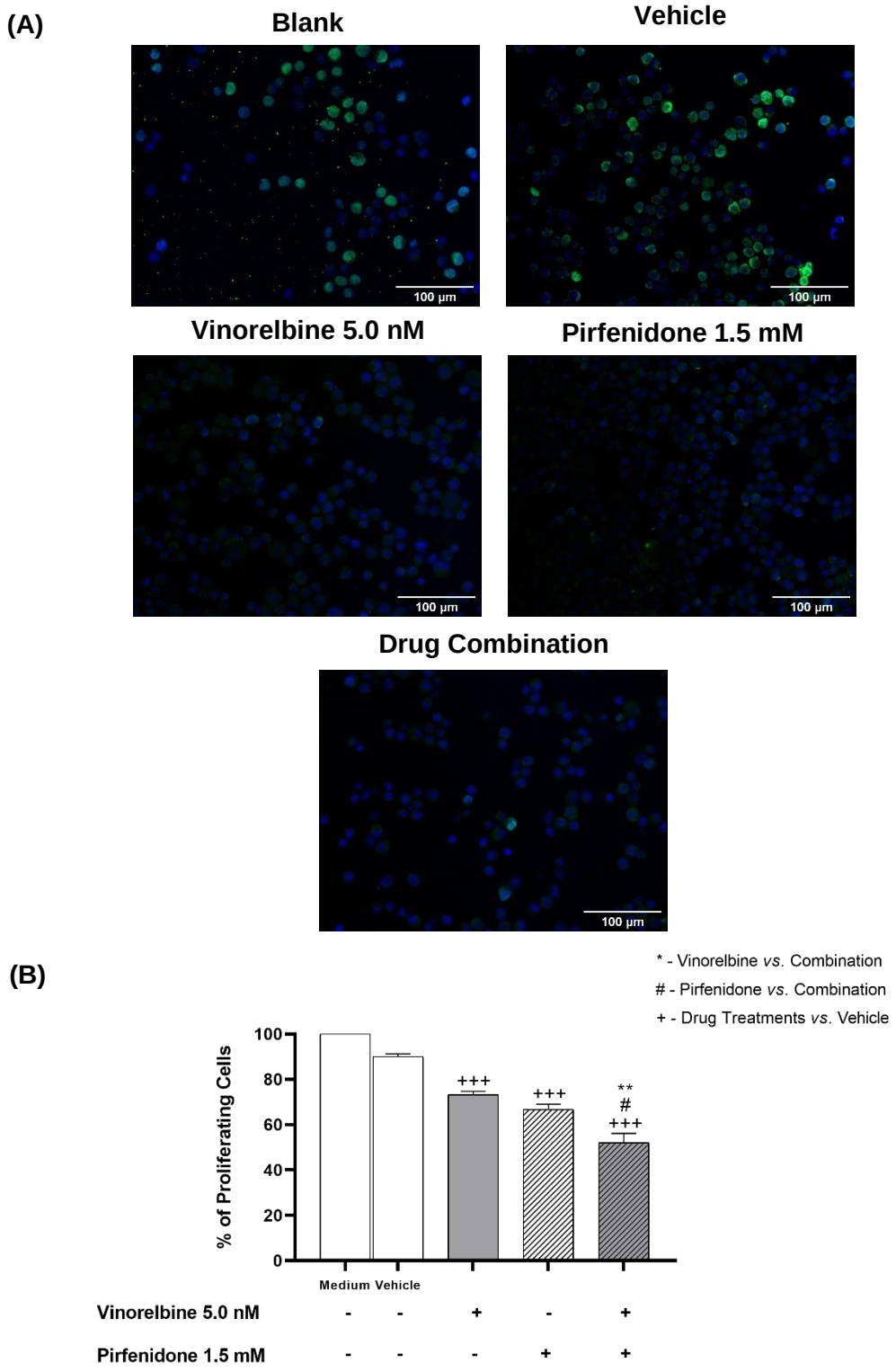

Figure 14 – Effect of the combined treatment with Vinorelbine and Pirfenidone on the cell proliferation of A549 cells assessed by the BrdU incorporation assay. Cells were treated with Vinorelbine at 5.0 nM and Pirfenidone at 1.5 mM, either alone or in combination, for 48 h. The effect of the vehicle at the highest concentration tested was also analyzed. **(A)** Representative fluorescence microscopy images of BrdU incorporation (green) and DAPI stained nuclei (blue). Amplification = 200×. Scale bar = 100 micrometers. **(B)** Percentage of BrdU-incorporating cells. Results are the mean ± SEM of at least three independent experiments. # $p < 0.05$, ** $p < 0.01$ and +++ $p < 0.001$.

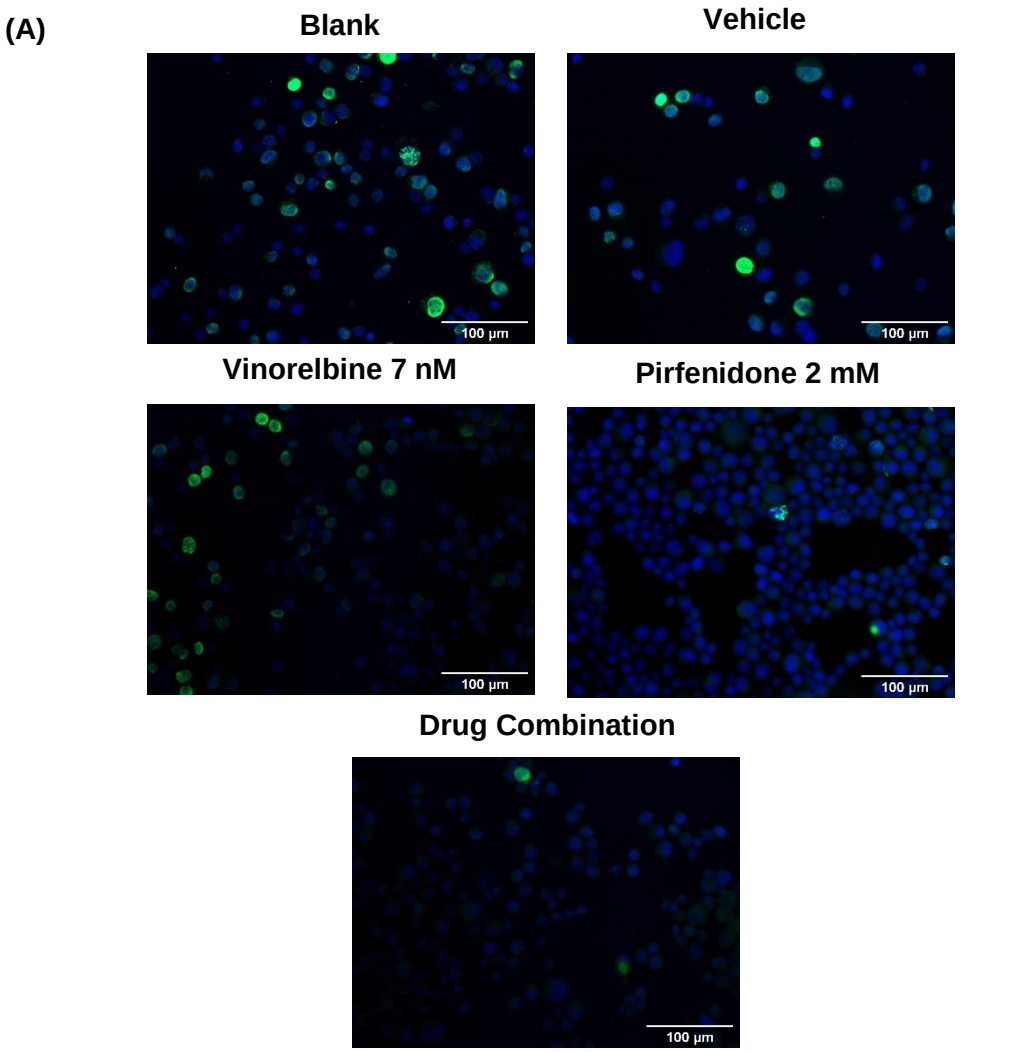

Figure 15 – Effect of the combined treatment with Vinorelbine and Pirfenidone on the cell proliferation of NCI-H322 cells assessed by the BrdU incorporation assay. Cells were treated with Vinorelbine at 7 nM and Pirfenidone at 2 mM, either alone or in combination, for 48 h. The effect of the vehicle at the highest concentration tested was also analyzed. **(A)** Representative fluorescence microscopy images of BrdU incorporation (green) and DAPI stained nuclei (blue). Amplification = 200×. Scale bar = 100 micrometers**. (B)** Percentage of BrdU-incorporating cells. Results are the mean ± SEM of at least three independent experiments. * or + $p < 0.05$, ## or ++ $p < 0.01$ and +++ $p < 0.001$.

4.2.4. Effect on the Cell Cycle Profile of NSCLC Cell Lines

Cancer cell proliferation is frequently linked to a dysregulated cell cycle progression, thus targeting the mechanisms underlying cell cycle control is one of the processes by which anticancer drugs can limit cancer cell proliferation [102]. Preliminary results from our group demonstrated that the combined treatment of VR with PF caused a slight increase in the % of cells in the sub-G1 phase of NCI-H460 cell cycle [83]. Therefore, considering the previously demonstrated antiproliferative effect of the combined treatment of VR with PF, the present work further assessed whether this effect was related to alterations in the cell cycle profile in the A549 and NCI-H322 cell lines.

The results for the A549 cell line are presented in **Figure 16**. Doxorubicin at 50 nM was used as a positive control and, as predicted, altered the cell cycle profile according to what is described in the literature [103]. Our data showed that VR statistically significantly increased the % of cells in the G0/G1 phase of the cell cycle, accompanied by a decrease in the % of cells in the S phase. Furthermore, an increase in the sub-G1 cell population was also observed, which is suggestive of apoptosis. These results are supported by those of Zhu K. *et al.* (2014), who demonstrated the same effect for VR in this particular cell line [104]. Regarding the PF treatment, this drug also increased the % of cells in the G0/G1 phase and decreased the % of cells in the S phase of the cell cycle. The results obtained are also consistent with the results found in the literature [71, 72, 75]. Regarding the combination treatment of VR and PF in the A549 cell line, even though no statistical significance was found when comparing the combination treatment with each drug individually, this drug combination slightly increased the % of cells in G0/G1 phase, decreased the % of cells in the S phase of the cell cycle and increased the % of cells in the sub-G1 phase (which is suggestive of apoptosis).

In the NCI-H322 cell line, PAC at a concentration of 20 nM was used as a positive control, and as expected it caused a G2/M cell cycle arrest [105]. The results presented in **Figure 17** demonstrated no alterations in the cell cycle profile when NCI-H322 cells were treated with VR and PF alone. Regarding the drug combination of VR with PF, even though results were not statistically significant when compared to each drug individually, the combination slightly decreased the % of cells in the S phase of the cell cycle and increased the % of cells in the sub-G1 phase.

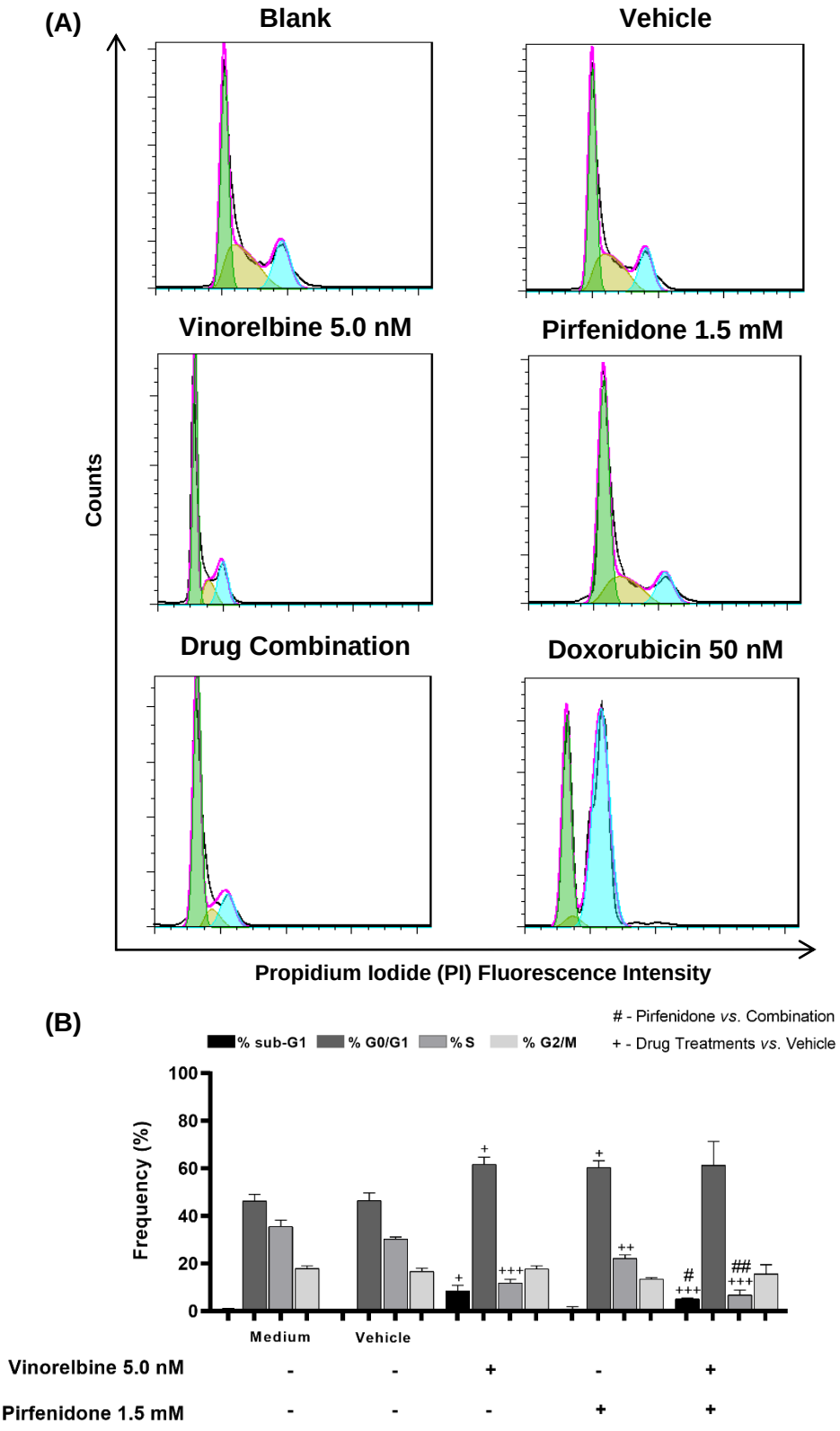

Figure 16 – Effect of the combined treatment with Vinorelbine and Pirfenidone on the cell cycle profile of A549 cells analyzed by flow cytometry following PI staining. Cells were treated with Vinorelbine at 5.0 nM and Pirfenidone at 1.5 mM, either alone or in combination, for 48 h. **(A)** Representative cell cycle histograms and **(B)** Frequency of the cell cycle phases for each condition. Doxorubicin (50 nM) was used as positive control. Results are the mean ± SEM of at least 3 independent experiments. # or + $p < 0.05$, ## or ++ $p < 0.01$ and +++ $p < 0.001$.

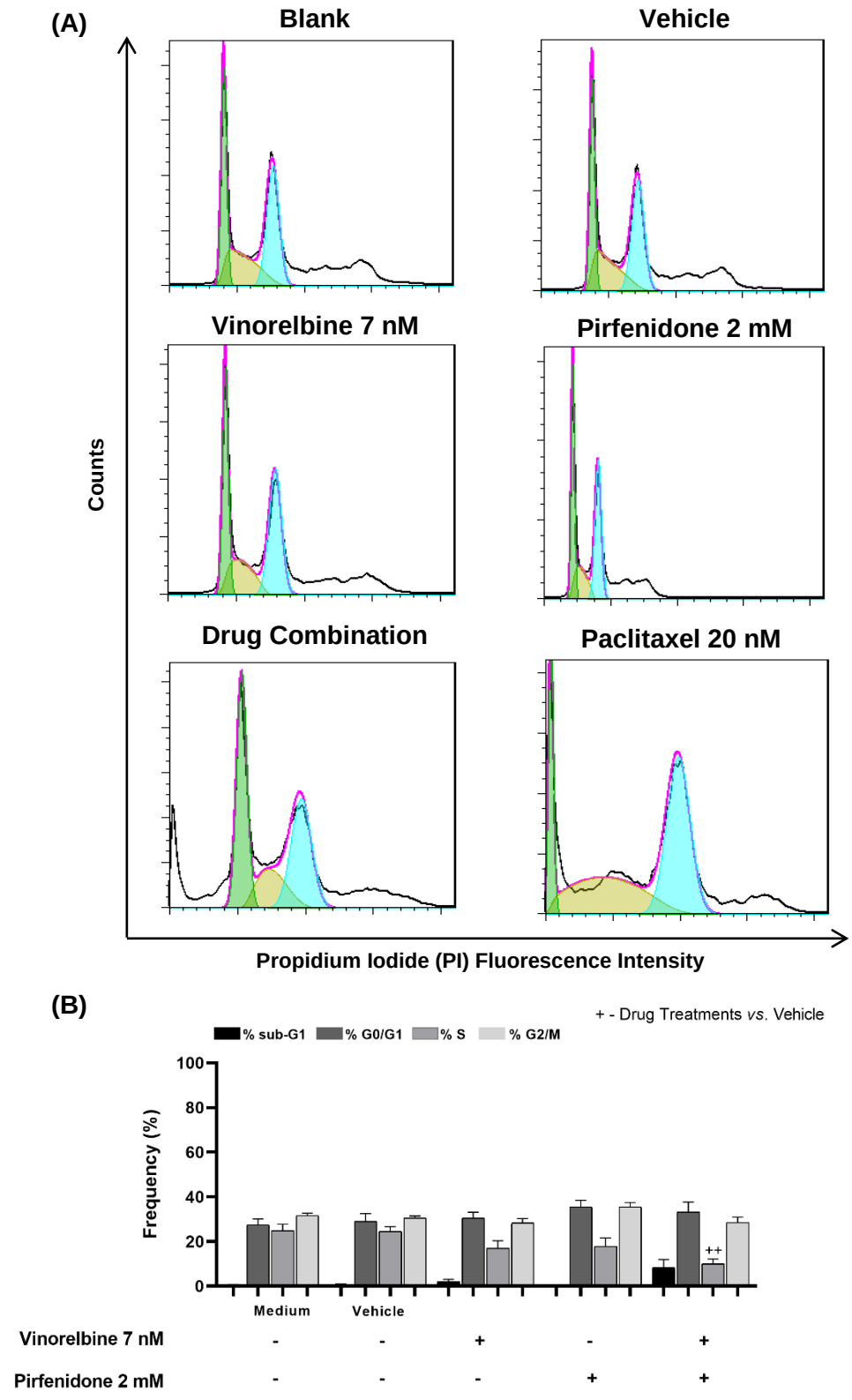

Figure 17 – Effect of the combined treatment with Vinorelbine and Pirfenidone on the cell cycle profile of NCI-H322 cells analyzed by flow cytometry following PI staining. Cells were treated with Vinorelbine at 7 nM and Pirfenidone at 2 mM, either alone or in combination, for 48 h. **(A)** Representative cell cycle histograms and **(B)** Frequency of the cell cycle phases for each condition. Paclitaxel (20 nM) was used as positive control. Results are the mean ± SEM of at least 3 independent experiments. ++ $p < 0.01$.

4.2.5. Effect on the Levels of Cell Death of NSCLC Cell Lines

Programmed cell death is a tightly regulated process that acts to prevent the accumulation of potentially harmful mutations and to eliminate cells with abnormal cell growth or that carry DNA damage. The deregulation of this mechanism is at the basis of various pathologies including cancer [106, 107]. In fact, one of the hallmarks of cancer is the ability to evade programmed cell death [84].

As mentioned above, preliminary results from our research group found an increase in the % of cells in the sub-G1 phase of the cell cycle after treatment of NCI-H460 cells with the combined treatment of VR and PF, which was suggestive of apoptosis [83]. Moreover, our results, although not statistically significant, also showed an increase in the sub-G1 phase of the cell cycle when A549 and NCI-H322 cells were treated with VR plus PF. Thus, the effect of this combined treatment on cell death of NCI-H460, A549 and NCI-H322 cell lines was assessed using flow cytometry following Annexin V-FITC/PI staining. Doxorubicin at 50 nM was used as a positive control for the NCI-H460 and A549 cell lines, while Paclitaxel at 20 nM was used as a positive control for the NCI-H322 cell line.

The results presented in **Figures 18, 19 and 20** demonstrated that the combination of VR and PF statistically significantly increased the % of cell death (here described as apoptosis, late-apoptosis and necrosis) in the three NSCLC cell lines, when compared with the effect of each drug individually.

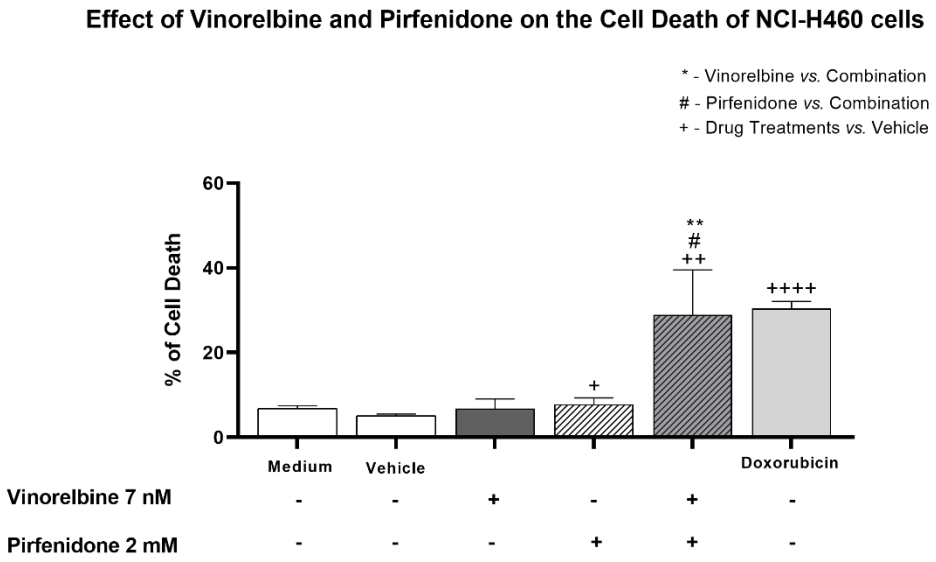

Figure 18 – Effect of the combined treatment with Vinorelbine and Pirfenidone on the % of cell death of NCI-H460 cells determined by flow cytometry following Annexin V-FITC/PI staining. Cells were treated with Vinorelbine at 7 nM and Pirfenidone at 2 mM, either alone or in combination, for 48 h. The effect of the vehicle at the highest concentration tested was also analyzed. Doxorubicin (50 nM) was used as positive control.

Results are the mean ± SEM of at least three independent experiments. # or + $p < 0.05$, ** or ++ $p < 0.01$ and ++++ $p < 0.0001$.

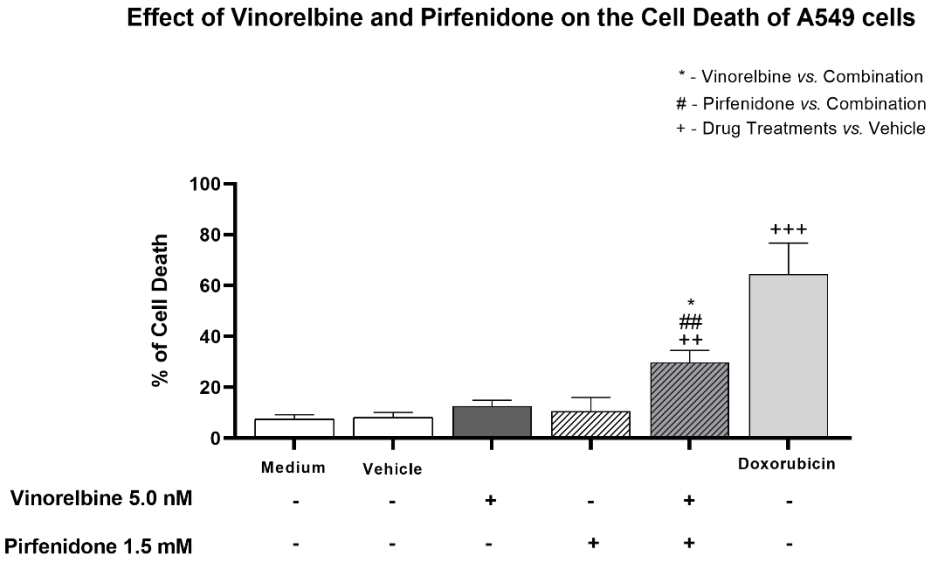

Figure 19 – Effect of the combined treatment with Vinorelbine and Pirfenidone on the % of cell death of A549 cells determined by flow cytometry following Annexin V-FITC/PI staining. Cells were treated with Vinorelbine at 5.0 nM and Pirfenidone at 1.5 mM, either alone or in combination, for 48 h. The effect of the vehicle at the highest concentration tested was also analyzed. Doxorubicin (50 nM) was used as positive control. Results are the mean ± SEM of at least three independent experiments. * $p < 0.05$, ## or ++ $p < 0.01$ and +++ $p < 0.001$.

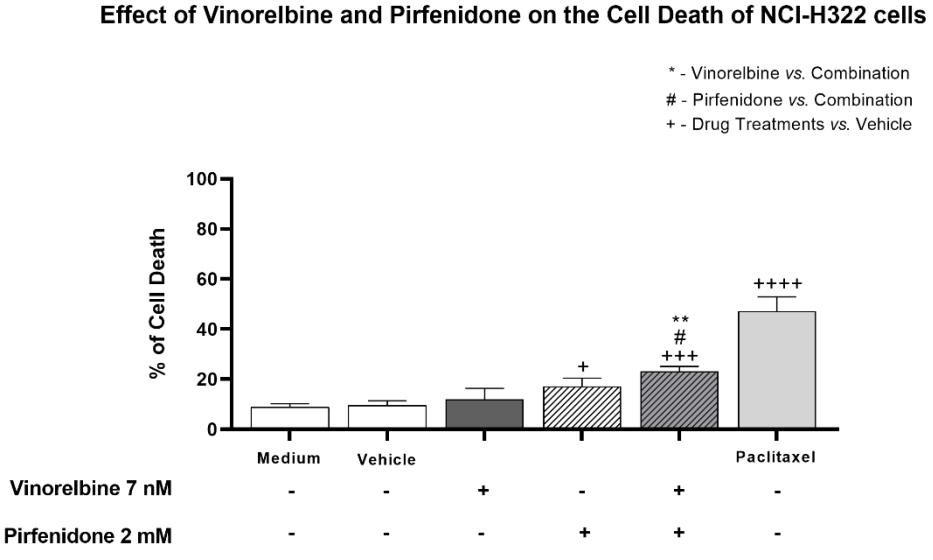

Figure 20 – Effect of the combined treatment with Vinorelbine and Pirfenidone on the % of cell death of NCI-H322 cells determined by flow cytometry following Annexin V-FITC/PI staining. Cells were treated with Vinorelbine at 7 nM and Pirfenidone at 2 mM, either alone or in combination, for 48 h. The effect of the vehicle at the highest concentration tested was also analyzed. Paclitaxel (20 nM) was used as positive control.

Results are the mean ± SEM of at least three independent experiments. # or + $p < 0.05$, ** $p < 0.01$, +++ $p < 0.001$ and ++++ $p < 0.0001$.

4.3. Study of the Drug Combination: Paclitaxel (PAC) plus Pirfenidone (PF)

4.3.1. Effect on the % of Cell Growth of Human NSCLC cell lines

In this dissertation, the effect of the combined treatment of PAC with PF (also used in the clinical practice) on the % of cell growth of the three NSCLC cell lines was also explored.

First, the NCI-H460 cell line was treated with drug combinations consisting of: 1) PF at 2 mM with increasing concentrations of PAC (**Figure 21A**) or 2) PAC at 5.7 nM with increasing concentrations of PF (**Figure 21B**). Our results revealed that the combined treatment of PAC 5.7 nM with PF 2.0 mM statistically significantly reduced NCI-H460 cell growth, when compared with each individual drug, suggesting that PF also sensitizes this cell line to PAC treatment.

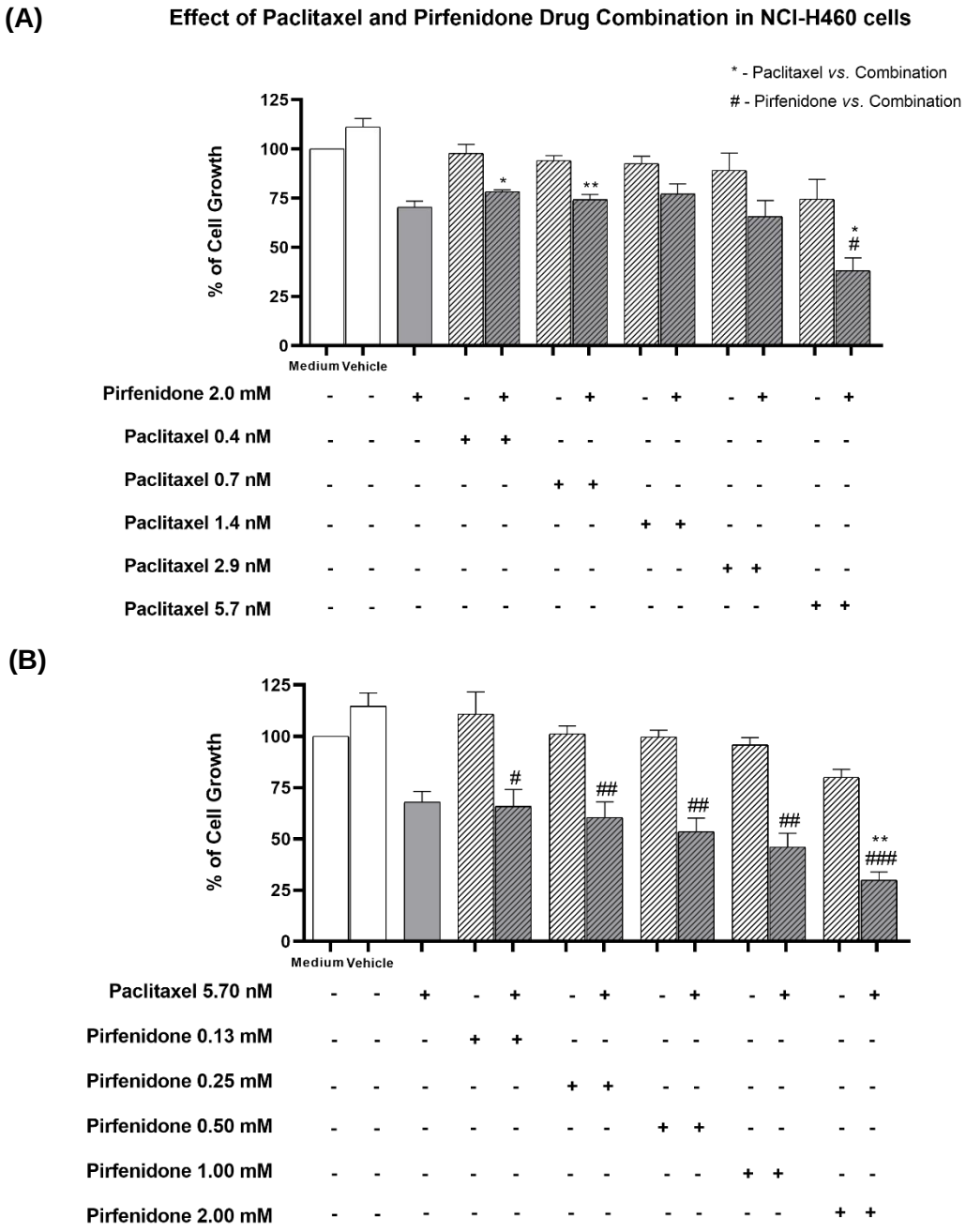

Figure 21 – Effect of the combined treatment with Paclitaxel and Pirfenidone on the % of cell growth of NCI-H460 cells, assessed by the SRB assay. Cells were treated with drug combinations consisting of **(A)** Pirfenidone at 2.0 mM with five serial dilutions of Paclitaxel; or **(B)** Paclitaxel at 5.70 nM with five serial dilutions of Pirfenidone for 48 h. The effect of the vehicle at the highest concentration tested was also analyzed. Results are presented as a % of cell growth and are the mean ± SEM of at least three independent experiments. * or # $p < 0.05$, ** or ## $p < 0.01$ and ### $p < 0.001$.

Then, these results were validated in another NSCLC cell line, A549, which was treated with the drug combination of PAC 2.7 nM and PF 1.5 mM. The results presented in **Figure 22** show that this combined treatment did not bring advantage over PAC treatment alone, in the A549 cells.

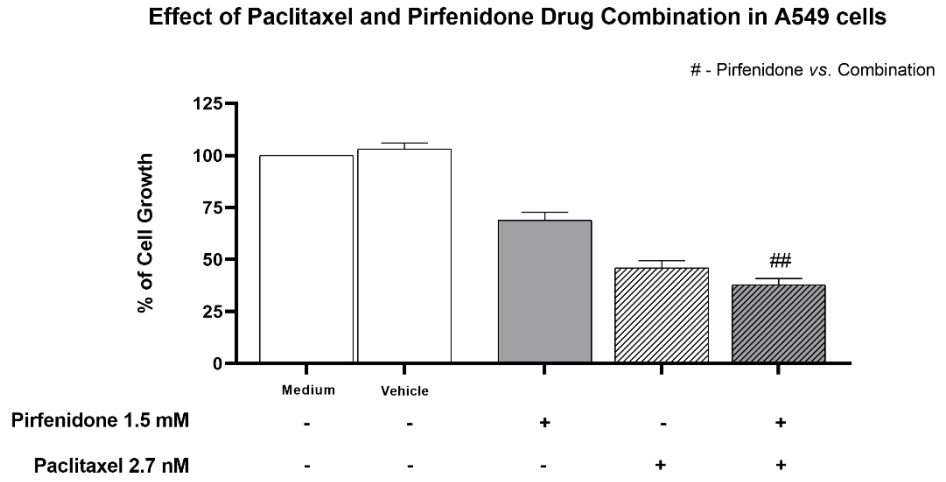

Figure 22 – Effect of the combined treatment with Paclitaxel and Pirfenidone on the % of cell growth of A549 cells, assessed by the SRB assay. Cells were treated with a drug combination consisting of Pirfenidone at 1.5 mM and Paclitaxel at 2.7 nM for 48 h. The effect of the vehicle at the highest concentration tested was also analyzed. Results are presented as a % of cell growth and are the mean ± SEM of at least three independent experiments. ## $p < 0.01$.

The same outcome was observed when NCI-H322 cells were treated with PAC 5.7 nM and PF 2 mM (concentrations that produced the best results in the NCI-H460 cell line) (**Figure 23**). Therefore, since the combined treatment of PAC with PF has only advantage over PAC treatment alone in the NCI-H460 cell line, subsequent assays were only performed in this particular cell line.

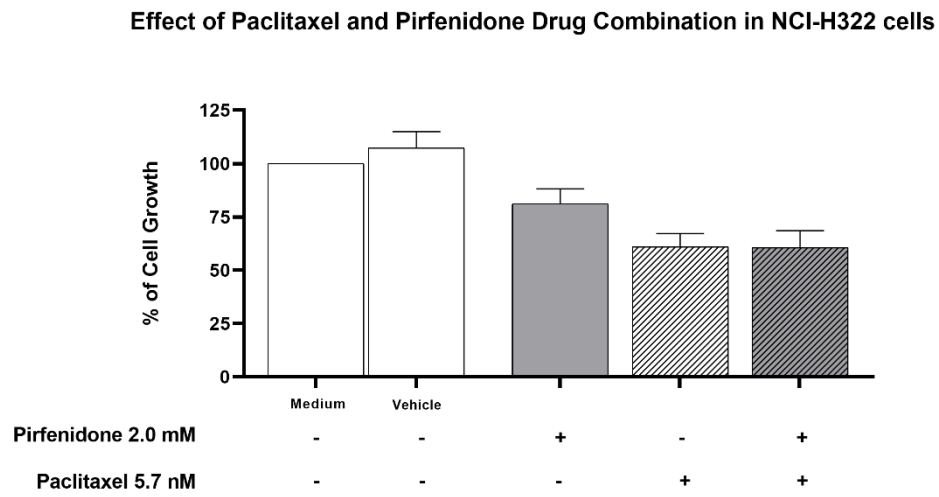

Figure 23 – Effect of the combined treatment with Paclitaxel and Pirfenidone on the % of cell growth of NCI-H322 cells, assessed by the SRB assay. Cells were treated with a drug combination consisting of Pirfenidone at 2.0 mM and Paclitaxel at 5.7 nM for 48 h. The effect of the vehicle at the highest concentration tested was also analyzed. Results are presented as a % of cell growth and are the mean ± SEM of at least three independent experiments.

4.3.2. Effect on the Viability of NCI-H460 Cells

The effect of the combined treatment with PAC and PF on NCI-H460 cell viability was analyzed with the trypan blue exclusion assay. The results presented in **Figure 24** demonstrated that PAC and PF statistically significantly reduced the % of NCI-H460 viable cells. These results are in agreement with the ones published by Zhu Z. *et al.* (2018) and Marwitz *et al.* (2019), who demonstrated a reduction in NSCLC cell viability following treatment with PAC and PF, respectively [75, 108]. Importantly, the combined treatment of PAC with PF statistically significantly decreased the % of NCI-H460 viable cells, when compared with the treatment with PAC or PF individually

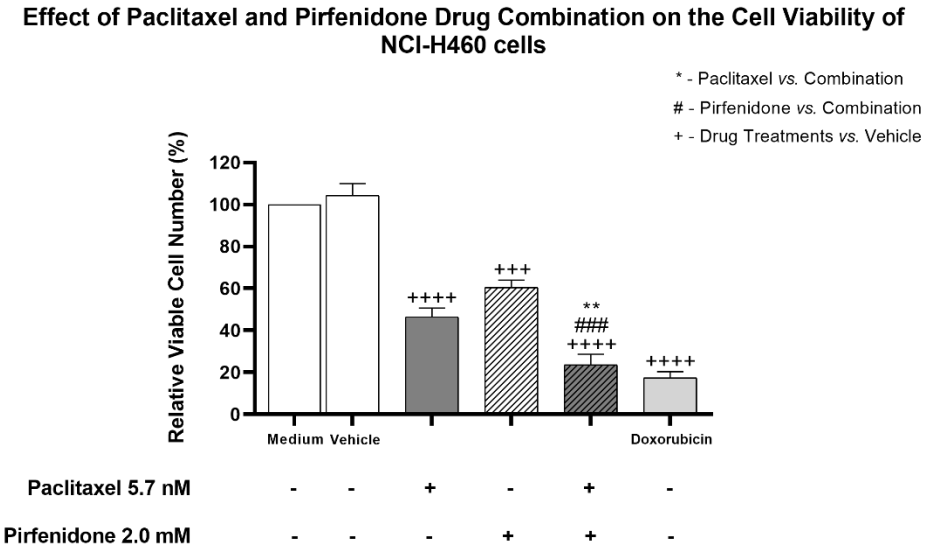

Figure 24 – Effect of the combined treatment with Paclitaxel and Pirfenidone on the viable cell number of NCI-H460 cells determined by the trypan blue exclusion assay. Cells were treated with Paclitaxel at 5.7 nM and Pirfenidone at 2 mM, either alone or in combination, for 48 h. The effect of the vehicle at the highest concentration tested was also analyzed. Results are the mean ± SEM of at least three independent experiments. ** $p < 0.01$, ### or +++ $p < 0.001$ and ++++ $p < 0.0001$.

4.3.3. Effect on the Proliferation of NCI-H460 Cells

Since the combined treatment of PAC with PF reduced the growth and viability of the NCI-H460 cells, we then studied the possible effect of this drug combination on cell proliferation. Thus, the effect of the combined treatment consisting of PAC at 5.7 nM with PF at 2 mM on the proliferation of this large cell carcinoma cell line was verified using the BrdU incorporation assay.

Our results, presented in **Figure 25,** demonstrated that NCI-H460 cells treated with PAC or PF alone statistically significantly reduced the % of proliferating cells, as described in the literature for other NSCLC cell lines [75, 108]. Regarding the drug treatment of PAC combined with PF, even though not statistically significant when compared with each drug individually, a slight decrease in the % of proliferating NCI-H460 cells was found.

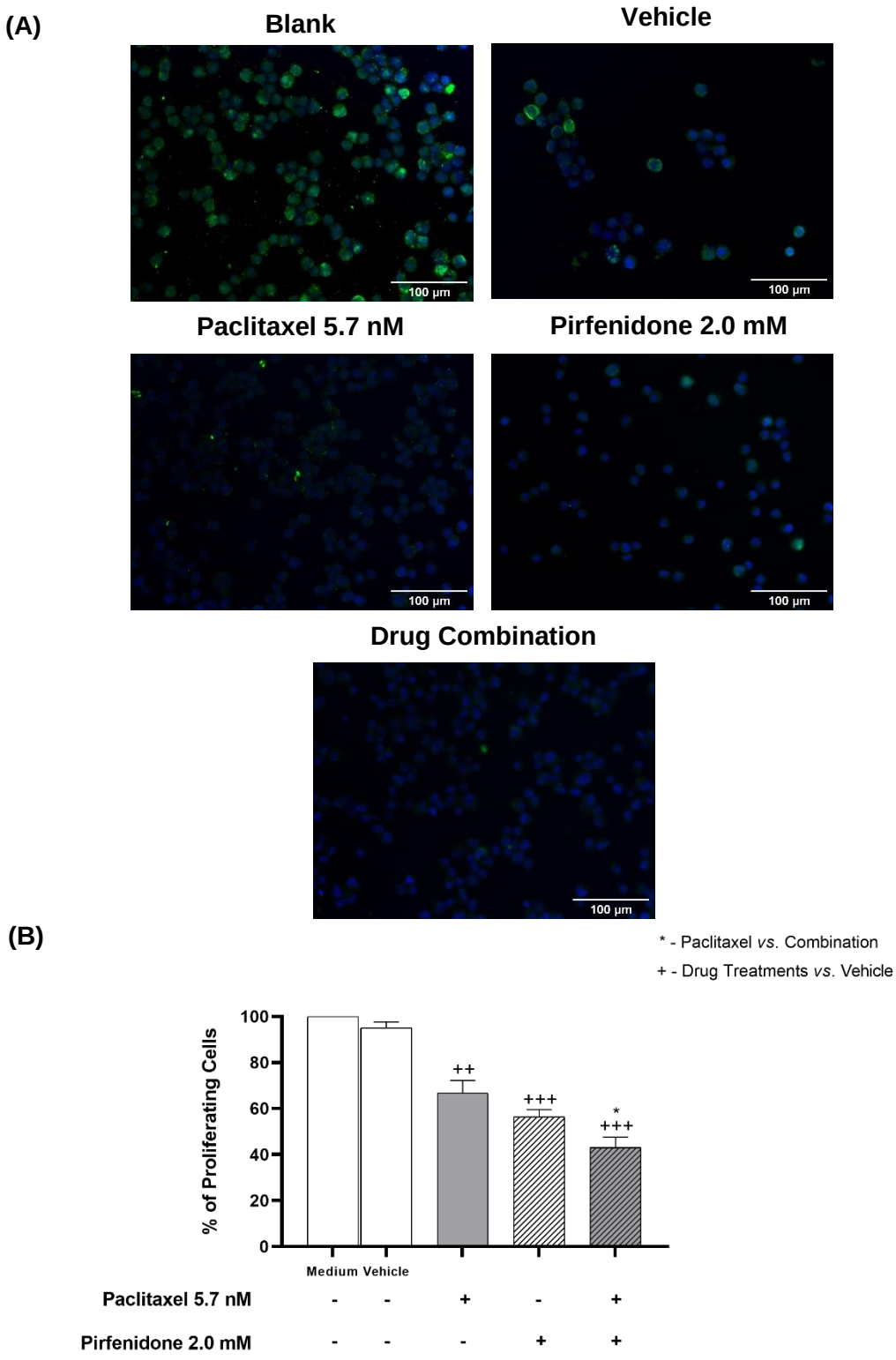

Figure 25 – Effect of the combined treatment with Paclitaxel and Pirfenidone on the cell proliferation of NCI-H460 cells assessed by the BrdU incorporation assay. Cells were treated with Paclitaxel at 5.7 nM and Pirfenidone at 2.0 mM, either alone or in combination, for 48 h. The effect of the vehicle at the highest concentration tested was also analyzed. **(A)** Representative fluorescence microscopy images of BrdU incorporation (green) and DAPI stained nuclei (blue). Amplification = 200×. **(B)** Percentage of BrdU-incorporating cells. Results are the mean ± SEM of at least three independent experiments. * $p < 0.05$, ++ $p < 0.01$ and +++ $p < 0.001$

4.3.4. Effect on the Cell Cycle Profile of NCI-H460 Cells

Then, the effect of the combined treatment of PAC with PF on the cell cycle profile of the NCI-H460 cells was evaluated. The results are presented in **Figure 26**. As described in the literature for this particular cell line, Doxorubicin at 50 nM, the positive control, caused visible alteration in the histograms of the cell cycle profile [109, 110].

The treatment of NCI-H460 cells with PAC alone statistically significantly decreased the % of cells in the G0/G1 phases of the cell cycle, as well as, increased the % of cell population in the sub-G1 phase. These findings were previously reported by Park S. *et al.* (2014) for the same cell line [111]. Regarding the NCI-H460 cells treated with PF alone, a statistically significant increase in the % of cells in G0/G1, accompanied by a significant reduction in the % of cells in the S phase of the cell cycle was found. These results are in line with what was previously described in the literature for several tumor models, including NSCLC [71, 72, 75].

With regard to the combined treatment of PAC with PF, our results showed a statistically significant reduction in the % of cells in the G2/M phases, accompanied by a prominent increase in the % of cells in sub-G1, when compared with the effect of each drug alone. Moreover, although not statistically significant when compared with each drug individually, when compared with the vehicle this drug combination also decreased the % of cells in the S phase of the cell cycle.

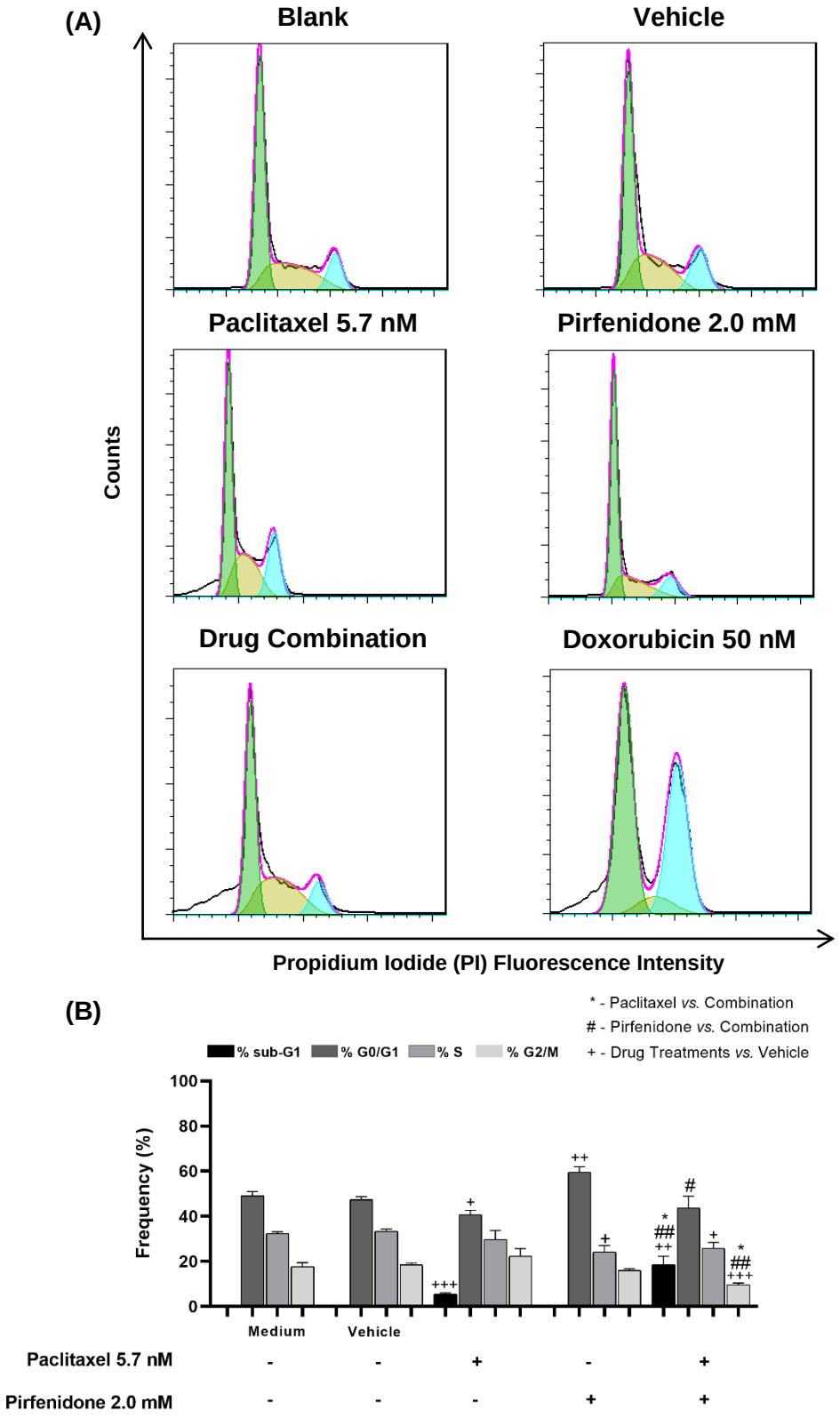

Figure 26 – Effect of the combined treatment with Paclitaxel and Pirfenidone on the cell cycle profile of NCI-H460 cells analyzed by flow cytometry following PI staining. Cells were treated with Paclitaxel at 5.7 nM and Pirfenidone at 2.0 mM, either alone or in combination, for 48 h. **(A)** Representative cell cycle histograms and **(B)** Frequency of cell cycle phases for each condition. Doxorubicin (50 nM) was used as positive control. Results are the mean ± SEM of at least 3 independent experiments. *, # or + $p < 0.05$, ## or ++ $p < 0.01$ and +++ $p < 0.001$.

4.3.5. Effect on the Levels of Cell Death of NCI-H460 Cells

Our previous results revealed that the combination of PAC with PF decreased cell growth and viability, which was not related to an antiproliferative effect. Furthermore, a substantial increase in the % of cells in the sub-G1 phase of the cell cycle after treatment with this drug combination was observed. Thus, our findings pointed out to the possibility that this drug combination could induce cell death. Therefore, the effect of the combination of PAC with PF on NCI-H460 cell death was evaluated, using an assay specific to detect cell death (Annexin V-FITC/PI labelling followed by flow cytometry analysis). The results are presented in **Figure 27**. Doxorubicin at 50 nM was used as a positive control.

Our results demonstrated that the combined treatment of PAC with PF statistically significantly increased the % of NCI-H460 cell death, when compared to the treatment with each drug individually.

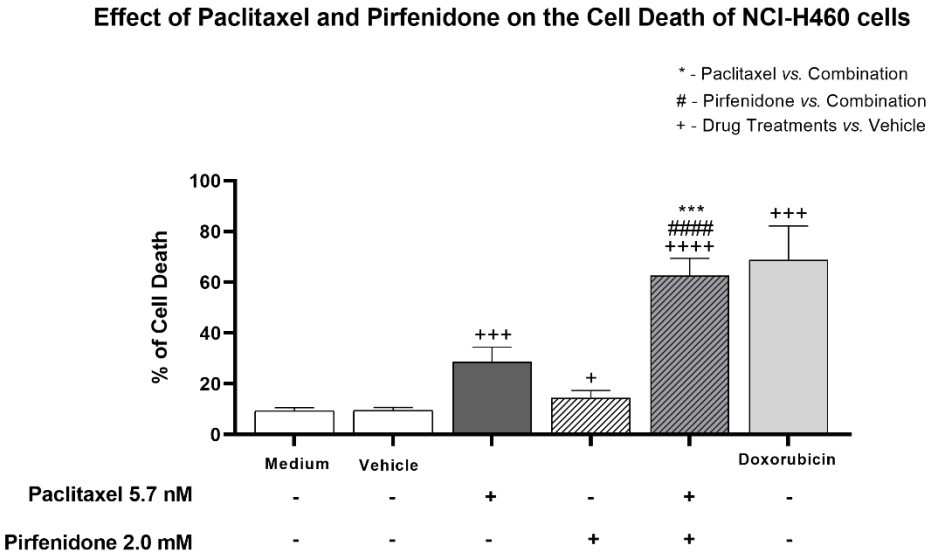

Figure 27 – Effect of the combined treatment with Paclitaxel and Pirfenidone on the % of cell death of NCI-H460 cells determined by flow cytometry following Annexin V-FITC/PI staining. Cells were treated with Paclitaxel at 5.7 nM and Pirfenidone at 2.0 mM, either alone or in combination, for 48 h. The effect of the vehicle at the highest concentration tested was also analyzed. Doxorubicin (50 nM) was used as positive control. Results are the mean ± SEM of at least three independent experiments. + $p < 0.05$, *** or +++ $p < 0.001$ and #### or ++++ $p < 0.0001$.

4.4. Study of the Drug Combination: Etoposide (ETP) plus Pirfenidone (PF)

4.4.1. Effect on the % of Cell Growth of Human NSCLC Cell Lines

In order to verify whether PF sensitizes NSCLC cell lines to ETP treatment, the NCI-H460 cell line was treated with a drug combination consisting of: i) PF at its GI_{50} concentration (2 mM) with increasing concentrations of Etoposide (from 0.04 to 0.60 µM, **Figure 28A**); or ii) ETP at its GI_{50} concentration (0.60 µM) with increasing concentrations of PF (from 0.30 to 2.00 mM, **Figure 28B**). Our results showed that the combined treatment of ETP with PF did not provide a statistically significant advantage, in terms of cell growth inhibition, over the treatment with ETP alone.

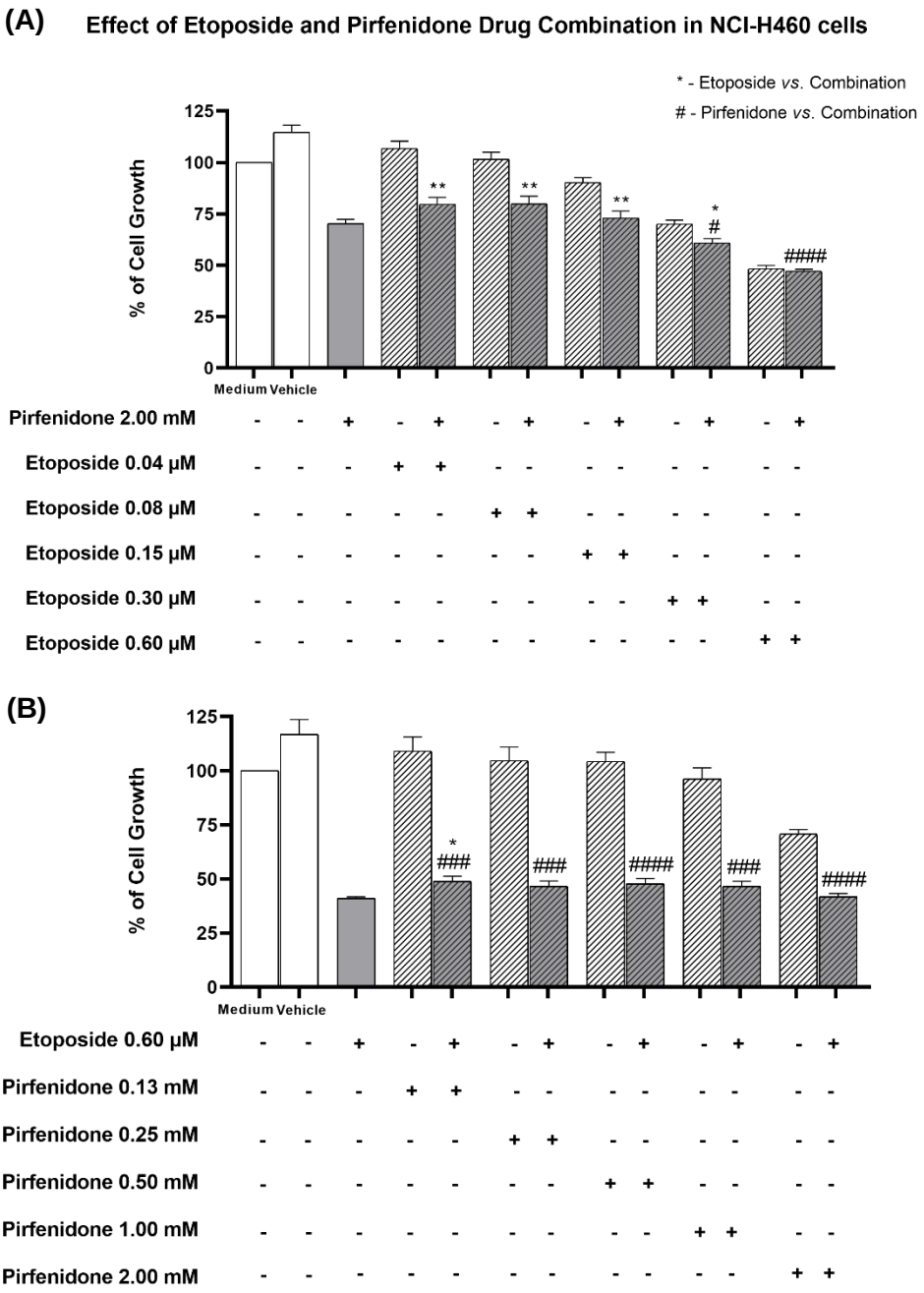

Figure 28 – Effect of the combined treatment with Etoposide and Pirfenidone at different concentrations on the % of cell growth of NCI-H460 cells, assessed by the SRB assay. Cells were treated with drug combinations consisting of **(A)** Pirfenidone at 2.0 mM with five serial dilutions of Etoposide; or **(B)** Etoposide at 0.60 µM with five serial dilutions of Pirfenidone for 48 h. The effect of the vehicle at the highest concentration tested was also analyzed. Results are presented as a % of cell growth and are the mean ± SEM of at least three independent experiments. * or # $p < 0.05$, ** $p < 0.01$, ### $p < 0.001$ and #### $p < 0.0001$.

Similar results were obtained when A549 cells were treated with the drug combination of ETP at 5.0 µM and PF at 1.5 mM for 48 h (**Figure 29**).

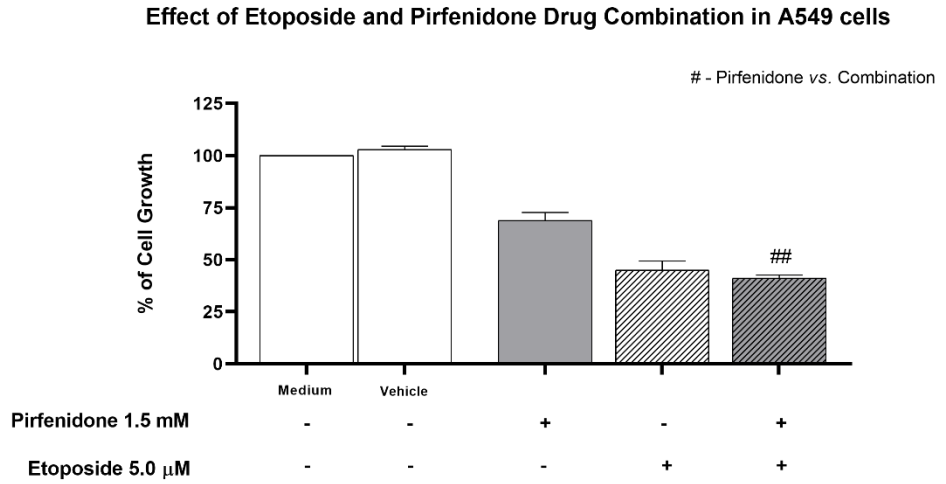

Figure 29 – Effect of the combined treatment with Etoposide and Pirfenidone on the % of cell growth of A549 cells, assessed by the SRB assay. Cells were treated with a drug combination consisting of Pirfenidone at 1.5 mM and Etoposide at 5.0 µM for 48 h. The effect of the vehicle at the highest concentration tested was also analyzed. Results are presented as a % of cell growth and are the mean ± SEM of at least three independent experiments. ## $p < 0.01$.

Therefore, the combination of ETP plus PF was not pursued with further studies in NSCLC cell lines. Interestingly, the drug ETP is frequently used in combination with platinum-based drugs to treat another lung cancer subtype, the SCLC [12].

4.5. Study of the Drug Combination: Gemcitabine (GEM) plus Pirfenidone (PF)

4.5.1. Effect on the % of Cell Growth of Human NSCLC Cell Lines

The effect of the combined treatment of GEM with PF on the % of cell growth of NSCLC cell lines was also analyzed. The NCI-H460 cells were treated for 48 h using two different experimental approaches: i) PF at a concentration of 2 mM with increasing concentrations of GEM (from 0.79 to 12.60 nM, **Figure 30A**); and ii) GEM at a concentration of 12.60 nM with increasing concentrations of PF (from 0.13 to 2 mM, **Figure 30B**).

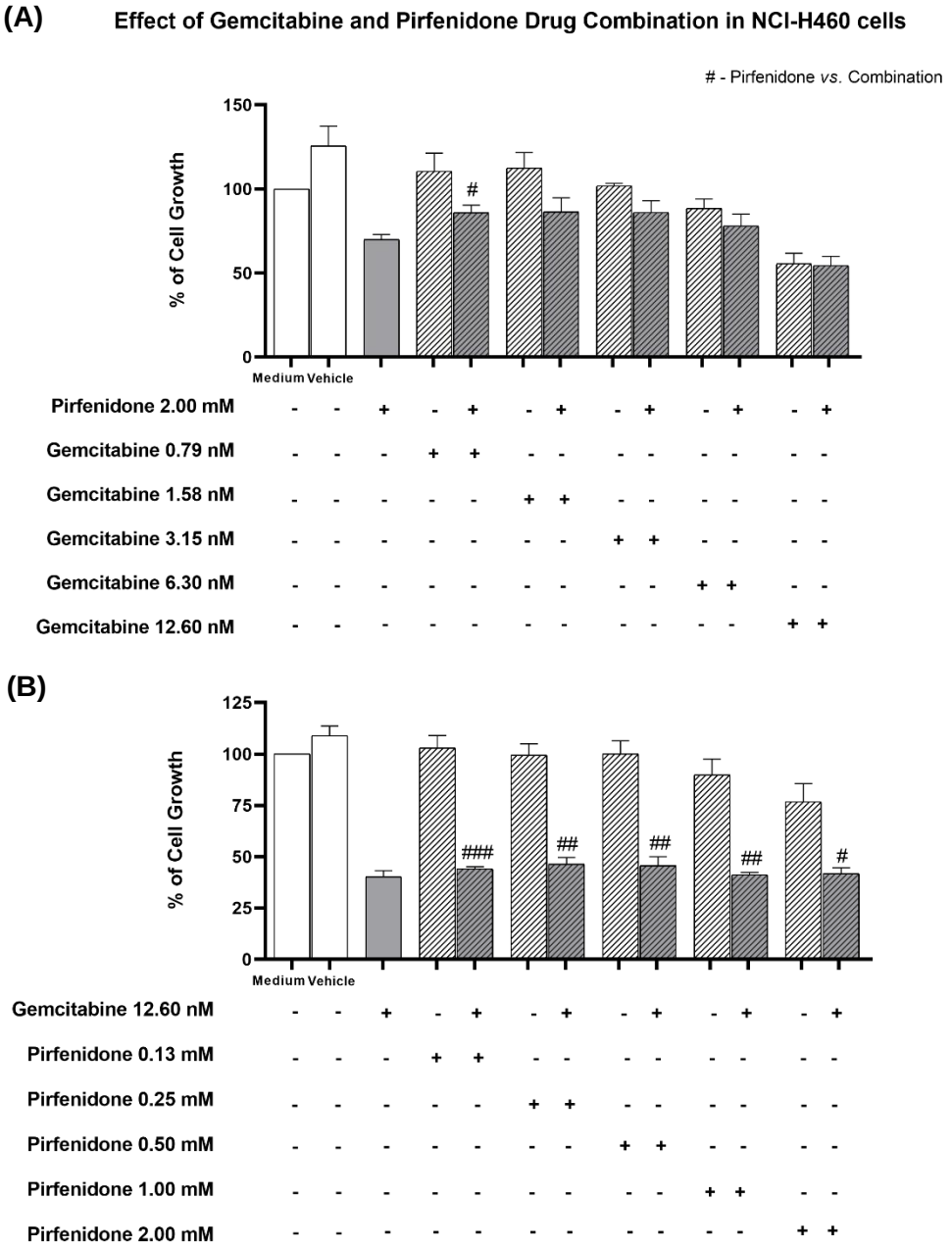

Figure 30 – Effect of the combined treatment with Gemcitabine and Pirfenidone at different concentrations on the % of cell growth of NCI-H460 cells, assessed by the SRB assay. Cells were treated with drug combinations consisting of **(A)** Pirfenidone at 2.0 mM with five serial dilutions of Gemcitabine; or **(B)** Gemcitabine at 12.60 nM with five serial dilutions of Pirfenidone for 48 h. The effect of the vehicle at the highest concentration tested was also analyzed. Results are presented as a % of cell growth and are the mean ± SEM of at least three independent experiments. # $p < 0.05$, ## $p < 0.01$ and ### $p < 0.001$.

Our results demonstrated that this drug combination did not alter the % of cell growth, when compared with the drugs used individually in the NCI-H460 cell line. The same outcome was observed when the A549 cell line was treated with PF at 1.5 mM and GEM at 26.0 nM for 48 h (**Figure 31**).

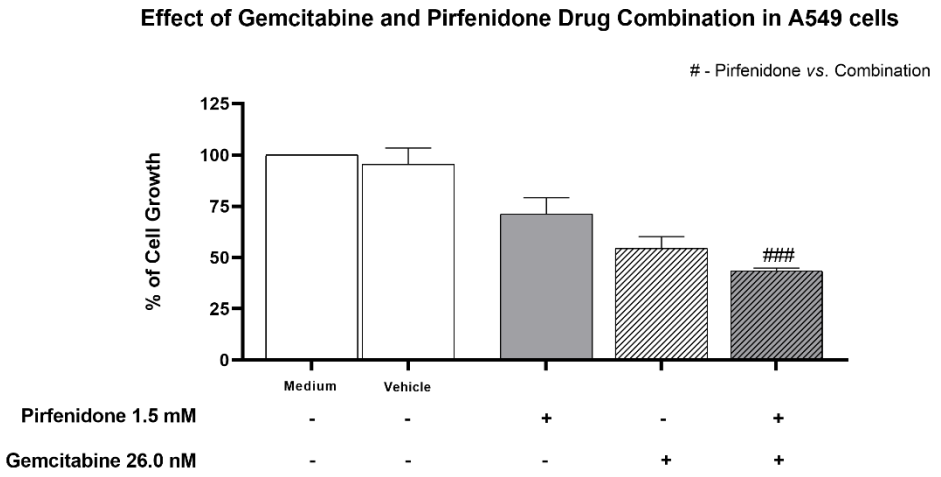

Figure 31 – Effect of the combined treatment with Gemcitabine and Pirfenidone on the % of cell growth of A549 cells, assessed by the SRB assay. Cells were treated with a drug combination consisting of Pirfenidone at 1.5 mM and Gemcitabine at 26.0 nM for 48 h. The effect of the vehicle at the highest concentration tested was also analyzed. Results are presented as a % of cell growth and are the mean ± SEM of at least three independent experiments. ### $p < 0.001$.

4.6. Study of the Triplet Drug Combination: Vinorelbine (VR) and Carboplatin (CBP) plus Pirfenidone (PF)

4.6.1. Effect on the % of Cell Growth of Human NSCLC Cell Lines

As previously stated, platinum-based chemotherapy is the standard of care for NSCLC patients who do not respond to targeted therapies or express lower levels of PD-L1. In addition, this type of combinational regimen is also applied in a neo-adjuvant setting [5, 14, 28]. Recently, in 2020, a retrospective study suggested that combining carboplatin-based regimens with PF could be safe for the treatment of patients with idiopathic pulmonary fibrosis and lung cancer [88]. These facts, along with the previously presented results suggesting that PF sensitizes NSCLC cell lines to VR treatment, led us to verify whether PF also sensitizes cells to the combined treatment with VR and CBP (duplet currently used in the clinic). Thus, the effect of this triplet drug combination (VR and CBP plus PF) on the cell growth of the three NSCLC cell lines was also analyzed.

The results, presented in **Figures 32, 33 and 34,** demonstrated that the triplet drug combination statistically significantly reduced the % of cell growth of NCI-H460, A549 and NCI-H322 cells, when compared to the cells treated with the duplet (VR and CBP), which is currently used in the clinical practice.

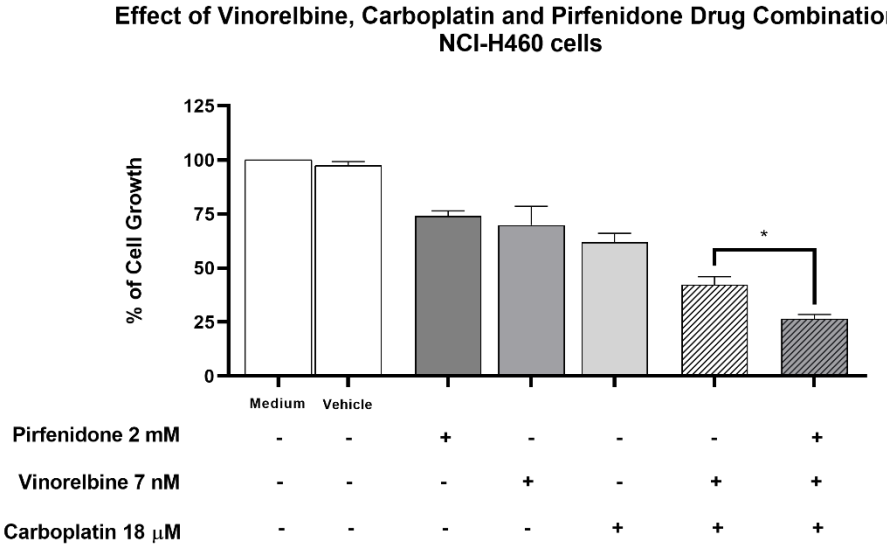

Figure 32 – Effect of the combined treatment with Pirfenidone, Vinorelbine and Carboplatin on the % of cell growth of NCI-H460 cells, assessed by the SRB assay. Cells were treated with a drug combination consisting of Pirfenidone at 2 mM, Vinorelbine at 7 nM and Carboplatin at 18 μM (triplet) for 48 h. The effect of the combined treatment consisting of Vinorelbine at 7 nM and Carboplatin at 18 μM, used in the clinical practice, was compared with the triplet under study. The effect of the vehicle at the highest concentration tested was also analyzed. Results are presented as a % of cell growth and are the mean ± SEM of at least three independent experiments. * $p < 0.05$.

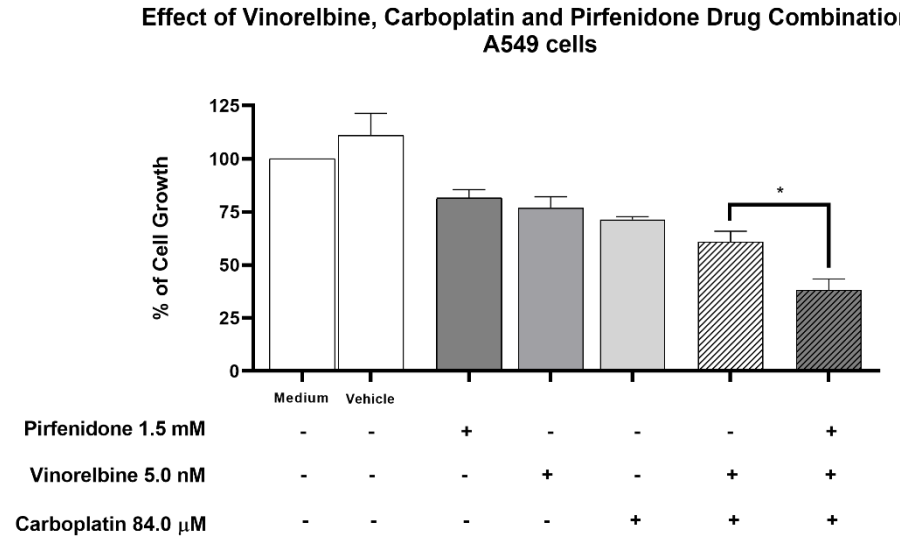

Figure 33 – Effect of the combined treatment with Pirfenidone, Vinorelbine and Carboplatin on the % of cell growth of A549 cells, assessed by the SRB assay. Cells were treated with a drug combination consisting

of Pirfenidone at 1.5 mM, Vinorelbine at 5.0 nM and Carboplatin at 84.0 µM (triplet) for 48 h. The effect of the combined treatment consisting of Vinorelbine at 5.0 nM and Carboplatin at 84.0 µM, used in the clinical practice, was compared with the triplet under study. The effect of the vehicle at the highest concentration tested was also analyzed. Results are presented as a % of cell growth and are the mean ± SEM of at least three independent experiments. * $p < 0.05$.

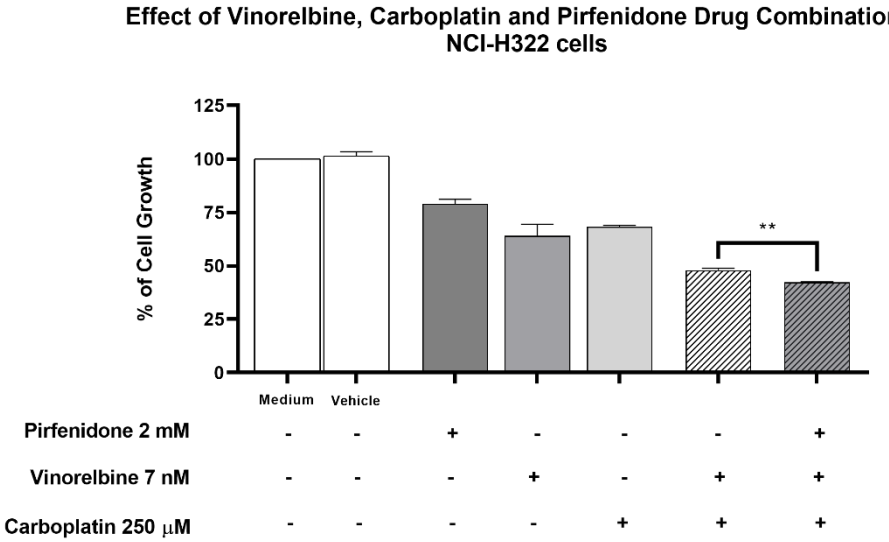

Figure 34 – Effect of the combined treatment with Pirfenidone, Vinorelbine and Carboplatin on the % of cell growth of NCI-H322 cells, assessed by the SRB assay. Cells were treated with a drug combination consisting of Pirfenidone at 2 mM, Vinorelbine at 7 nM and Carboplatin at 250 µM (triplet) for 48 h. The effect of the combined treatment consisting of Vinorelbine at 7 nM and Carboplatin at 250 µM, used in the clinical practice, was compared with the triplet under study. The effect of the vehicle at the highest concentration tested was also analyzed. Results are presented as a % of cell growth and are the mean ± SEM of at least three independent experiments. ** $p < 0.01$.

4.7. Study of the Effect of the Combined Drug Treatments in Non-Tumorigenic Cell Lines

The cytotoxic effect of the most promising combined drug treatments was evaluated in two non-tumorigenic cell lines (MCF-10A and MCF-12A).

First, the cytotoxic effect of the combined treatments of VR or PAC with PF (duplets) on non-tumorigenic cell lines was evaluated in both MCF-10A (**Figure 35A**) and MCF-12A cells (**Figure 35B**). Our results demonstrated that these combined treatments did not cause toxicity to either of the non-tumorigenic cell lines, when compared with the individual drugs, VR or PAC.

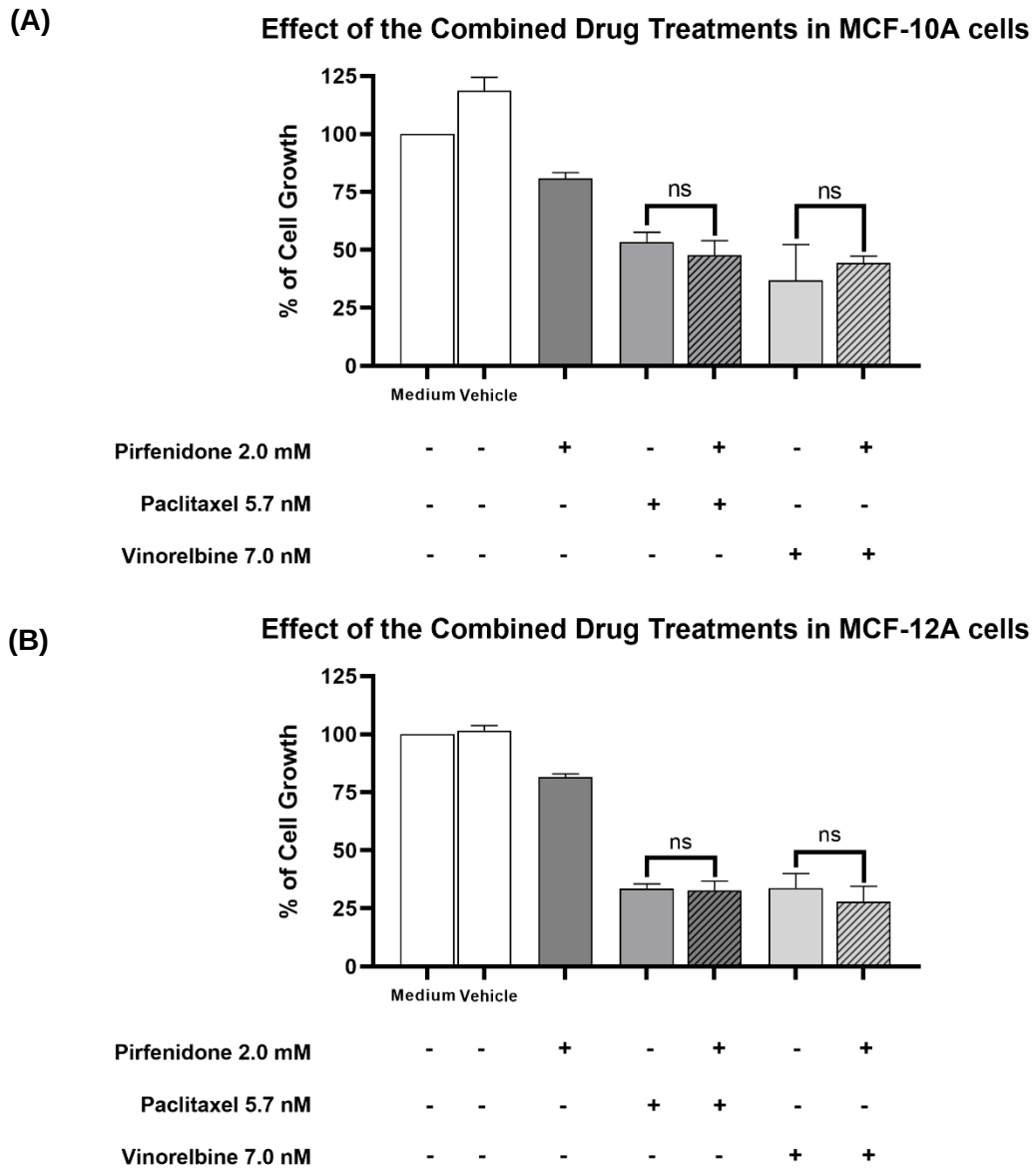

Figure 35 – Effect of the combined treatment with Pirfenidone plus Vinorelbine or Paclitaxel in (A) MCF-10A and (B) MCF-12A non-tumorigenic cells, assessed by the SRB assay. Cells were treated with the drug combinations consisting of Pirfenidone 2.0 mM plus Paclitaxel 5.7 nM or Vinorelbine 7.0 nM, for 48 h. The effect of the vehicle at the highest concentration tested was also analyzed. Results are presented as a % of cell growth and are the mean ± SEM of at least three independent experiments.

Finally, the cytotoxic effect of the triple combination of VR, CBP and PF was also evaluated in both MCF-10A (**Figure 36A**) and MCF-12A cell lines (**Figure 36B**). Our results revealed that this triplet drug combination did not cause cytotoxicity to either of the non-tumorigenic cell lines, when compared with the cells treated with the duplet consisting of VR plus CBP.

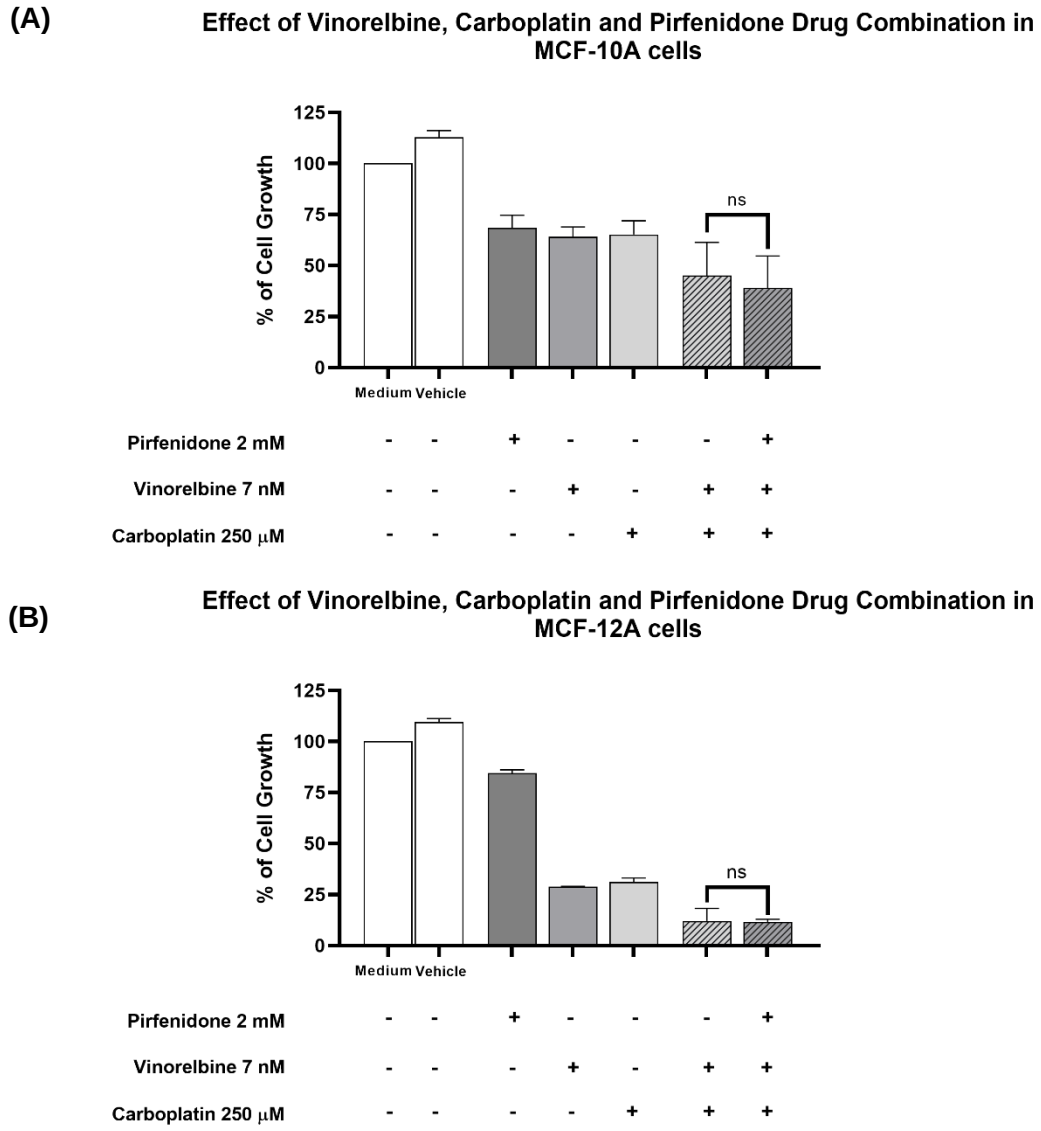

Figure 36 – Effect of the combined treatment with Vinorelbine, Carboplatin and Pirfenidone in (A) MCF-10A and (B) MCF-12A non-tumorigenic cells, assessed by the SRB assay. Cells were treated with the drug combination consisting of Vinorelbine 7 nM, Carboplatin 250 µM and PF 2 mM, for 48 h. The effect of the combined duplet treatment consisting of Vinorelbine at 7 nM and Carboplatin at 250 µM was compared with the effect of treatment with the triplet under study. The effect of the vehicle at the highest concentration tested was also analyzed. Results are presented as a % of cell growth and are the mean ± SEM of at least three independent experiments.

4.8. Next Generation Sequencing (NGS) of NSCLC Cell Lines

To validate the NSCLC cell lines' molecular profile, a Next Generation Sequencing analysis for a panel of specific genes was performed with the Ion Torrent™ Oncomine™ Focus Assay. The results, presented in **Figure 37**, obtained from the Ion Torrent™ Software, confirmed that the mutations detected by NGS for the three cell lines currently in culture in our laboratory match with those described by ATCC. Indeed, a *KRAS* G12S mutation was detected in the A549 adenocarcinoma cell line. Furthermore, the NCI-H460 cell line presented a *KRAS* Q61H mutation. Mutations in the *PIK3CA* and *MYC* genes were also detected in the NCI-H460 cell line. As expected, the NCI-H322 cell line did not present any of the mutations considered in this NGS analysis.

These results also allowed the selection of the NSCLC cell line that best mimics the molecular profile of patients who could potentially benefit from the combined drug treatments under study, and thus, to be tested in xenograft mice models. Thus, the A549 cell line was selected as, in addition to be representative of the most common histological subtype (adenocarcinoma), it also carries a *KRAS* G12S mutation, for which there are currently no approved targeted therapies. Furthermore, as previously stated, the presence of this mutation is associated with a poor prognosis.

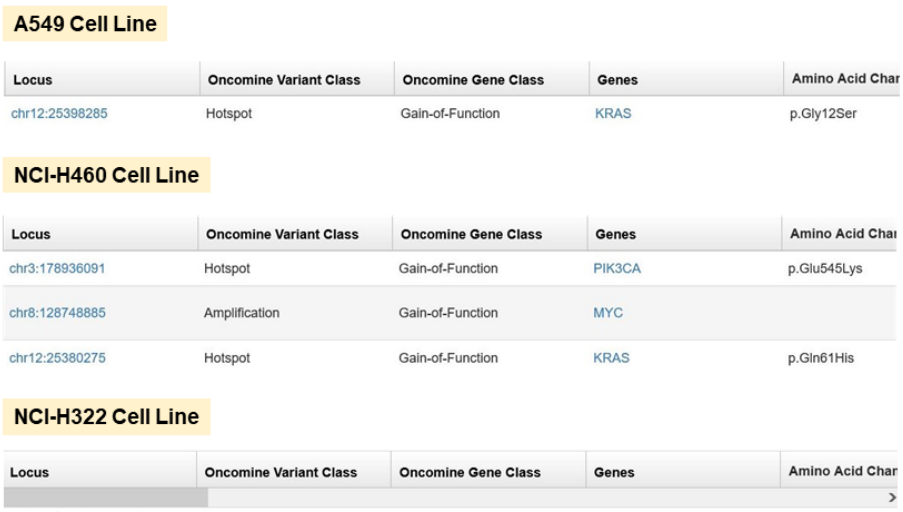

A549 Cell Line

Locus	Oncomine Variant Class	Oncomine Gene Class	Genes	Amino Acid Char
chr12:25398285	Hotspot	Gain-of-Function	KRAS	p.Gly12Ser

NCI-H460 Cell Line

Locus	Oncomine Variant Class	Oncomine Gene Class	Genes	Amino Acid Char
chr3:178936091	Hotspot	Gain-of-Function	PIK3CA	p.Glu545Lys
chr8:128748885	Amplification	Gain-of-Function	MYC	
chr12:25380275	Hotspot	Gain-of-Function	KRAS	p.Gln61His

NCI-H322 Cell Line

Locus	Oncomine Variant Class	Oncomine Gene Class	Genes	Amino Acid Char

Figure 37 – Mutations detected in A549, NCI-H460 and NCI-H322 cell lines using the Ion Torrent™ Oncomine™ Focus Assay. Results generated from Ion Reporter™ Software following Next Generation Sequencing.

Chapter

Conclusion and Future Perspectives

5

Lung cancer remains the second cancer with highest incidence and the leading cause of cancer-related deaths worldwide. Non-small cell lung cancer (NSCLC) accounts for a major part of the cases. Chemotherapy is still the major treatment option for patients with NSCLC. However, drug resistance occurs, also as a result of a highly fibrotic tumor, thus the development of new therapeutic approaches is crucial. Pirfenidone is an anti-fibrotic drug that revealed antitumor potential, as well as the capability to sensitize some tumor models to chemotherapy. Preliminary results from our research group demonstrated that PF sensitized the NSCLC NCI-H460 cell line to Vinorelbine treatment. Therefore, the purpose of this dissertation was to study the sensitizing effect of Pirfenidone to chemotherapeutic drugs currently used in the clinic for the treatment of NSCLC, by validating the previous preliminary results and evaluating new potential combined drug treatments.

Our results demonstrated that Pirfenidone sensitized the A549 and NCI-H322 lung adenocarcinoma cell lines to Vinorelbine treatment. This drug combination caused a reduction in cell growth and viability, a decrease in the % of proliferating cells, as well as an alteration in the cell cycle profile, when compared to the treatment with each of these drugs individually. Moreover, this drug combination also induced cell death in the NCI-H460, A549, and NCI-H322 cell lines, when compared with the drugs used alone. Importantly, this drug combination was not more cytotoxic to non-tumorigenic cells than the individual drug treatments. Therefore, our data validated the previous preliminary results and further showed the relevance of combining Pirfenidone with Vinorelbine in other NSCLC cell lines.

Interestingly, Pirfenidone also sensitized the three NSCLC cell lines under study to the combined treatment with Vinorelbine with Carboplatin (which has been used in the clinical practice in patients with advanced NSCLC or as a neo-adjuvant measure). Our data clearly demonstrated that this triple drug combination has advantages, in terms of cell growth inhibition, over Vinorelbine plus Carboplatin.

Furthermore, our work also demonstrated that Pirfenidone sensitized the NCI-H460 cells to Paclitaxel treatment. This drug combination reduced the % of cell growth

and viability, altered the cell cycle profile and induced cell death, when compared with the effect of the drugs alone. Again, when non-tumorigenic cells were treated with this drug combination the observed cytotoxicity was similar to that observed when cells were treated with the individual chemotherapeutic drugs. Therefore, the combination of Pirfenidone plus Paclitaxel also revealed to be potentially advantageous over Paclitaxel treatment alone, however only in the NCI- H460 cells, a specific histologic type. Unfortunately, Pirfenidone did not sensitize either of the NSCLC cells under study to Etoposide or Gemcitabine treatment.

Overall, the findings presented in this dissertation provide pre-clinical evidence to support the possibility of repurposing Pirfenidone, in combination with Vinorelbine alone or combined with Carboplatin, for the treatment of NSCLC.

Future work will study the combination treatment consisting of Pirfenidone plus Vinorelbine and Carboplatin in mice xenografts of human NSCLC cell lines, to further evaluate their toxicity and antitumor efficacy. The mechanisms of action underlying these drug combination will also be further explored both *in vitro* and *vivo.* Finally, future work will also aim to explore the effect of Pirfenidone in combination with targeted therapies or immune-checkpoint inhibitors.

Chapter

References 6

1. Sung, H., et al., *Global Cancer Statistics 2020: GLOBOCAN Estimates of Incidence and Mortality Worldwide for 36 Cancers in 185 Countries.* CA Cancer J Clin, 2021. **71**(3): p. 209-249.
2. International Agency for Research on Cancer. *Global Cancer Observatory: Cancer Tomorrow.* Available online: https://gco.iarc.fr/tomorrow/en (accessed October 5, 2021).
3. Duma, N., R. Santana-Davila, and J.R. Molina, *Non-Small Cell Lung Cancer: Epidemiology, Screening, Diagnosis, and Treatment.* Mayo Clin Proc, 2019. **94**(8): p. 1623-1640.
4. International Agency for Research on Cancer. *Global Cancer Observatory: Cancer Today.* Available online: https://gco.iarc.fr/tomorrow/en (accessed October 5, 2021).
5. Gridelli, C., et al., *Non-small-cell lung cancer.* Nat Rev Dis Primers, 2015. **1**: p. 15009.
6. Carioli, G., et al., *European cancer mortality predictions for the year 2020 with a focus on prostate cancer.* Ann Oncol, 2020. **31**(5): p. 650-658.
7. Siegel, R.L., K.D. Miller, and A. Jemal, *Cancer statistics, 2020.* CA Cancer J Clin, 2020. **70**(1): p. 7-30.
8. Nooreldeen, R. and H. Bach, *Current and Future Development in Lung Cancer Diagnosis.* Int J Mol Sci, 2021. **22**(16).
9. Mao, Y., et al., *Epidemiology of Lung Cancer.* Surg Oncol Clin N Am, 2016. **25**(3): p. 439-45.
10. Matakidou, A., T. Eisen, and R.S. Houlston, *Systematic review of the relationship between family history and lung cancer risk.* Br J Cancer, 2005. **93**(7): p. 825-33.
11. Herbst, R.S., J.V. Heymach, and S.M. Lippman, *Lung cancer.* N Engl J Med, 2008. **359**(13): p. 1367-80.
12. Rudin, C.M., et al., *Small-cell lung cancer.* Nat Rev Dis Primers, 2021. **7**(1): p. 3.
13. Bernhardt, E.B. and S.I. Jalal, *Small Cell Lung Cancer.* Cancer Treat Res, 2016. **170**: p. 301-22.

14. Lemjabbar-Alaoui, H., et al., *Lung cancer: Biology and treatment options.* Biochim Biophys Acta, 2015. **1856**(2): p. 189-210.
15. Chen, Z., et al., *Non-small-cell lung cancers: a heterogeneous set of diseases.* Nat Rev Cancer, 2014. **14**(8): p. 535-46.
16. Travis, W.D., et al., *The 2015 World Health Organization Classification of Lung Tumors: Impact of Genetic, Clinical and Radiologic Advances Since the 2004 Classification.* J Thorac Oncol, 2015. **10**(9): p. 1243-1260.
17. Subba R. Digumarthy, T.C.M., *Chapter 11 - Pulmonary Neoplasms.* The Requisites, 2010: p. 253-287.
18. Yasufuku, K. and T. Fujisawa, *Staging and diagnosis of non-small cell lung cancer: invasive modalities.* Respirology, 2007. **12**(2): p. 173-83.
19. Brierley, J., M. K. Gospodarowicz, and Ch. Wittekind., *TNM Classification of Malignant Tumours*. Eighth ed. 2017: Chichester, West Sussex, UK ; Hoboken, NJ: John Wiley & Sons, Inc.
20. Videtic, G.M., *The role of radiation therapy in small cell lung cancer.* Curr Oncol Rep, 2013. **15**(4): p. 405-10.
21. Wang, X., et al., *Pulmonary function after segmentectomy versus lobectomy in patients with early-stage non-small-cell lung cancer: a meta-analysis.* J Int Med Res, 2021. **49**(9): p. 3000605211044204.
22. Feng, J., et al., *Survival Outcomes of Lobectomy Versus Segmentectomy in Clinical Stage I Non-Small Cell Lung Cancer: A Meta-Analysis.* Adv Ther, 2021. **38**(7): p. 4130-4137.
23. Palussière, J., et al., *Radiofrequency ablation of stage IA non-small cell lung cancer in patients ineligible for surgery: results of a prospective multicenter phase II trial.* J Cardiothorac Surg, 2018. **13**(1): p. 91.
24. *Platinum Coordination Complexes*, in *LiverTox: Clinical and Research Information on Drug-Induced Liver Injury*. 2012, National Institute of Diabetes and Digestive and Kidney Diseases: Bethesda (MD).
25. Sinkule, J.A., *Etoposide: a semisynthetic epipodophyllotoxin. Chemistry, pharmacology, pharmacokinetics, adverse effects and use as an antineoplastic agent.* Pharmacotherapy, 1984. **4**(2): p. 61-73.
26. Hertel, L.W., et al., *Evaluation of the antitumor activity of gemcitabine (2',2'-difluoro-2'-deoxycytidine).* Cancer Res, 1990. **50**(14): p. 4417-22.
27. Hardin, C., et al., *Emerging treatment using tubulin inhibitors in advanced non-small cell lung cancer.* Expert Opin Pharmacother, 2017. **18**(7): p. 701-716.
28. Pignon, J.P., et al., *Lung adjuvant cisplatin evaluation: a pooled analysis by the LACE Collaborative Group.* J Clin Oncol, 2008. **26**(21): p. 3552-9.

29. Devarakonda, S., D. Morgensztern, and R. Govindan, *Genomic alterations in lung adenocarcinoma.* Lancet Oncol, 2015. **16**(7): p. e342-51.
30. Suster, D.I. and M. Mino-Kenudson, *Molecular Pathology of Primary Non-small Cell Lung Cancer.* Arch Med Res, 2020. **51**(8): p. 784-798.
31. Martinez-Marti, A., A. Navarro, and E. Felip, *Epidermal growth factor receptor first generation tyrosine-kinase inhibitors.* Transl Lung Cancer Res, 2019. **8**(Suppl 3): p. S235-s246.
32. Karachaliou, N., et al., *EGFR first- and second-generation TKIs—there is still place for them in EGFR -mutant NSCLC patients.* 2018, 2018: p. S23-S47.
33. Hirsch, F.R., et al., *Lung cancer: current therapies and new targeted treatments.* Lancet, 2017. **389**(10066): p. 299-311.
34. Blair, H.A., *Sotorasib: First Approval.* Drugs, 2021. **81**(13): p. 1573-1579.
35. D'Incecco, A., et al., *PD-1 and PD-L1 expression in molecularly selected non-small-cell lung cancer patients.* Br J Cancer, 2015. **112**(1): p. 95-102.
36. Alexander, M., S.Y. Kim, and H. Cheng, *Update 2020: Management of Non-Small Cell Lung Cancer.* Lung, 2020. **198**(6): p. 897-907.
37. Roviello, G., et al., *Advances in anti-BRAF therapies for lung cancer.* Invest New Drugs, 2021. **39**(3): p. 879-890.
38. Suresh, K., et al., *Immune Checkpoint Immunotherapy for Non-Small Cell Lung Cancer: Benefits and Pulmonary Toxicities.* Chest, 2018. **154**(6): p. 1416-1423.
39. Rafei, H., et al., *Immune-based Therapies for Non-small Cell Lung Cancer.* Anticancer Res, 2017. **37**(2): p. 377-387.
40. Arbour, K.C. and G.J. Riely, *Systemic Therapy for Locally Advanced and Metastatic Non-Small Cell Lung Cancer: A Review.* Jama, 2019. **322**(8): p. 764-774.
41. Oguntade, A.S., et al., *Anti-angiogenesis in cancer therapeutics: the magic bullet.* J Egypt Natl Canc Inst, 2021. **33**(1): p. 15.
42. Assoun, S., et al., *Bevacizumab in advanced lung cancer: state of the art.* Future Oncol, 2017. **13**(28): p. 2515-2535.
43. Xie, S., et al., *The metastasizing mechanisms of lung cancer: Recent advances and therapeutic challenges.* Biomed Pharmacother, 2021. **138**: p. 111450.
44. Rotow, J. and T.G. Bivona, *Understanding and targeting resistance mechanisms in NSCLC.* Nat Rev Cancer, 2017. **17**(11): p. 637-658.
45. Carnio, S., et al., *Prognostic and predictive biomarkers in early stage non-small cell lung cancer: tumor based approaches including gene signatures.* Transl Lung Cancer Res, 2013. **2**(5): p. 372-81.
46. Uramoto, H. and F. Tanaka, *Recurrence after surgery in patients with NSCLC.* Transl Lung Cancer Res, 2014. **3**(4): p. 242-9.

47. Reita, D., et al., *Molecular Mechanism of EGFR-TKI Resistance in EGFR-Mutated Non-Small Cell Lung Cancer: Application to Biological Diagnostic and Monitoring.* Cancers (Basel), 2021. **13**(19).
48. Błach, J., et al., *Failure of Immunotherapy-The Molecular and Immunological Origin of Immunotherapy Resistance in Lung Cancer.* Int J Mol Sci, 2021. **22**(16).
49. Assaraf, Y.G., et al., *The multi-factorial nature of clinical multidrug resistance in cancer.* Drug Resist Updat, 2019. **46**: p. 100645.
50. Bremnes, R.M., et al., *The role of tumor stroma in cancer progression and prognosis: emphasis on carcinoma-associated fibroblasts and non-small cell lung cancer.* J Thorac Oncol, 2011. **6**(1): p. 209-17.
51. Han, X., et al., *Emerging nanomedicines for anti-stromal therapy against desmoplastic tumors.* Biomaterials, 2020. **232**: p. 119745.
52. Cha, Y., et al., *Drug repurposing from the perspective of pharmaceutical companies.* Br J Pharmacol, 2018. **175**(2): p. 168-180.
53. Austin, B.A. and A.D. Gadhia, *New Therapeutic Uses for Existing Drugs.* Adv Exp Med Biol, 2017. **1031**: p. 233-247.
54. Ashburn, T.T. and K.B. Thor, *Drug repositioning: identifying and developing new uses for existing drugs.* Nat Rev Drug Discov, 2004. **3**(8): p. 673-83.
55. Langedijk, J., et al., *Drug repositioning and repurposing: terminology and definitions in literature.* Drug Discov Today, 2015. **20**(8): p. 1027-34.
56. Jourdan, J.P., et al., *Drug repositioning: a brief overview.* J Pharm Pharmacol, 2020. **72**(9): p. 1145-1151.
57. Pushpakom, S., et al., *Drug repurposing: progress, challenges and recommendations.* Nat Rev Drug Discov, 2019. **18**(1): p. 41-58.
58. Xue, H., et al., *Review of Drug Repositioning Approaches and Resources.* Int J Biol Sci, 2018. **14**(10): p. 1232-1244.
59. Nosengo, N., *Can you teach old drugs new tricks?* Nature, 2016. **534**(7607): p. 314-6.
60. Gupta, S.C., et al., *Cancer drug discovery by repurposing: teaching new tricks to old dogs.* Trends Pharmacol Sci, 2013. **34**(9): p. 508-17.
61. Schein, C.H., *Repurposing approved drugs for cancer therapy.* Br Med Bull, 2021. **137**(1): p. 13-27.
62. Bertolini, F., V.P. Sukhatme, and G. Bouche, *Drug repurposing in oncology--patient and health systems opportunities.* Nat Rev Clin Oncol, 2015. **12**(12): p. 732-42.
63. Gonzalez-Fierro, A. and A. Dueñas-González, *Drug repurposing for cancer therapy, easier said than done.* Semin Cancer Biol, 2021. **68**: p. 123-131.

64. Saxena, A., et al., *Therapeutic Effects of Repurposed Therapies in Non-Small Cell Lung Cancer: What Is Old Is New Again.* Oncologist, 2015. **20**(8): p. 934-45.
65. Sun, W., P.E. Sanderson, and W. Zheng, *Drug combination therapy increases successful drug repositioning.* Drug Discov Today, 2016. **21**(7): p. 1189-95.
66. King, T.E., Jr., et al., *A phase 3 trial of pirfenidone in patients with idiopathic pulmonary fibrosis.* N Engl J Med, 2014. **370**(22): p. 2083-92.
67. Taniguchi, H., et al., *Pirfenidone in idiopathic pulmonary fibrosis.* Eur Respir J, 2010. **35**(4): p. 821-9.
68. Zou, W.J., et al., *Pirfenidone Inhibits Proliferation and Promotes Apoptosis of Hepatocellular Carcinoma Cells by Inhibiting the Wnt/β-Catenin Signaling Pathway.* Med Sci Monit, 2017. **23**: p. 6107-6113.
69. Li, C., et al., *Pirfenidone decreases mesothelioma cell proliferation and migration via inhibition of ERK and AKT and regulates mesothelioma tumor microenvironment in vivo.* Sci Rep, 2018. **8**(1): p. 10070.
70. Burghardt, I., et al., *Pirfenidone inhibits TGF-beta expression in malignant glioma cells.* Biochem Biophys Res Commun, 2007. **354**(2): p. 542-7.
71. Ishii, K., et al., *Pirfenidone, an Anti-Fibrotic Drug, Suppresses the Growth of Human Prostate Cancer Cells by Inducing G_1 Cell Cycle Arrest.* J Clin Med, 2019. **8**(1).
72. Usugi, E., et al., *Antifibrotic Agent Pirfenidone Suppresses Proliferation of Human Pancreatic Cancer Cells by Inducing G0/G1 Cell Cycle Arrest.* Pharmacology, 2019. **103**(5-6): p. 250-256.
73. Kozono, S., et al., *Pirfenidone inhibits pancreatic cancer desmoplasia by regulating stellate cells.* Cancer Res, 2013. **73**(7): p. 2345-56.
74. Aboulkheyr Es, H., et al., *Pirfenidone reduces immune-suppressive capacity of cancer-associated fibroblasts through targeting CCL17 and TNF-beta.* Integr Biol (Camb), 2020. **12**(7): p. 188-197.
75. Marwitz, S., et al., *The Multi-Modal Effect of the Anti-fibrotic Drug Pirfenidone on NSCLC.* Front Oncol, 2019. **9**: p. 1550.
76. Fujiwara, A., et al., *Pirfenidone plays a biphasic role in inhibition of epithelial-mesenchymal transition in non-small cell lung cancer.* Lung Cancer, 2017. **106**: p. 8-16.
77. Kurimoto, R., et al., *Pirfenidone may revert the epithelial-to-mesenchymal transition in human lung adenocarcinoma.* Oncol Lett, 2017. **14**(1): p. 944-950.
78. Krämer, M., et al., *Pirfenidone inhibits motility of NSCLC cells by interfering with the urokinase system.* Cell Signal, 2020. **65**: p. 109432.
79. Choi, S.H., et al., *Pirfenidone enhances the efficacy of combined radiation and sunitinib therapy.* Biochem Biophys Res Commun, 2015. **462**(2): p. 138-43.

80. Polydorou, C., et al., *Pirfenidone normalizes the tumor microenvironment to improve chemotherapy.* Oncotarget, 2017. **8**(15): p. 24506-24517.
81. Mediavilla-Varela, M., et al., *The anti-fibrotic agent pirfenidone synergizes with cisplatin in killing tumor cells and cancer-associated fibroblasts.* BMC Cancer, 2016. **16**: p. 176.
82. Qin, W., et al., *Pirfenidone facilitates immune infiltration and enhances the antitumor efficacy of PD-L1 blockade in mice.* Oncoimmunology, 2020. **9**(1): p. 1824631.
83. Antunes, C.T., *Studying the combined effect of Pirfenidone and Vinorelbine in lung and breast cancer cell lines*. 2020, University of Porto.
84. Hanahan, D. and R.A. Weinberg, *Hallmarks of cancer: the next generation.* Cell, 2011. **144**(5): p. 646-74.
85. Ballester, B., J. Milara, and J. Cortijo, *Idiopathic Pulmonary Fibrosis and Lung Cancer: Mechanisms and Molecular Targets.* Int J Mol Sci, 2019. **20**(3).
86. Vancheri, C., *Common pathways in idiopathic pulmonary fibrosis and cancer.* Eur Respir Rev, 2013. **22**(129): p. 265-72.
87. Miura, Y., et al., *Reduced incidence of lung cancer in patients with idiopathic pulmonary fibrosis treated with pirfenidone.* Respir Investig, 2018. **56**(1): p. 72-79.
88. Yamamoto, Y., et al., *Safety and effectiveness of pirfenidone combined with carboplatin-based chemotherapy in patients with idiopathic pulmonary fibrosis and non-small cell lung cancer: A retrospective cohort study.* Thorac Cancer, 2020. **11**(11): p. 3317-3325.
89. Strober, W., *Trypan Blue Exclusion Test of Cell Viability.* Curr Protoc Immunol, 2015. **111**: p. A3.B.1-a3.B.3.
90. Vichai, V. and K. Kirtikara, *Sulforhodamine B colorimetric assay for cytotoxicity screening.* Nat Protoc, 2006. **1**(3): p. 1112-6.
91. Martí-Clúa, J., *Incorporation of 5-Bromo-2'-deoxyuridine into DNA and Proliferative Behavior of Cerebellar Neuroblasts: All That Glitters Is Not Gold.* Cells, 2021. **10**(6).
92. Darzynkiewicz, Z., X. Huang, and H. Zhao, *Analysis of Cellular DNA Content by Flow Cytometry.* Curr Protoc Immunol, 2017. **119**: p. 5.7.1-5.7.20.
93. Lekshmi, A., et al., *A quantitative real-time approach for discriminating apoptosis and necrosis.* Cell Death Discov, 2017. **3**: p. 16101.
94. Berger, M.F. and E.R. Mardis, *The emerging clinical relevance of genomics in cancer medicine.* Nat Rev Clin Oncol, 2018. **15**(6): p. 353-365.
95. Hu, L., et al., *Synthesis and structure-activity relationship studies of cytotoxic vinorelbine amide analogues.* Bioorg Med Chem Lett, 2012. **22**(24): p. 7547-50.

96. Willuda, J., et al., *Preclinical Antitumor Efficacy of BAY 1129980-a Novel Auristatin-Based Anti-C4.4A (LYPD3) Antibody-Drug Conjugate for the Treatment of Non-Small Cell Lung Cancer.* Mol Cancer Ther, 2017. **16**(5): p. 893-904.
97. Chang, Y.C., et al., *Discovery of Novel Agents on Spindle Assembly Checkpoint to Sensitize Vinorelbine-Induced Mitotic Cell Death Against Human Non-Small Cell Lung Cancers.* Int J Mol Sci, 2020. **21**(16).
98. Yamori, T., et al., *Anti-tumor efficacy of paclitaxel against human lung cancer xenografts.* Jpn J Cancer Res, 1997. **88**(12): p. 1205-10.
99. Yu, Y., et al., *Synthesis and anticancer activity of lipophilic platinum(II) complexes of 3,5-diisopropylsalicylate.* Eur J Med Chem, 2008. **43**(7): p. 1438-43.
100. Belani, C.P., *Incorporation of paclitaxel and carboplatin in combined-modality therapy for locally advanced non-small cell lung cancer.* Semin Oncol, 1999. **26**(1 Suppl 2): p. 44-54.
101. Liu, H., et al., *Anti-tubulin agent vinorelbine inhibits metastasis of cancer cells by regulating epithelial-mesenchymal transition.* Eur J Med Chem, 2020. **200**: p. 112332.
102. Matthews, H.K., C. Bertoli, and R.A.M. de Bruin, *Cell cycle control in cancer.* Nat Rev Mol Cell Biol, 2021.
103. Litwiniec, A., et al., *Features of senescence and cell death induced by doxorubicin in A549 cells: organization and level of selected cytoskeletal proteins.* J Cancer Res Clin Oncol, 2010. **136**(5): p. 717-36.
104. Zhu, K., et al., *TNF-related apoptosis-inducing ligand enhances vinorelbine-induced apoptosis and antitumor activity in a preclinical model of non-small cell lung cancer.* Oncol Rep, 2014. **32**(3): p. 1234-42.
105. Wang, T.H., H.S. Wang, and Y.K. Soong, *Paclitaxel-induced cell death: where the cell cycle and apoptosis come together.* Cancer, 2000. **88**(11): p. 2619-28.
106. Brown, J.M. and L.D. Attardi, *The role of apoptosis in cancer development and treatment response.* Nat Rev Cancer, 2005. **5**(3): p. 231-7.
107. Kepp, O., et al., *Cell death assays for drug discovery.* Nat Rev Drug Discov, 2011. **10**(3): p. 221-37.
108. Zhu, Z., et al., *Modulation of alternative splicing induced by paclitaxel in human lung cancer.* Cell Death Dis, 2018. **9**(5): p. 491.
109. Rathos, M.J., et al., *Potentiation of in vitro and in vivo antitumor efficacy of doxorubicin by cyclin-dependent kinase inhibitor P276-00 in human non-small cell lung cancer cells.* BMC Cancer, 2013. **13**: p. 29.

110. Magalhães, D.B., et al., *Melissa officinalis L. ethanolic extract inhibits the growth of a lung cancer cell line by interfering with the cell cycle and inducing apoptosis.* Food Funct, 2018. **9**(6): p. 3134-3142.

111. Park, S., et al., *Schedule-Dependent Effect of Epigallocatechin-3-Gallate (EGCG) with Paclitaxel on H460 Cells.* Tuberc Respir Dis (Seoul), 2014. **76**(3): p. 114-9.